

VALIDATION AND IMPLEMENTATION OF  
EFFICIENT SIMULATION TECHNIQUES TO  
DETERMINE COUPLING TO A WIRE IN AN  
OVERMODED ENCLOSURE

By

ENDEGENA ASSEFA

Bachelor of Science in Electrical Engineering

Bahir Dar University

Bahir Dar, Ethiopia

2005

Submitted to the Faculty of the  
Graduate College of the  
Oklahoma State University  
in partial fulfillment of  
the requirements for  
the Degree of  
MASTER OF SCIENCE  
May, 2012

VALIDATION AND IMPLEMENTATION OF  
EFFICIENT SIMULATION TECHNIQUES TO  
DETERMINE COUPLING TO A WIRE IN AN  
OVERMODED ENCLOSURE

Thesis Approved:

Dr. Charles F. Bunting

---

Thesis Adviser

Dr. James C. West

---

Dr. Keith A. Teague

---

Dr. Sheryl A. Tucker

---

Dean of the Graduate College

## TABLE OF CONTENTS

I. INTRODUCTION .....	1
II. TECHNIQUES TO EVALUATE EM FIELD COUPLING TO EMPTY AND LOADED ENCLOSURES.....	7
2.1 Deterministic coupling methods using MoM .....	6
2.2 Analytical coupling method.....	9
2.3 Statistical coupling method using MODAL/MoM .....	10
2.4 Numerical and Experimental methods to determine coupling in an overmoded enclosure .....	12
2.5 Semi-analytic method to determine coupling in an overmoded enclosure .....	13
2.6 Statistical and experimental methods to determine coupling into physically small and electrically large enclosures .....	14
2.7 Statistical coupling method to determine below-deck environment.....	16
2.8 Statistical coupling methods using random plane wave approach.....	17
2.9 Random plane wave approach using FDTD .....	18
2.10 Determination of correlation of the random variables .....	19
III. BASIC CONFIGURATION AND PRELIMINARY ASSESSMENT OF FIELD PENETRATION IMPACTS.....	21
3.1 Impacts of varying parameters on the field and current coupling .....	21

3.2 Simulation of structure used in the study.....	22
3.2.1 Simulation steps .....	23
IV. STATISTICAL ANALYSIS .....	25
4.1 The need for statistical analysis .....	25
4.2 RC probability distribution model for current induced on a wire.....	26
4.3 Monte Carlo simulation .....	31
4.4 Evaluation of susceptibility based on emissions (Reciprocity) .....	32
V. RESULTS AND DISCUSSION.....	39
5.1 Observations of effects of variation of parameters on the current coupling....	39
5.1.1 Field calculation for normal incidence angle.....	39
5.1.2 Change of position of wire.....	41
5.1.3 Current calculation for normal incidence angle.....	43
5.1.4 Field calculation for varying incidence angle.....	44
5.1.5 Field calculation for different aperture size .....	46
5.2 Statistics of the current in a complex environment represented by superposition of plane waves .....	49
5.2.1 MC simulation: Random plane wave approach .....	49
5.2.2 Validation of method for using reciprocity.....	53
5.2.2.1 Fixed phi and frequency, change in theta (Moving along the shorter aperture side).....	57
5.2.2.2 Fixed phi and theta, change in frequency (Changing the frequency and changing steps along the shorter aperture side) ...	61
5.2.2.3 Fixed phi and theta, change in frequency (Changing the	

frequency and changing steps along the longer aperture side) ....	64
5.2.2.4 Fixed theta and frequency, change in phi (Moving along the longer aperture side).....	67
5.2.3 Statistics of the reciprocity field data.....	70
5.2.3.1 Summation of reciprocal fields.....	70
5.2.3.2 Accurate uniform sampling of the reciprocal field.....	74
5.2.3.3 Validation of Legendre/uniform sampling for the wire in box .....	78
VI. CONCLUSIONS AND FUTURE WORK.....	84
REFERENCES .....	88
APPENDICES .....	95

## LIST OF FIGURES

Figure	Page
Figure 2.1 Application of the equivalence principle.....	9
Figure 2.2 Electromotive force method to evaluate coupling to a linear dipole.....	12
Figure 3.1 Rectangular box model for EM simulation .....	23
Figure 4.1.a Evaluation of current induced on the dipole at the center of the dipole .....	35
Figure 4.1.b Far field radiated by the source on the center of the dipole. ....	35
Figure 4.2.a Evaluation of current induced on the wire at the test point (end of the wire).....	36
Figure 4.2.b Far field radiated by the source on the Wire (end of the wire).....	36
Figure 4.3 Wire on a ground used to validate reciprocity.....	37
Figure 5.1.1.1 Electric field at monitor points 1' and 2' for normal incidence .....	40
Figure 5.1.1.2 Empty cavity resonances .....	40
Figure 5.1.2.1 Electric field as a function of frequency at point 1' for 16 wire positions .....	42
Figure 5.1.3.1 Current as a function of frequency for 16 wire positions.....	43
Figure 5.1.4.1 Electric field as a function of frequency at point 1' for 16	

wire positions (theta = 90 degrees, phi = 0 degree). .....	44
Figure 5.1.4.2 Electric field as a function of frequency at point 1' for 16	
wire positions (theta = 120 degrees, phi = 0 degree). .....	45
Figure 5.1.4.3 Electric field as a function of frequency at point 1' For 16	
wire positions (theta = 130 degrees, phi = 0 degree). .....	45
Figure 5.1.4.4 Electric field as a function of frequency at point 1' For 16	
wire positions (theta = 120 degrees, phi = 0 degree). .....	46
Figure 5.1.5.1 Electric field versus frequency	
(for aperture size of 15cm x 6cm and 14cm x 6cm). .....	47
Figure 5.1.5.2 Electric field versus frequency	
(for aperture size of 12cm x 6cm and 6cm x 6cm). .....	47
Figure 5.2.1.1.a Cumulative distribution function of the simulated current induced	
to the wire on the ground plane for 150 iterations compared with a	
Rayleigh distribution.....	50
Figure 5.2.1.1.b Cumulative distribution function of the simulated	
current induced to the wire on the ground plane for 400 iterations	
compared with a Rayleigh distribution. ....	50
Figure 5.2.1.1.c Cumulative distribution function of the simulated	
current induced to the wire on the ground plane for 1500 iterations	
compared with a Rayleigh distribution. ....	51
Figure 5.2.1.2.a Cumulative distribution function of the simulated current	
induced to the wire on in the box for 150 iterations	
compared with a Rayleigh distribution. ....	51

Figure 5.2.1.2.b Cumulative distribution function of the simulated current induced to the wire on in the box for 400 iterations compared with a Rayleigh distribution. ....	52
Figure 5.2.1.2.c Cumulative distribution function of the simulated current induced to the wire on in the box for 1500 iterations compared with a Rayleigh distribution. ....	52
Figure 5.2.2.1 Comparison of forward and reciprocal data for the wire on the ground plane .....	54
Figure 5.2.2.1 Comparison of forward and reciprocal data for the wire on the ground plane (for a finer mesh size) .....	56
Figure 5.2.2.1.1 Comparison of forward and reciprocal data for the wire in the box for variation in theta ( $\phi = 90$ degrees, Frequency = 800MHz). ....	57
Figure 5.2.2.1.2 Comparison of forward and reciprocal data for the wire in the box for variation in theta ( $\phi = 90$ degrees, Frequency = 1000MHz). ....	58
Figure 5.2.2.1.3 Comparison of forward and reciprocal data for the wire in the box for variation in theta ( $\phi = 90$ degrees, Frequency = 1500MHz). ....	58
Figure 5.2.2.1.4 Comparison of forward and reciprocal data for the wire in the box for variation in theta ( $\phi = 90$ degrees, Frequency = 2000MHz). ....	59
Figure 5.2.2.1.5 Comparison of forward and reciprocal data for the wire in the box for variation in theta, for a finer mesh size ( $\phi = 90$ degrees,	

Frequency = 2000MHz).....	60
Figure 5.2.2.2.1 Comparison of forward and reciprocal data for the wire in the box for variation in frequency (theta = 45 degrees, phi = 90 degrees).....	61
Figure 5.2.2.2.2 Comparison of forward and reciprocal data for the wire in the box for variation in frequency (theta = 90 degrees, phi = 90 degrees).....	62
Figure 5.2.2.2.3 Comparison of forward and reciprocal data for the wire in the box for variation in frequency (theta = 45 degrees, phi = 90 degrees).....	62
Figure 5.2.2.2.4 Comparison of forward and reciprocal data for the wire in the box for variation in frequency (theta = 45 degrees, phi = 90 degrees).....	63
Figure 5.2.2.2.5 Comparison of forward and reciprocal data for the wire in the box for variation in frequency (theta = 45 degrees, phi = 45 degrees).....	64
Figure 5.2.2.2.6 Comparison of forward and reciprocal data for the wire in the box for variation in frequency (theta = 45 degrees, phi = 180 degrees).....	65
Figure 5.2.2.2.7 Comparison of forward and reciprocal data for the wire in the box for variation in frequency (theta = 45 degrees, phi = 235 degrees).....	65
Figure 5.2.2.2.8 Comparison of forward and reciprocal data for the wire	

in the box for variation in frequency ( $\theta = 45$ degrees, $\phi = 350$ degrees).....	66
Figure 5.2.2.3.1 Comparison of forward and reciprocal data for the wire in the box for variation in $\phi$ ( $\theta = 45$ degrees, Frequency = 800MHz).....	67
Figure 5.2.2.3.2 Comparison of forward and reciprocal data for the wire in the box for variation in $\phi$ ( $\theta = 45$ degrees, Frequency = 1000MHz).....	68
Figure 5.2.2.3.3 Comparison of forward and reciprocal data for the wire in the box for variation in $\phi$ ( $\theta = 45$ degrees, Frequency = 2000MHz).....	68
Figure 5.2.2.3.4 Comparison of forward and reciprocal data for the wire in the box for variation in $\phi$ ( $\theta = 45$ degrees, Frequency = 2500MHz).....	69
Figure 5.2.3.1.1 Sum of far field data taking 5 consecutive values at a time for change of $\theta$ from 0 to 180 degrees in 1 degrees variation, at frequency = 800MHz .....	71
Figure 5.2.3.1.2 Sum of far field data taking 5 consecutive values at a time for change of $\theta$ from 0 to 180 degrees in 1 degrees variation, at frequency = 1000MHz .....	72
Figure 5.2.3.1.3 Sum of far field data taking 10 consecutive values at a time for change of $\theta$ from 0 to 180 degrees in 1 degrees variation, at frequency = 800MHz .....	72

Figure 5.2.3.1.4 Sum of far field data taking 10 consecutive values at a time for change of $\theta$ from 0 to 180 degrees in 1 degrees variation, at frequency = 1000MHz .....	73
Figure 5.2.3.2.1. Cumulative distribution function of the simulated current Induced to the wire on in the box for 150 iterations compared with a Rayleigh distribution. ....	76
Figure 5.2.3.2.2. Cumulative distribution function of the simulated current Induced to the wire on in the box for 400 iterations compared with a Rayleigh distribution.....	76
Figure 5.2.3.2.3. Cumulative distribution function of the simulated current Induced to the wire on in the box for 1500 iterations compared with a Rayleigh distribution.....	77
Figure 5.2.3.3.1. Cumulative distribution function of the simulated current Induced to the wire on in the box for 300 field realizations compared with a Rayleigh distribution. ....	80
Figure 5.2.3.3.2. Cumulative distribution function of the simulated current Induced to the wire on in the box for 1000 field realizations compared with a Rayleigh distribution .....	80
Figure 5.2.3.3.3. Cumulative distribution function of the simulated current Induced to the wire on in the box for 10000 field realizations compared with a Rayleigh distribution .....	81

## CHAPTER I

### INTRODUCTION

The advancement of electronics and wireless communication technologies has been a major cause of increased electromagnetic emissions and radiation to the environment. If not properly controlled, these electromagnetic (EM) radiations from different equipment interfere with nearby equipment which has the same radiation frequency. Metallic enclosures are commonly used to protect sensitive electrical components against these EM radiations and to improve the immunity of the equipment. Frequently, the enclosures contain apertures located on their walls for ventilation and input output purposes. The possible penetration of electromagnetic field through the apertures dramatically deteriorates the shielding properties of the enclosure creating interference to the materials inside. Such materials include wires carrying signals for communication and different purposes throughout the enclosure. The field coupled to the enclosures may induce excessive current on the wires inside the enclosures causing damage to the equipment, such as an electric discharge or ignition. To analyze the level of damage caused by field penetration, various studies have been carried out. Emission tests, susceptibility studies and shielding effectiveness have been studied widely. A susceptibility study involves analyzing the level of exposure by the EM field by evaluating the possible coupling to the

cavity concerned. Among the various ways to evaluate field coupling, analytical methods are the most precise. However applying analytical solutions to solve electromagnetic coupling and emission problems such as by applying Maxwell's equations can be very lengthy and tedious even for a simple structure [1]. Moreover analytical solutions require a geometrically defined structure which is not widely applicable in real environment. Another method of coupling analysis is to apply electromagnetic topology [2]. This refers to making a 3-D model of the incident field using computer code and decomposing complex systems into simple components. However this method is not efficient enough to include all the complexity of internal structures. Even though they take a much longer processing time, numerical methods are more efficient to consider the details of a complex environment. To account for complex geometries, various numerical methods have been implemented. Some of the implemented numerical methods are Finite Element Method (FEM) [3], Finite Difference Time Domain (FDTD) [4], Method of Moments (MoM) [5]-[6] , and Multi-Level Fast Multipole Algorithm (MLFMA) [7]. The choice between these numerical methods is mostly based on memory usage and time taken to compute the coupling solutions. Even though numerical methods are efficient methods in order to discretize a complex environment into grids and solve required parameters more accurately, they take much computational time and memory usage. Moreover, these deterministic approaches mentioned become less applicable for a constantly changing environment. A statistical approach provides a more general solution for field coupling in a complex and constantly varying environment. Among the various statistical methods proposed, reverberation chamber (RC) techniques are widely implemented. Reverberation chambers have been used as source of random waves for field coupling

measurements [8]-[9] and it are also under a continuous research and investigation in order to develop a general characterization of emissions and radiation phenomena[10]-[11]. Mechanical stirring in a reverberation chamber creates a statistically uniform field which couples energy into a cavity with apertures. Various numerical methods have been implemented to model the RC and equipment under test. The finite element technique [12] was used to model a 2D and 3D RC environment. FDTD is also used to model RC by considering the real losses inside the RC environment [13]-[14]. The statistically uniform distribution in a reverberation chamber can be achieved either by mechanical stirring [15] or frequency stirring [16]-[17]. Mechanical stirring involves rotating a metal paddle inside the reverberation chamber stirring the field due to reflections from the paddle and the cavity walls. Frequency stirring implies varying the source frequency disturbing the cavity resonances.

The purpose of this study is to investigate the EM coupling to a simple rectangular cavity which is exposed to a varying environment in order to develop a meaningful statistical study. A preliminary study is performed to observe the effects of variation of random variables on the field coupling to the cavity with and without a wire. A plane wave is used as electromagnetic source and its parameters are varied to represent a varying electromagnetic field environment. To observe the effects of varying parameters of random variables, field and current values are evaluated and examined by varying angle of incidence, polarization, frequency of the plane wave, and aperture size. Commercial software FEKO, which uses the moment method, is used to calculate current on a wire for each plane wave encounter. Even though statistical methods are helpful to give general description of the random variables required such as random current values

induced due to random field encounter, which is the case in this particular work, large number of data is required for a valid statistical investigation to be implemented. If efficient methods of evaluating the required parameters and collection of data are not employed, it limits the ability to efficiently define statistical methods. In this thesis, an effort is made to choose the most efficient simulation method for evaluating and collecting the necessary current data for the statistical approach. The validation, implementation and comparison of three different methods of evaluation of random current values are implemented. The methods basically use the random plane wave model of representation of RC in order to represent a stochastic field environment. The first technique is random plane wave model using evaluation of current for random incidence of plane waves, the second method is implementing the accurate sampling method over the sphere and optimization of the random plane wave model using reciprocity, i.e. using reciprocity to evaluate the current values from the far field evaluation and the third method is evaluation of the current data using the Legendre/uniform sampling method. The comparison of the different methods is discussed in detail. In order to validate the software and the codes for using the reciprocity approach and reduce computational time, comparison of the forward and reciprocal problems is made. MC iterations are performed for each method in order to collect random current evaluations. An effort is made to compare the statistics of the simulated current with the well-known RC statistical model.

The organization of the thesis is as follows: Chapter 2 reviews literatures describing the theoretical and numerical methods used in studying coupling. Chapter 3 discusses the preliminary analysis procedures in order to evaluate coupling to a wire inside an enclosure for changing parameters. Chapter 4 presents the details of different methods

implemented in order to evaluate statistical data efficiently from random values of current coupling. Chapter 5 contains the results validation of the reciprocal method and the comparisons of different statistical methods. Finally, the conclusion of this thesis along with recommendation for future work is presented in chapter 6.

## CHAPTER II

### TECHNIQUES TO EVALUATE EM FIELD COUPLING TO EMPTY AND LOADED ENCLOSURES

#### **2.1. Deterministic coupling methods using MoM**

Most coupling studies involve evaluating coupled quantities to certain equipment in an enclosure or evaluating the SE of the enclosure. The coupling analysis is accomplished by exposing the enclosures or the equipment under test (EUT) with an external field source and measuring the field levels in the enclosures or the current induced at the loads inside the enclosures. This is usually done either by simulation or by making measurements in real field environments or comparing both. These coupling analyses may involve implementation of either deterministic or statistical methods to evaluate the coupling response by the EUT and may require utilization of numerical methods such as MoM, FDTD, and FEM, to solve for the required coupling parameters. The moment method was proposed [22] to estimate electromagnetic coupling to a wire in a rectangular enclosure with a rectangular aperture. This work modifies the previous MoM method which deal with only the normal incidence of plane waves [23] by considering oblique incidence and arbitrary polarization. This method allows the evaluation of fields at any point in the cavity for any arbitrary plane wave incidence. It was also possible to consider various cavity modes. The field evaluation which is used for shielding effectiveness is

done by varying frequency, incidence angle, polarization and the number of apertures. The apertures are represented as thin waveguides and hence the aperture fields are represented by modal expansions. The aperture being assumed very small compared to the walls, is represented using equivalent magnetic currents and the equivalence principle. The internal fields are found using cavity Green's functions and external fields are found using free space Green's functions with the magnetic currents as the radiating source. The external and internal fields are then matched at the aperture to obtain an integro-differential equation to be solved for the unknown magnetic currents using the method of moments. It is shown that the assumption that maximum field coupling happens for normal incidence and at the center of the apertures is not always true for multiple number of apertures. It is suggested that the field interaction from multiple apertures may create a field of maximum magnitude at a location away from the center of the apertures. The advantage of this method is that it allows arbitrary number of apertures on both front and back side of the cavity and is a faster method compared to other numerical methods. However there are some limitations to the method as it is only applicable to rectangular lossless cavities and for small apertures relative to the size of the wall. Moreover, the effects of diffraction of fields at the edges are neglected.

The equivalence principle is also applied to evaluate the coupling to wires through apertures of arbitrary shapes [24]-[25]. Another application of moment method was employed to evaluate coupling through infinite two dimensional screens with wires crossing apertures [26]. Field coupling to an aperture of a two dimensional infinite screen is evaluated with and without a wire crossing the aperture. When a wire is crossing the aperture, the electric distribution at the wires on both sides of the screen is represented by

an equivalent electric current distribution and the aperture is represented by equivalent magnetic current distribution by employing the equivalence principle. Applying boundary condition for the tangential components of magnetic and electric currents at the aperture and wire interfaces produces an integral equation with the unknowns of equivalent magnetic current at the apertures and equivalent current distributions on the wire as shown in figure 2.1 below. This integral equation is then solved by the method of moments. The limitation of this method is that the application of this method becomes more intensive as the structure becomes more complicated.

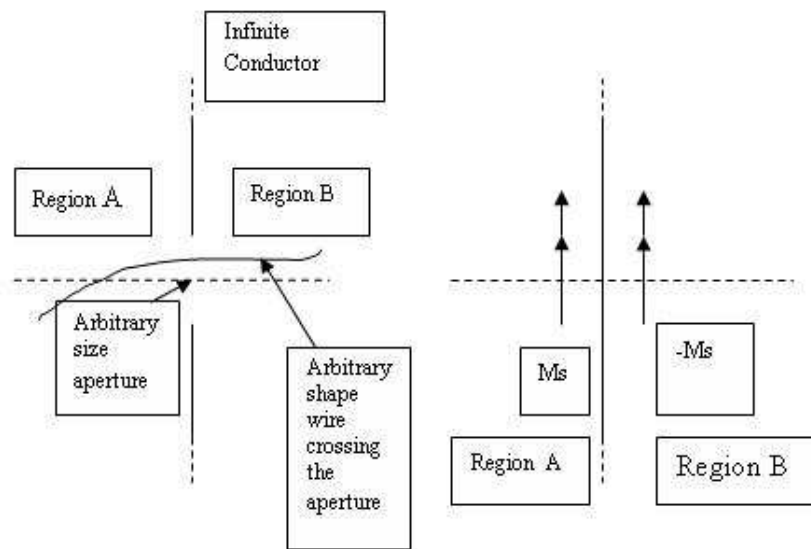


Figure 2.1. Application of the Equivalence principle

A fast multipole moment method (MLFMM) is used [27] to study the coupling behavior for normal incidence of field penetration to a rectangular enclosure. The shielding

effectiveness is evaluated at the center of the cavity for variation of frequency. It is observed that the cavity resonance is disturbed near the frequency value which matches the slot resonance. Changing the rectangular slot size to other different values demonstrated similar observations by introducing deterioration of the shielding effectiveness near their respective slot resonances. It is also shown that as the slot resonance frequency is increased by changing the slot size; the disturbance to the cavity resonances disappears. It is shown that even narrow slots on enclosures can affect the coupling to the cavity due to cavity-slot interactions. A further observation is made by introducing a wire in the slotted cavity. Additional peaks are observed which indicate a remarkable interference at lower frequencies where the wire exhibits its resonances. According to this work, it is concluded that the coupling of fields to a slotted enclosure can highly be affected by slot, cavity and wire resonances, especially at lower frequencies where the cavity resonance is not dominant. The limitation of this work is that it is only applicable for coupling evaluation only at the center of the cavity and for normal incidence field penetration.

## **2.2. Analytical coupling method**

Hill [28] presented an analytical method to evaluate coupling to a coaxial air line placed in a cavity. To evaluate the SE of the cavity, polarizability theory was used to evaluate the ratio of the average power received by a reference antenna and the coaxial line. Moreover, an effort was made to compare the results with a reverberation chamber environment by evaluating the coupling over incidence angle and polarization. In his other analytical work Hill [29] proposed a method to evaluate field excitation to an electrically large cavity with apertures and loading. This improved the SE evaluation by

using an electrically large environment where the dimension of the equipment is small compared to the wavelength. In Hill's work, field excitation in an electrically large cavity with apertures and loading is presented. Additionally, a detailed analysis for loss mechanisms due to loading, wall loss, aperture leakage and antenna power loss is studied. By matching power coming in through the apertures and power dissipated due to wall loss, leakage through the cavity and antenna power loss, an equation for the shielding effectiveness is derived in terms of the cavity quality factor. The expression obtained for the quality factor (Q) for each corresponding loss mechanisms is used together with power balance theory to evaluate shielding effectiveness of the cavity. The theoretical study is then followed by a validation. Even though this work can give a simplified solution of field excitation with loss analysis, it is limited to only cavities with circular apertures. On the other hand, more than 15 dB difference is observed between theoretical and experimental comparisons. This difference shows that a further effort should be made to accommodate cavity losses in the theoretical analysis. Hill suggested that difficulty associated with the evaluation of the typical materials makes it difficult to obtain an accurate solution. A lot of power compensation mechanisms were needed in the cavity to get good comparison between theory and measurement. The other drawback with this technique is that it is not valid for long, narrow apertures, which have strong resonances.

### **2.3. Statistical coupling method using MODAL/MoM**

Modal/MoM method [3] was employed to perform the simulation in order to determine the coupling statistically. In order to implement the well-known reverberation chamber statistics, the field inside the cavity is disturbed using frequency stirring. The source frequency was varied to include the higher-order cavity modes to create an electrically

large environment which gives statistics similar to a mechanically stirred reverberation chamber. The statistics for the shielding effectiveness at various locations was evaluated based on probability plots. The result was compared with similar procedure to that implemented using finite element method [30]. The uniformity of the shielding effectiveness at various points is checked as a uniform field distribution is expected for a well stirred field environment. The Modal/MoM method was able to provide the average shielding effectiveness in the cavity at various points. However, its limitation is that the analysis is made by taking only one component of the field and normal incidence. Moreover, inclusion of the total field and arbitrary incidence and polarization may increase the computational overhead.

Coupling to a linear dipole in a reverberation chamber was analyzed [31] based on the spatial correlation function of the incident field and the induced electromotive force method.

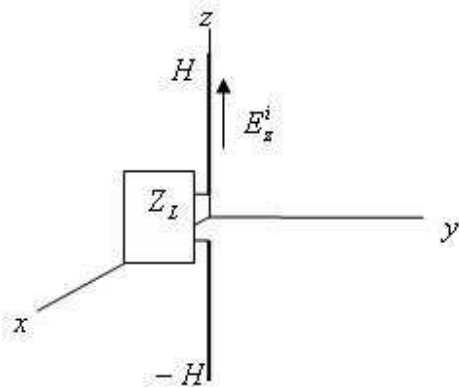


Figure 2.2. Electromotive force method to evaluate coupling to a linear dipole

The open circuit voltage is evaluated using the induced EMF method, which uses reciprocity to evaluate the voltage induced from the current. The experiment setup for this work is shown in figure 2.2 above. The voltage is expressed in terms of the incident electric field and the current on the dipole. The received power is then expressed in terms of the random voltage. The average power is expressed in terms of the derived spatial correlation function yielding the common power received by a general antenna inside a reverberant environment. This analysis gives an advantage in that it can be done analytically without the need of numerical methods.

#### **2.4. Numerical and Experimental methods to determine coupling in an overmoded enclosure**

Numerical and experimental methods have been proposed [4] to evaluate field coupling to a wire loop placed in an electrically large enclosure. The numerical computation uses FDTD numerical method which uses plane waves as a source of the incident field to a rectangular enclosure. Both reverberation chambers and anechoic chambers (AC) are simulated. Random plane waves are used for representing the RC and plane waves of certain variations are used to represent fields in the AC. The current induced on the wire loop in a small enclosure placed both in RC and AC is simulated. An experiment is made by measuring an average current coupled to the loop in a real RC and AC. A mechanical stirrer in an RC is rotated to generate random field environment. The field at any position is measured using a three dimensional probe. The average current on the loop is also measured. The analytical and experimental current values are compared showing a good agreement. It is suggested that this result can be used for cavity design with less field penetration. The comparison between analytical and experimental methods shows a good

agreement. Statistical analysis can be done on the data presented to give a field susceptibility probability reference. The author of this paper explains how RC is useful over AC as the former can reveal every direction of field exposure and the latter can have a probability of missing a field coupling that can be very critical. However, this work doesn't consider the field situations near the cavity walls which can affect the coupling if the loop is placed close to the walls.

### **2.5. Semi-analytic method to determine coupling in an overmoded enclosure**

In another coupling study [32], an effort is made to consider the field evaluation at the cavity walls, proposing a semi analytic procedure to evaluate coupling to a wire in an overmoded enclosure. An effort is made to accommodate for coupling evaluation near the cavity walls. This method implements transmission line theory to evaluate the coupling in relation to the mean coupling cross section at one end of the wire. The coupling cross section is expressed in terms of the mean power induced at the end of the wire. To accommodate the coupling at any position in the cavity, the position and length of the wire are introduced as variables in the analysis. The field environment is represented by superposition of random plane waves whose statistical properties are derived from reverberation chamber theory and are input to the transmission line model through correlation functions. The coupling solution for locations near the cavity walls is included by deriving the correlation functions in terms of the distance of the wire from the cavity walls. This work gives a better computational time compared to Monte Carlo simulation by avoiding computation of induced current for every plane wave incidence. It also gives a better coupling solution by accommodating locations near the cavity walls. The result shows different values for distances close to and far from the cavity walls. The result for

far from the cavity walls corresponds to previous results obtained from Monte Carlo technique. However since loss is not considered in the simulation small resonances could not be shown which were shown in the measurement. Comparison is made with the Monte Carlo approach for a wire at 3 cm and 9 cm from the walls, since normal statistics or correlation functions are made for farther distances the one with 9 cm gave the same result with that of Monte Carlo approach.

## **2.6. Statistical and experimental methods to determine coupling into physically small and electrically large enclosures**

Holloway [33] evaluated the SE of physically small but electrically large cavities by conducting an experiment in a reverberation chamber where a small enclosure is placed inside a large reverberation chamber which is excited by the method of frequency stirring. A small wall mounted monopole probe is used to measure the power level in the cavity. The monopole was chosen in order to minimize the field disturbance in the enclosure. The monopole must be rotated to different positions to measure the power levels so that it can be compared with a reference measurement to calculate the shielding effectiveness. The SE of the small cavity is evaluated in four different reverberation chamber configurations. It is shown that the SE of the small enclosure is similar in the four cases. Even though the analysis given by this work indicated that the SE is independent of the monopole position, it was also restrictive of the probe from being in the corners. Using the monopole has its own disadvantage as it requires dealing with large reflections. Moreover, the compensation done by adding antenna mismatch correction factors in the calculations introduces additional work. Even though the measurements give good agreement with theoretical, measuring with a monopole

mounted on the wall may miss the statistics of the central cavity since the measurement near the walls may be affected by boundary problems. This work [33] avoided the need for a paddle stirrer which otherwise will be impossible to insert into small enclosures by using a frequency stirring technique. However implementing frequency stirring has its own drawbacks at lower frequencies. One of the drawbacks is that the field measurement is strongly dependent on the probe position if frequency stirring is used at lower frequencies.

In order to accommodate the field coupling of the center of physically small electrically large enclosures, Wang [34] describes a method of measuring field coupling at the center of a rectangular cavity using a measuring probe which moves along the center of the enclosure instead of mounting the probe at the walls. This is to accommodate the common assumption that the center of the cavity is more susceptible to maximum value of field coupling resulting in less shielding effectiveness, hence requiring more attention. In the effort to evaluate the shielding effectiveness of small dimension enclosures, the field coupled to a small enclosure is evaluated using simulation and experiment. Instead of evaluating the field at single point for different stirrer positions, the field is evaluated at different locations by using a moving probe along a chosen position inside the cavity. The enclosure is simulated with FEKO simulation software and the sampling positions are chosen along the center axis as it is expected that maximum coupling occurs at the centers rather than the edges. Random plane waves are used as random sources coming from all directions and with random polarizations. Mode stirring is used by using plane wave superposition representation of various cavity mode configurations. This method

avoids the difficulty in inserting a paddle stirrer in small enclosures and also avoids issues related to frequency stirring.

## **2.7. Statistical coupling method to determine below-deck environment**

Among the efforts done to characterize complex environments statistically is [35] which is an effort to characterize an electromagnetic environment of below deck spaces in ships. The statistics for the reverberation chamber environment are used to find the maximum field values. Because of the inconvenience to place a mechanical stirrer in the below-deck environment, frequency stirring is used. The statistics for the power received by an antenna in the space appeared to have a chi square distribution which helps to demonstrate the environment as reverberant and uniform. The insertion loss between transmit and received antennas placed in the space is used as a parameter for the statistics. The insertion loss is measured at 12 different locations by rotating the receiver antenna at 12 different positions. The experiment is conducted in two different environments, a large ordnance magazine and a small pyrotechnics storage room. The measured max to mean and standard deviation of the mean normalized power are compared with the theoretical values for 12 independent samples and a good agreement is found. Similarly for frequency stirring around 2.4GHz for 20% bandwidth, 134 independent samples are evaluated using autocorrelation analysis. The measured max to mean ratio is compared with theoretical expected value. K-S test on the frequency stirred power data is done and compared with theoretical CDF of chi square data and showed good agreement. The maximum power is evaluated from the mean power and the max to mean ratio of the measured data.

## **2.8. Statistical coupling methods using random plane wave approach**

One of the well-known representations of a stochastic field environment, which leads to statistical investigations, is the random plane wave approach, i.e. representing the field environment as superposition of plane waves. Hill [18] presented a plane wave integral representation to model a reverberation chamber environment. In this approach, the field at a point is represented as superposition of plane waves over all incidence angles and polarizations. The statistics for the fields are introduced by allocating a random variable for the angular spectrum of the plane waves. Each field represented by superposition of plane waves satisfies Maxwell's equations. This method of plane wave representation of fields is suitable for evaluation of test object responses which is important for immunity test implementation of RC analysis. The analysis made to evaluate the test object responses also shows that the power received by the test objects is due to all plane waves over all incidence angles and polarizations.

In another approach, the statistics for the current coupling is analyzed using Monte Carlo (MC) simulation [19]. This approach is based on Hill's plane wave integration method to represent a field at a point. The value of the current at one position is evaluated by adding all the current induced due to each finite number of plane waves coming from random directions. The current for each plane wave interaction should be calculated using one of the deterministic methods. The randomness of the plane waves is introduced by taking the angle of incidence, polarization, and phase of the plane waves randomly from their respective distributions. MC simulation approximates the plane wave integral representation by Hill with a finite number of plane waves. For a well stirred uniform field, the fields causing a current flow in the wire will have a random propagation

direction and polarization and can radiate from any direction with in a sphere with the same probability. Therefore, the uniform distribution is chosen to describe random values for these field parameters. A uniform distribution is also chosen for the phase due to multiple scattering of waves inside the RC environment. A random number generator is used to obtain the random values from the respective ranges and these values were used to calculate the current coupled due to each plane wave attack with the corresponding random parameters. According to a MC approach the mean value of current induced is obtained as superposition of current values for each plane wave encounter. In order to minimize the number of computations for the plane wave superposition methods, the reciprocity theorem has been used [20]-[21]. According to this theorem, the current induced on a material due to an incident wave can be computed from a far field radiation by putting the same source at the point of susceptibility.

## **2.9. Random plane wave approach using FDTD**

The superposition of plane wave technique with FDTD simulation is used to evaluate coupling to a loaded transmission line and field coupling to an empty cavity [4]. Instead of simulating the whole chamber, EUT and the paddle stirrer, a EUT with the specification of its separation field region is specified. The RC environment is represented by superposition of incident plane waves. N plane waves are chosen to excite the EUT by running M times, to represent M different random field distributions. N of 100 plane waves and M of 200 simulations times are chosen compromising the number of computations and accuracy of results. The incidence angles are generated in order to get uniform sampling both in the azimuth and elevation directions. The incidence angles are generated using an algorithm which enables sampling the angles and avoiding the

thickening of the points at the poles. Polarization angles are evaluated with a uniform distribution from  $[0, 2\pi]$  and the field magnitude is chosen to be one. The points at the separation plane, chosen according to the uniform sampling method, which separates the total field and the scattered field region, are used by the FDTD simulation to calculate the fields coupled to the environment. The current coupled to a transmission line is evaluated and compared with the experimental results giving a good result. Even though this method gives a susceptibility analysis method with less computational time and processing overhead, it does not indicate an efficient way to determine the number of plane waves needed for the simulation. This method is extended and used to compute the field penetration into a cavity with a large aperture, whose opening is protected by wire-mesh screen [36] and to determine the shielding properties of a coaxial cable [37].

#### **2.10. Determination of correlation of the random variables**

One of the characterization methods of fields which describe the spatial properties of fields in a reverberant environment is field spatial correlation [38]. In a reverberation chamber simulation, the spatial correlations are used to predict the response of fields in the environment simulated. In this simulation, different field configurations are created for each variation of stirrer position which is represented by different superposition plane waves each time for each stirrer position. According to this result, the spatial correlation decays for a larger separation between field points in an oscillating manner which also indicates that the correlation between corresponding fields decreases as the separation between them increases. The most common measurement of independence is the autocorrelation function. The statistical theories for RC environment are built assuming independence between the values of field values evaluated at a particular position for

different boundary conditions. For an independent field distribution, the autocorrelation function yields a small value. However, the reverse is absolutely true only for normally distributed data values. Even though it is not absolutely true for all data, a small value of autocorrelation suggests independence. Field correlation between random fields in a complex environment is derived using the modal sum representation of fields [39] as well as for plane wave representation of fields [40] Hill derived the spatial correlation function for the complex electric or magnetic fields, and also for the total field of both electric and magnetic fields. In this work, the spatial correlation function is also derived for the complex electric and magnetic fields, for the squared magnitudes, for the components of the electric and magnetic energy densities and for the total energy. Moreover, it is derived for the mixed electric and magnetic components and it has been shown that most of the electrical and magnetic field components are uncorrelated when evaluated at different positions except the transverse components of E and H which are correlated for fields evaluated at different locations. All the correlation functions for all cases are equal to 1 for a zero separation between field points and decays in oscillatory manner as the separation distance increases. However, when evaluated at the same location, all electric and magnetic field components are uncorrelated. In order to account for fields near the RC walls, a plane wave integral representation is used to evaluate the statistics of field near the cavity walls [41]. The field near the walls and corners is evaluated using the spatial correlation functions. The results show that the field gets statistically uniform as the location gets farther from the chamber walls.

## CHAPTER III

### BASIC CONFIGURATION AND PRELIMINARY ASSESSMENT OF FIELD PENETRATION IMPACTS

#### **3.1 Impacts of varying parameters on the field and current coupling**

Metallic enclosures are commonly used in shielding practice to mitigate unwanted emissions and improve the immunity of sensitive equipment against external electromagnetic fields. Frequently, the enclosure contains apertures located on its walls for input and output connections, control panels, visual-access windows, and ventilation panels. The possible penetration of electromagnetic fields through the apertures dramatically deteriorates the shielding properties of the enclosure creating interference or damage to equipments inside cavities, such as wires carrying signals through military equipments subsystems. An electric voltage/current carried by these wires inside the equipments may cause an electric discharge causing ignition. The excessive voltage/current can be caused due to a voltage surge in the electric system or external electromagnetic field coupled to these wires. In real life scenarios the electromagnetic environment both inside and outside is constantly changing. Therefore it is not possible to

foresee all possible scenarios in which a particular system will be placed.

The purpose of this thesis is to perform a preliminary analysis to evaluate the field coupling into a cavity due to an incident plane wave with varying angles of incidence angle and polarization. Also, to represent the uncertainty of the details of the cavity geometry and loading such as cable bundles, the coupling is computed for a wire at different positions. An observation is made on how the current induced on the wire is varied for different sizes of the aperture and for different coupling positions with respect to the incident field. In this preliminary assessment, FEKO is used as a simulation tool. Using MATLAB, the data is manipulated to make it easily accessible for model fidelity analysis. Based on the data found by varying the random variables, our goal is to observe the behavior of the random variables and also to identify the dominant random variable that causes the most variation. In this study an efficient method of collecting the necessary field and current data is done. A coupling analysis is done with the interest of evaluating the field and current coupled to a wire inside the cavity and the field disturbance/ sensitivity/ due to the presence of the wire, change in position of the wire, change in aperture size and change in incidence angle and frequency of operation of the incident plane wave. Based on the field and current computation results an observation is made.

### **3.2 Simulation of the structure used in the study**

To analyze the field and current coupling values, computational modeling was performed for a simplified metal box with dimensions of 30 cm x 12 cm x 30 cm with a wire inside the cavity and rectangular aperture of size 15 cm x 6 cm. A wire of length

10.4 cm is inserted fixed at the cavity floor. The origin is at the center of the aperture. The magnitude of field values at the two positions 1' and 2' and current values induced at the end of the wire while it is placed at the 16 different positions are evaluated. Since the current induced at the wire is expected to produce a field in the cavity which perturbs the original field in the cavity, an effort is made to compare the field without the wire and with the wire placed in the cavity. The model used for this simulation is shown in Figure 3.1 below. The exact location of the 16 points and 1' and 2' is shown in appendix A.

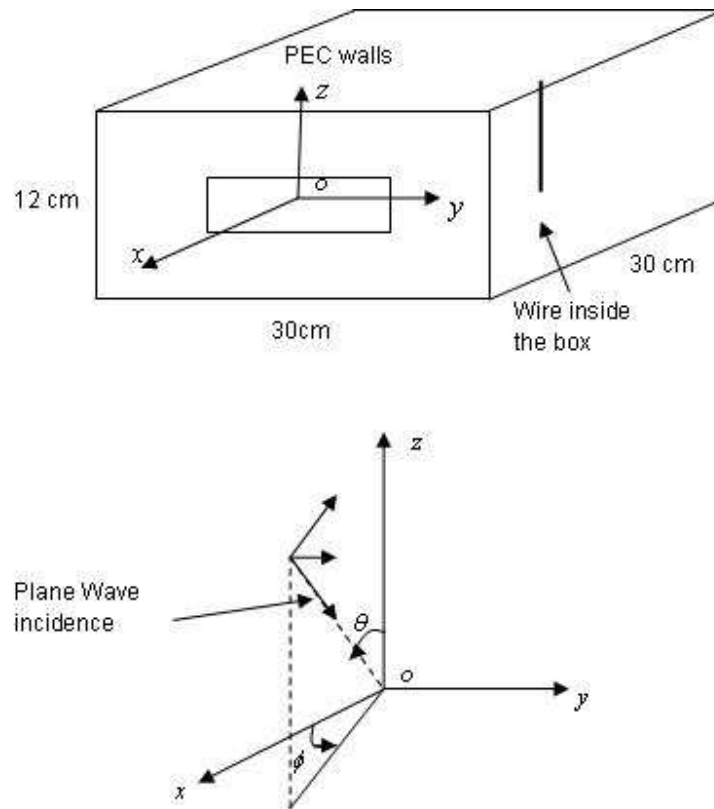


Figure 3.1. Rectangular box model and coordinate system for the EM simulation.

### 3.2.1 Simulation steps

In the structure shown in Figure 3.1 above,  $\theta$  is the elevation angle, theta, directed from the vertical  $z$  direction to the horizontal plane and  $\phi$  is the azimuth angle, phi, which represents rotation around the vertical  $z$  axis.

a. A y-polarized electric field is applied at normal incidence angle with respect to the front face of the cavity. The frequency is swept in 10 MHz steps from 300 MHz to 2000 MHz. The field is evaluated at the two defined field monitor points 1' and 2'.

b. A wire of diameter 0.082 cm and length 10.5 cm is introduced into the cavity and the fields for all field monitor positions is calculated by placing the wire at the defined 16 positions. The current at the end segment of the wire at each position of the wire is evaluated.

c. The incidence angle is varied from 0 to 180 in 5 degrees steps with respect to x and y axes; following the steps a & b, the fields and currents are calculated.

d. The aperture size on the front face of the cavity is changed from 15x6 cm to 15x1 cm; following the steps a, b and c, the fields and currents are calculated.

The result for change of each parameter will be shown and is discussed in the results and discussion section of this thesis. Even though examining the effects of change of random variables give better understanding of each variable individually, it is difficult to implement all the possible variations for a complex and constantly varying environment.

This problem leads to the need for statistical analysis which is presented in the next section. The geometry shown in Figure 3.1 is used for all simulations unless specified.

## CHAPTER IV

### STATISTICAL ANALYSIS

#### 4.1. The need for statistical analysis

The current induced in equipment inside a cavity with varying field interaction is better predicted statistically. The average and maximum values can be determined for placing equipment maintaining safety and protection. In order to obtain the average and maximum value of current, an appropriate statistical model should be chosen. For an overmoded cavity, in which the wavelength is small compared to the cavity dimensions  $a, b, c$ , the electromagnetic environment can be represented statistically. The number of modes is approximated by  $N = \frac{abc}{\lambda^2}$ , where  $\lambda$  is the wavelength [42].

The usual way of measuring coupling of external field into a cavity involves measuring the power level using probes. Since the field inside a high Q cavity demonstrates resonance, the coupling level varies significantly according to the position inside the cavity. Therefore the average coupling power should be found by taking measurements at different positions and calculating the average. However, moving the probe in the cavity may perturb the field. Moreover, this method can evaluate only the average power coupled and not the maximum value, which is sometimes the main parameter

needed to evaluate an electromagnetic susceptibility. Therefore a better way is to prove the uniformity of the environment and to evaluate the field at only one point representing the whole environment. Reverberation chamber is the well-known statistically uniform field environment.

#### **4.2. RC probability distribution model for current induced on a wire**

The coupling in an overmoded cavity can be modeled by placing the equipment under test either in an anechoic chamber or reverberation chamber to create a varying field interaction. To get a complex cavity in anechoic chamber, the plane wave must be incident at varying incidence angles. However it requires much effort to obtain a statistically distributed environment as it is difficult to vary the plane waves at every possible direction. On the other hand, a reverberation chamber provides statistically uniform field with random incidence angle, polarization and phase. The statistical uniformity of the field is achieved either using mechanical stirring or frequency stirring. To stir the field mechanically, a metal paddle is rotated inside the RC environment and the field being reflected from the paddle and the RC walls creates a statistically uniform field environment. Frequency stirring is accomplished by changing the source frequency which results in a disturbance to cavity modes creating a statistically uniform field environment. This statistically uniform environment in a RC can be used as a source of well-stirred field providing an appropriate variation of incident field for statistical analysis for coupling studies and immunity purposes. Moreover, the statistics of the RC environment is well studied and can be easily implemented.

When energy is input to a RC cavity, it will be reflected from the walls and resonance will be created. Therefore the field at a point is the sum of all the contributions of the

modes inside the chamber. Therefore the field in the chamber can be considered as a random variable which depends on the angular position of the paddle stirrer in the mechanically stirred chamber. The variation of the paddle stirrer position is represented in different ways to devise a computationally efficient method. The field at a point is represented by its real and imaginary components giving two field components at each of the three orthogonal directions for a total of six components. The six parameters are in-phase and quadrature components in each of three orthogonal directions. The large number of reflected waves from the RC walls and stirrer results a normal distribution for the field components according to the central limit theorem. If the direct path coupling between a transmit and receive antennas is small, the mean of the distribution can be assumed to be zero. The magnitude of the resultant is then the square root of the sum of the squares of six identically distributed, zero mean, normal random variables and is, therefore, chi distributed with six degrees of freedom. However, most field dependent measurements in a mode stirred RCs only respond to one dimension of the field. For example, when the antennas used are linearly polarized, when a one dimensional E-probe is used, and when the current induced to one dimensional wire is evaluated. In such cases, the magnitude of the received voltage (or current) is proportional to just one dimension of the field. Each dimension of the field has in-phase and quadrature components and is therefore chi distributed with two degrees of freedom, which is the same as a Rayleigh distribution. The chamber power is proportional to the square of the field, and is, therefore, a chi-squared or exponentially distributed.

Even though various techniques have been proposed to model RCs [7]-[9], it is difficult to model the RC itself using numerical methods. As RC is electrically very large,

modeling it may require an intensive computational time and memory usage. Therefore different methods have been suggested to model RC environment with less computational overhead. Most of these methods deploy a technique to represent the RC environment without modeling the RC itself but the source and the EUT.

In this present work, the statistics for coupled quantities is implemented based on plane wave integral representation originally proposed by Hill [18]. According to this method, the electric field at a point of the space  $\vec{r}$  can be represented as an integral over the solid angle of the plane wave spectrum:

$$\vec{E}(\vec{r}) = \iint_{4\pi} \vec{F}(\Omega) \exp(j\vec{k}\vec{r}) d\Omega \quad (4.1)$$

Where  $\vec{F}(\Omega)$  is the angular plane wave spectrum,  $\vec{r}$  is the position vector,  $\vec{k}$  is the vector wave number,  $d\Omega$  is the differential solid angle and is given by  $d\Omega = \sin\theta d\theta d\varphi$ .

The angular spectrum is represented as:

$$\vec{F}(\Omega) = \vec{a}_\alpha F_\alpha(\Omega) + \vec{a}_\beta F_\beta(\Omega) \quad (4.2)$$

Where  $\vec{a}_\alpha$  and  $\vec{a}_\beta$  are mutually orthogonal unit vectors and are also orthogonal to  $\vec{k}$ .

The complex amplitudes,  $F_\alpha$  and  $F_\beta$  are statistically independent.

The statistical properties of the field are introduced through the random angular spectrum. Based on the statistics chosen for the angular spectrum, the statistics for the field components and magnitude, as well as the power received by a receiver is determined. The statistics for the mean and squared mean values are found to follow Rayleigh and exponential distributions respectively. This plane wave integral

representation is reformulated in discrete form [19] representing the field in the complex environment as superposition of finite number of plane waves:

$$\bar{E}(\vec{r}) = \sum_{n=1}^n E_i \exp(j\vec{k}_i \cdot \vec{r}) \quad (4.3)$$

According to [11] the statistics for the components of the field, which is represented by a discrete number of plane waves, can be derived. The mean and variance of the components are found to be:

$$\text{mean}(\text{Re}\{E_{z,i}\}) = \text{mean}(J_m\{E_{z,i}\}) = 0 \quad (4.4)$$

$$\text{var}(\text{Re}\{E_{z,i}\}) = \text{var}(J_m\{E_{z,i}\}) = \frac{E_o^2}{6} \quad (4.5)$$

Where,  $E_o$  is the magnitude of the field.

For large number of plane waves taken, the real and imaginary components of field will have a Normal distribution, according to the Central Limit Theorem. The mean and variance of the distribution will have values of zero and  $\frac{nE_o^2}{6}$  respectively.

$$N\left[\mu=0, \sigma^2 = \frac{nE_o^2}{6}\right] \quad (4.6)$$

The statistics obtained for amplitudes and amplitude squared of field components and total field are found to be similar to that obtained for integral representation mentioned earlier [10]. This shows that this method can be a representation of field inside a RC. The current coupled to equipment inside the RC environment is represented as the sum of all currents induced due to each finite plane wave set:

$$I = \sum_{i=1}^n I_i , \quad (4.7)$$

where  $n$  is the number of plane waves and  $I_i$  is the current induced due to the  $I^{th}$  random plane wave. The statistical distribution of the magnitude and squared magnitude of the current is found to be Rayleigh and exponential respectively. An effort to determine the number of plane waves required to represent a reverberant environment has been done by different previous studies. Monte Carlo trials are used [11] to determine the number of plane waves required to achieve the required statistical behavior of the environment. However the implementation of this method also varies based on computational time and memory usage, depending on the number of computations required. Therefore different methods have been suggested to reduce the number of computation requirement by determining the optimal number of plane waves needed to get the required statistics [44]. Using reciprocity is also another method to reduce the computation required, as calculation of field in one run is required instead of calculating the coupling for different plane wave incidence. After defining the number of plane waves requires which can properly give the required statistics, the evaluation of coupling can be done using different numerical methods. In this particular study, the current is induced using commercial software FEKO and the data obtained is processed using MATLAB. This particular work involves the Monte Carlo (MC) iterative methods of coupling and using reciprocity to evaluate the statistics of current coupling to a wire on a ground plane and the wire in a box and compare the results.

### 4.3 Monte Carlo (MC) simulation

MC simulation has been widely implemented to represent a mechanically stirred reverberant environment. For every stirrer position, there is a distinct plane wave pattern, which is the superposition of some number of plane waves ( $N$ ). The pattern changes for a different stirrer position. MC iterative method is used to identify the number of plane waves that can be enough to represent a well-stirred RC environment, which can give the appropriate statistics. As the number of plane waves for each stirrer position ( $N$ ) and the number of stirrer positions considered ( $M$ ) increases, better statistics are obtained for a well stirred uniform, complex RC like environment. Hence, the total number of plane wave coupling computations required for the full stirrer rotation will be ( $N \times M$ ). The number of plane waves needed to properly represent a well-stirred RC like environment is chosen using MC trials. Even though the statistics get better as the number of plane waves increases, as few as 20 plane waves have been used [11]. In this thesis 20 plane waves are considered and the plane wave parameters are taken from a uniform distribution based on the following considerations.

For a well-stirred uniform field reverberation chamber like environment, the fields will have random propagation direction and polarization and radiate from any direction over the sphere with the same probability. Thus a uniform distribution is an appropriate choice to get random values for these field parameters. A uniform distribution is also chosen for the phase due to multiple scattering of waves inside the RC environment. Therefore, the azimuth and elevation angles of the plane waves are taken from uniform distribution over the solid angle, the polarization and phase angles are also taken from a uniform distribution with an interval  $[0, 2\pi]$ , a magnitude of 1 is chosen for the plane wave. A

random number generator is used to get the random values from the respective ranges and the values becomes an input to FEKO to calculate the current coupled due to each plane wave attack with the corresponding random parameters. The current coupling due to waves coming from different directions for one stirrer position are represented by the value of current produced when the 20 plane waves hit the wire at a time for one particular combination of parameters. This process is repeated (M) times representing the number of rotations of the mechanical stirrer. MC simulation can be done with different numerical methods and software to calculate the coupling and processing the data for each plane wave attack. In this work the current coupling calculation is computed using FEKO and the data is processed using a program written using MATLAB.

The FEKO processing of calculation of the statistical current values for the repeated times using plane waves with random parameters is shown in Appendix B.

#### **4.4 Evaluation of susceptibility based on emissions (Reciprocity)**

According to the simple definition of reciprocity, the same field value due to a source at a particular position will be created if the position of the source and the field evaluation point are interchanged. Therefore reciprocity involves both emission and susceptibility considerations. For the emission case hereafter called the (reciprocal problem), a source will be radiating from the given EUT and during the susceptibility case (forward problem), the EUT is attacked by an external source. It is found that there is a direct relation between the two problems. Applying this theory to the coupling problem reduces the number of computations needed for evaluating the current coupled for each plane wave incidence.

Instead of calculating the current coupling to different plane waves, a far field evaluation will be accomplished once at the respective field sampling points. The reciprocal model for representation of the RC environment is derived [44] by considering the forward and reciprocal problems. For the forward problem the coupling value on the EUT is evaluated for multiple plane wave incidences and for the reciprocal problem the far field is evaluated for a radiating source on the EUT. The derivation of implementing this reciprocity problem is performed using dipoles incident to the EUT from different angles and a dipole radiating to different directions for the forward and the reciprocal problems respectively. For the forward case, a dipole with dipole moment of

$$I_d^f l = \vec{a}_p \frac{4\pi r}{jk\eta} \exp(jkr) \quad (4.8)$$

is used, where  $I_d$  is a dipole current and  $l$  is the vector length of the dipole,  $k$  is the wave vector and  $\vec{a}_p$  is the wave vector that represents the polarization of the field incident. Thus, the current on the dipole will be

$$I_d^f = \frac{4\pi r}{jk\eta} \exp(jkr) \quad (4.9)$$

When this dipole is radiated, a current of  $I_t^f$  will be created at the test point on the EUT. The superscript  $f$  and  $r$  represents a forward and a reverse case respectively, while the subscripts  $d$  and  $t$  represents a dipole and EUT test point respectively.  $V_t^r$

To perform the reciprocal problem, the EUT will have a source of voltage,  $V_t^r$  which gives a field of  $E_d^r$  at the dipole. This radiation induces a voltage of  $V_d^r = E_d^r \cdot l$  hence a

current of  $I_d^r = \frac{V_d^r}{R_d}$ , where  $R_d$  is the dipole resistance. According to the reciprocity relationship,

$$V_d^f I_d^r = I_t^f V_t^r . \quad (4.10)$$

Substituting the values in the current equation above,

$$I_t^f = \frac{4\pi r}{jkl} 1/V_t^r E_d^r l = \frac{4\pi r}{jk} 1/V_t^r E_d^r \vec{a}_p \quad (4.11)$$

From this, it is deduced that the radiation from a plane wave of an electric field of magnitude 1V/m toward a EUT can be replaced by a reciprocal problem, placing a

voltage of  $V_t^r = \frac{4\pi r}{jk\eta}$  at the test point on the EUT and evaluating the radiating field

at the specified directions with the given polarization thus evaluating  $E_d^r \vec{a}_p$ . Therefore it

is shown that the voltage induced on the EUT during the susceptibility (forward) problem

is proportional to the transmitted far field obtained when the EUT is radiating during the

emission (reciprocal) problem with proportionality constant of  $\frac{4\pi r}{k\eta}$  which gives a

value of  $1.5 \times 10^{-3}$  for free space. The value of  $r$  in the equation indicates a large distance

representing a far field point and it is usually included in the computational methods, the

FEKO software in this case, and this fact is interpreted in this simulation work by giving

a value of 1 for  $r$ . In the work to follow, an effort is made to validate a method of using

reciprocity using a wire of length 10.4 cm on a ground plane, as shown in figures 4.2.a-b.

Moreover the validation of reciprocity continued on the 30cm x 12cm x 30cm box with

15cm x 6 cm aperture, when the wire is placed at position 7 which is indicated on APPENDIX A.

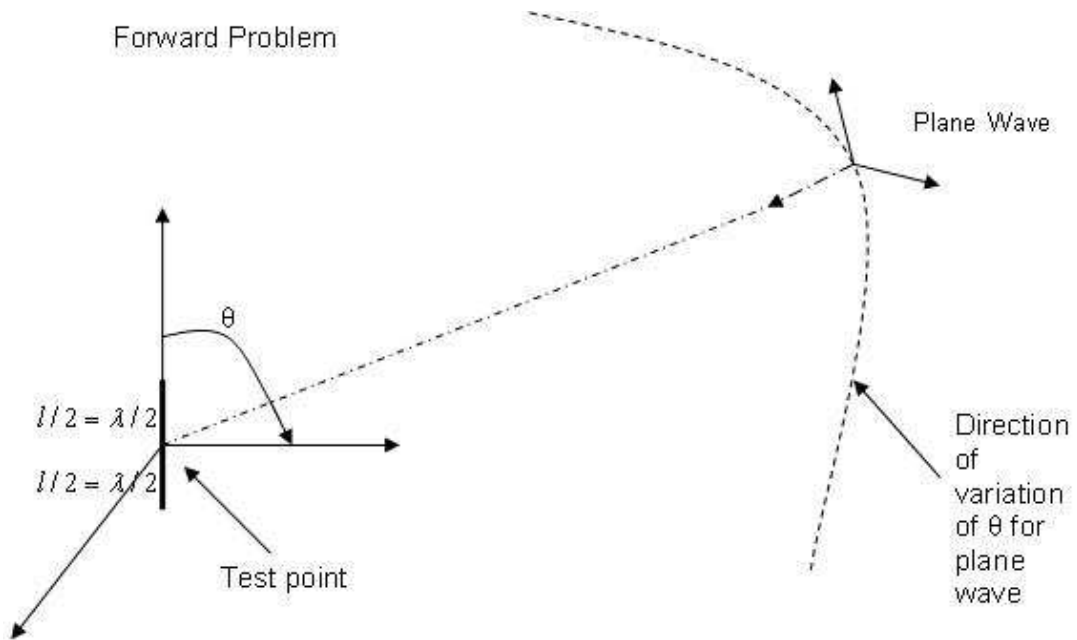


Figure 4.1.a. Evaluation of current induced on the dipole at the center of the dipole.

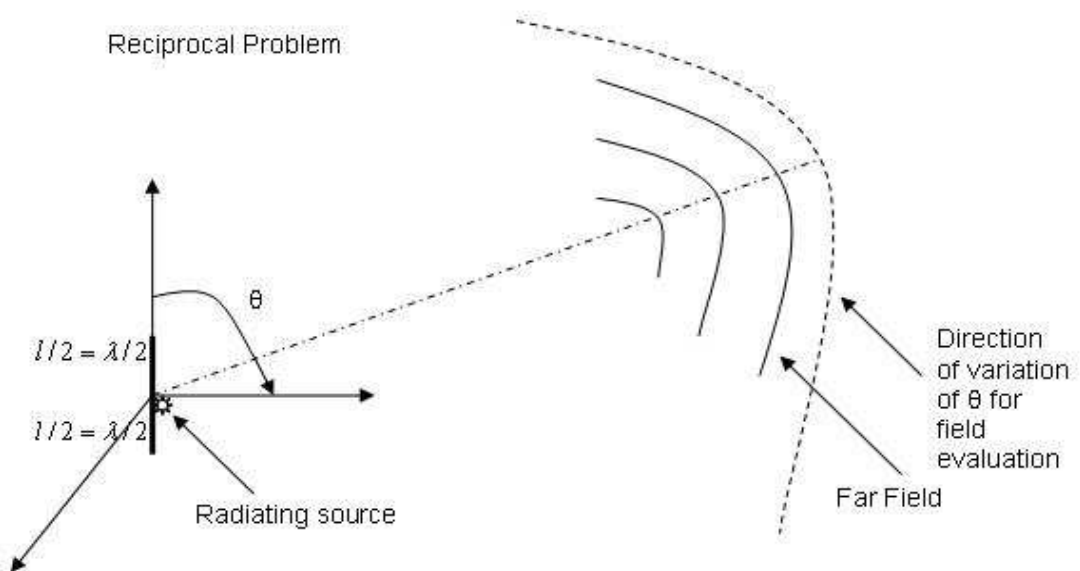


Figure 4.1.b. Far field radiated by the source on the center of the dipole.

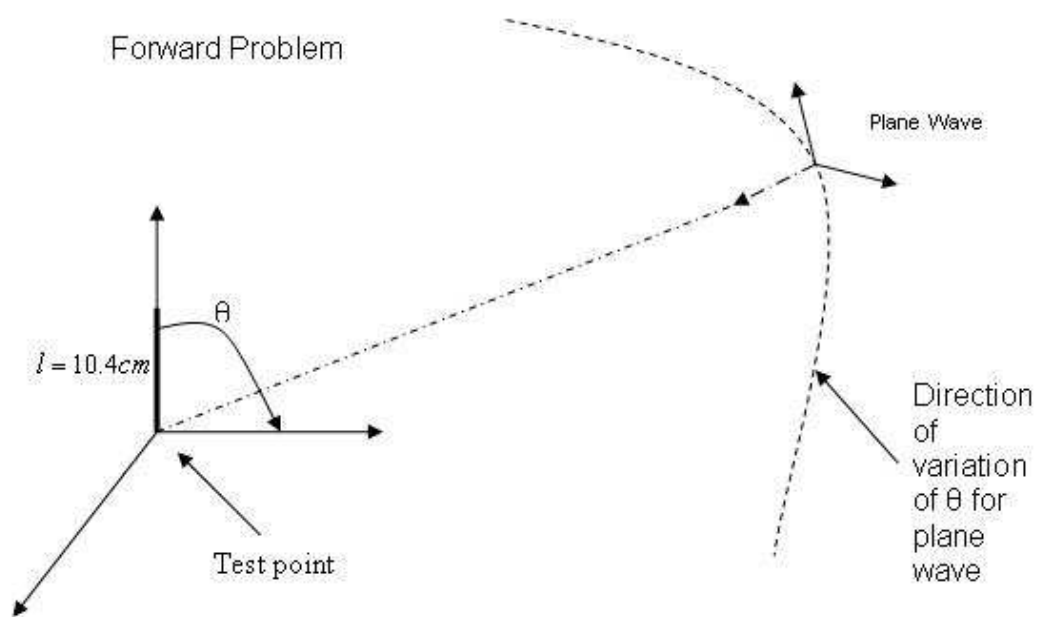


Figure 4.2.a. Evaluation of current induced on the wire at the test point (end of the wire).

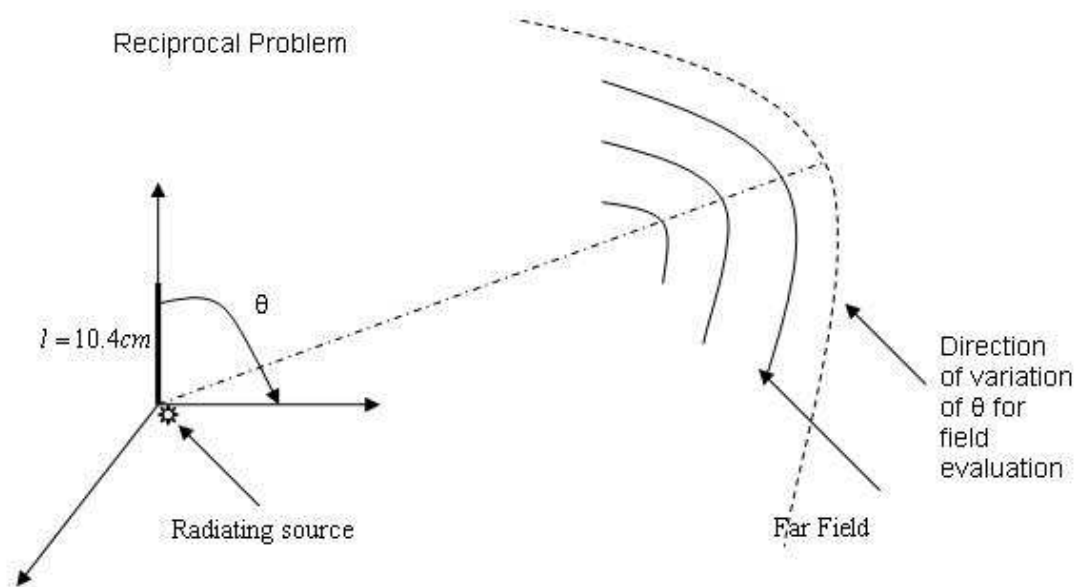


Figure 4.2.b. Far field radiated by the source on the wire (end of the wire).

A wire of length 10.4 cm is placed on a ground plane. In the forward problem, the wire is hit by a plane wave of Electric field magnitude 1 V/m with varying azimuth angle from 0 to 180 in 5 degrees difference. The current induced at the test point, which is the end of the wire, is evaluated. For the reciprocal case, a voltage source of magnitude 1 V is placed at the end segment of the wire and far field evaluation is made for the same variation of azimuth angle. Taking the sample values at different angles from both the forward and the reciprocal results, the ratio is calculated.

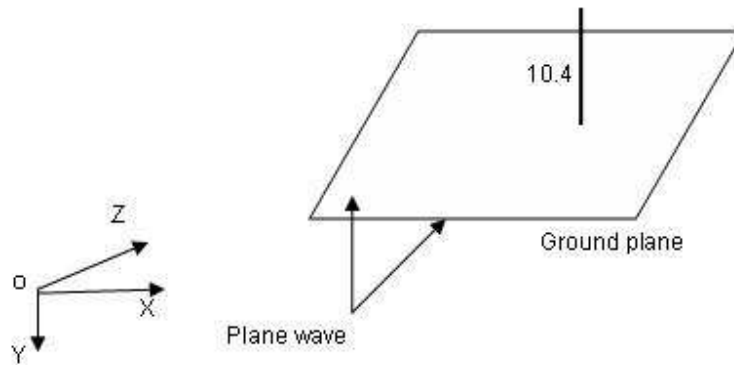


Figure 4.3. Wire on a ground used to validate reciprocity of computational solution.

The ratio of the electric field for the forward problem to the current obtained for the reciprocal problem is found to be the predicted constant value, which is  $1.5 \times 10^{-3}$  for free space. The same problem is repeated for a wire in a box, locating the test point at the end segment of the wire. The comparison is made for all points on the same plot. The result of the comparison between the forward and reciprocal problems considering the wire on a

ground plane and wire inside the box are described in detail in the results and discussion section.

## CHAPTER V

### RESULTS AND DISCUSSION

#### **5.1. Observations of effects of variation of parameters on the current coupling**

##### **5.1.1 Field calculation for normal incidence angle**

For a co-polarized, normally incident plane wave source, the electric field coupled to the cavity through the aperture is evaluated at points 1' and 2' of the model shown in Figures 3.1 and 3.2. Figure 5.1.1.1 shows a plot of the field calculation at the two points 1' and 2' without a wire in the cavity, where 1' is at the middle of the cavity where it's expected to have maximum coupling and 2' is a point near the corner of the cavity. The empty cavity modes are plotted in Figure 5.1.1.2 to investigate the relation between the cavity modes and the peak values of the field.

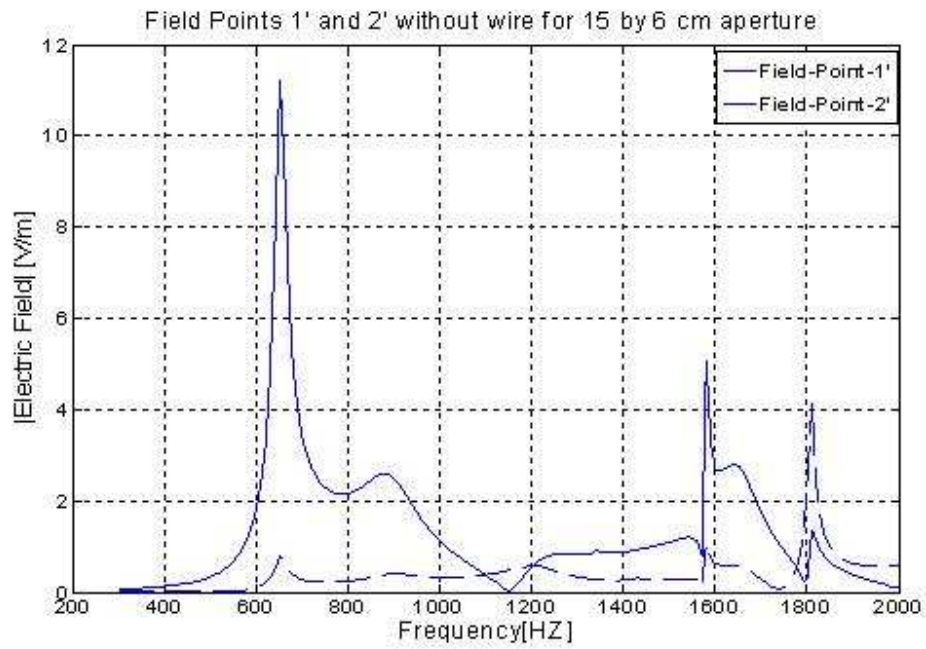


Figure 5.1.1.1 Electric field at monitor points 1' and 2' for normal incidence

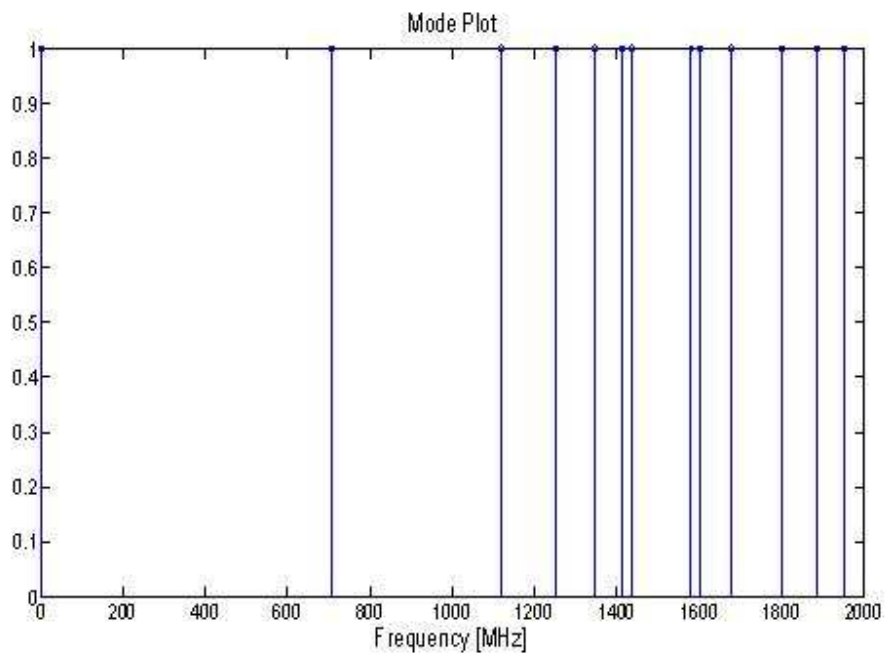


Figure 5.1.1.2 Empty cavity resonances

As was expected we observe a higher field magnitude at position 1' which is the cavity center. We note that most of the peaks of the electric field value coincide with the cavity resonances. However, we observe a peak at around 900 MHz which doesn't align with any of the cavity modes. It should be noted that, since the cavity modes are evaluated assuming a closed empty rectangular enclosure (without any openings). Therefore, some difference is expected between the field peak values and the empty cavity modes due to energy loss through the apertures.

### **5.1.2 Change of position of the wire**

The current induced on a wire due to incidence field radiates a field which may perturb the field measurement that could be obtained from empty cavity. In order to observe how the field is disturbed as the wire is moved inside the enclosure, the electric field is evaluated at the point 1' when a wire is introduced and moved to the 16 positions. The result is shown in Figure 5.1.2.1 below for a normally incident plane wave source and for a frequency sweep of 300 MHz to 2 GHz.

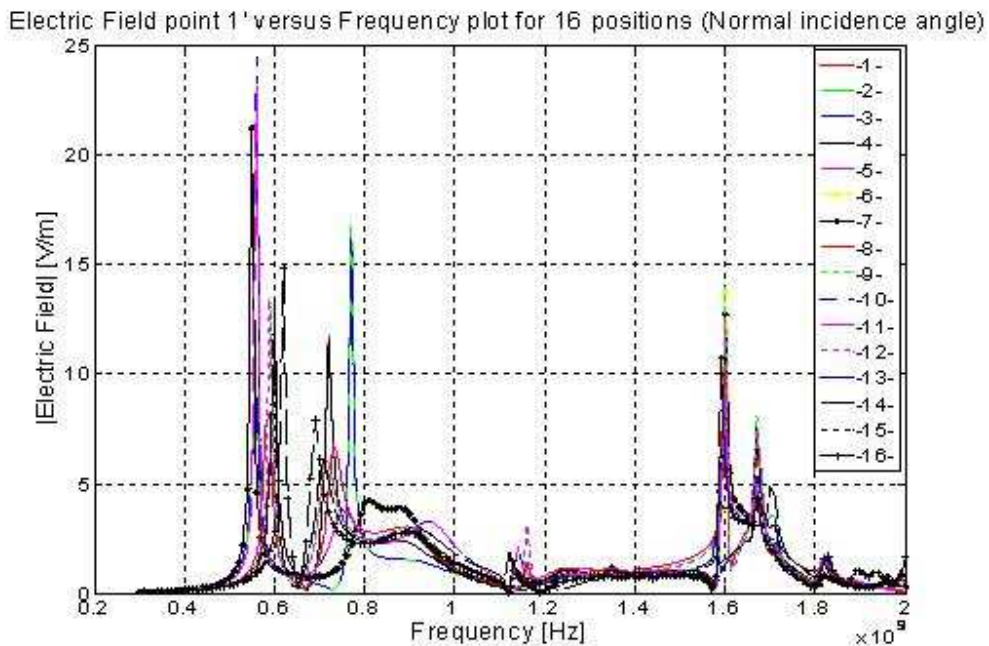


Figure 5.1.2.1 Electric field as a function of frequency at point 1' for 16 wire positions

From the slight variation of the field plot for different wire positions, it can be deduced that the field inside the cavity is slightly perturbed due to the movement of the wire. The difference caused by introducing the wire can also be observed by comparing these plots with the figure without wire (Figure 5.1.1.1). Introduction of a wire in the cavity resulted in a significant field resonance values at lower frequencies. Instead of the peak at 700 MHz of the empty cavity with aperture, two peaks are introduced at around 600 and 800 MHz. the frequency at around 900 MHz due to interaction of slot and cavity resonances still exist. For frequencies higher than 1000 MHz, the field resonances are in good agreement with the cavity resonances. At lower frequencies at around 600 and 800 MHz, we observe a change in field resonance frequency for change in positions of wire, however, no significant resonance change for higher frequencies and the field resonances

correspond to cavity modes. The possible reason for what happened at around the field resonance at 900 MHz will be explained later based on slot resonance and cavity resonance interaction effects. In general, except for slight change in magnitude, change in position of the wire doesn't have a significant effect compared to the effect of introducing a wire.

### 5.1.3 Current Calculation for Normal Incidence Angle

The current induced at the last segment of the wire for the 16 wire positions is plotted in figure 5.1.3.1. We can observe a direct relation between the field values and the current induced at the end of the wire. The current peak values also correspond to the cavity modes showing that the current is a direct result of coupling to the field at that position.

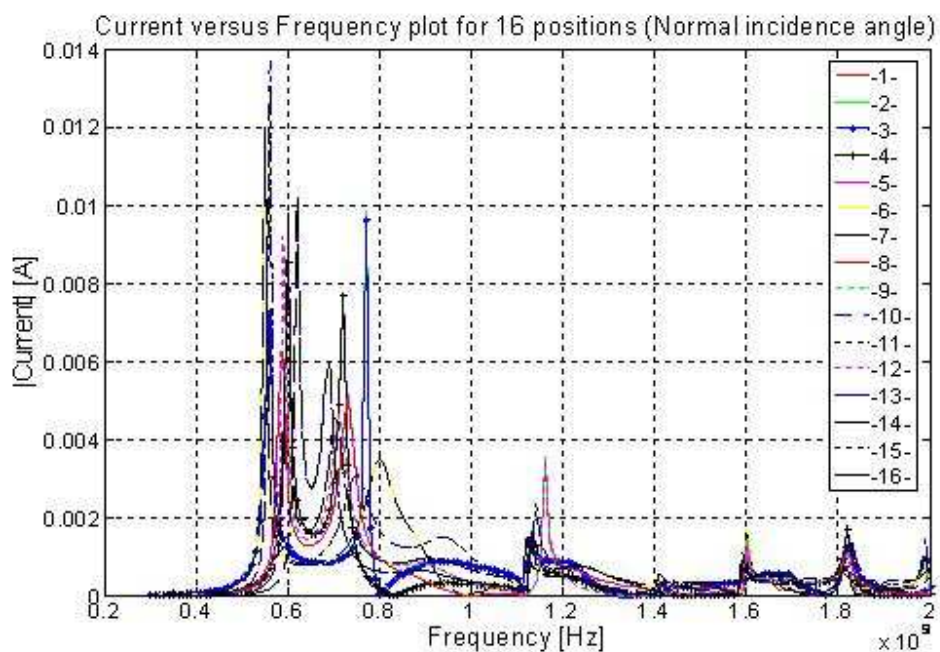


Figure 5.1.3.1 Current as a function of frequency for 16 wire positions

Fig

### 5.1.4 Field calculation for varying incidence angle

By taking the computations for field point 1', we can observe how the field changes as the incidence angle changes with respect to the x axis of the model shown in Figure 3.1. Figures 5.1.4.1 to 5.1.4.4 below show the field as the incidence angle rotates from the side of the box to the perpendicular direction. In these figures, theta is the elevation angle and phi is the azimuth angle with respect to the coordinate shown in the model of Figure 3.1. As we expect we observe an increase in magnitude as it gets closer to normal incidence. The increment is in a similar way for field point 2' and current on the wire. Otherwise there is no major difference for the different incidence angles shown. However a wider variation of incidence angles should be implemented in order to investigate the results for more incidence angle difference.

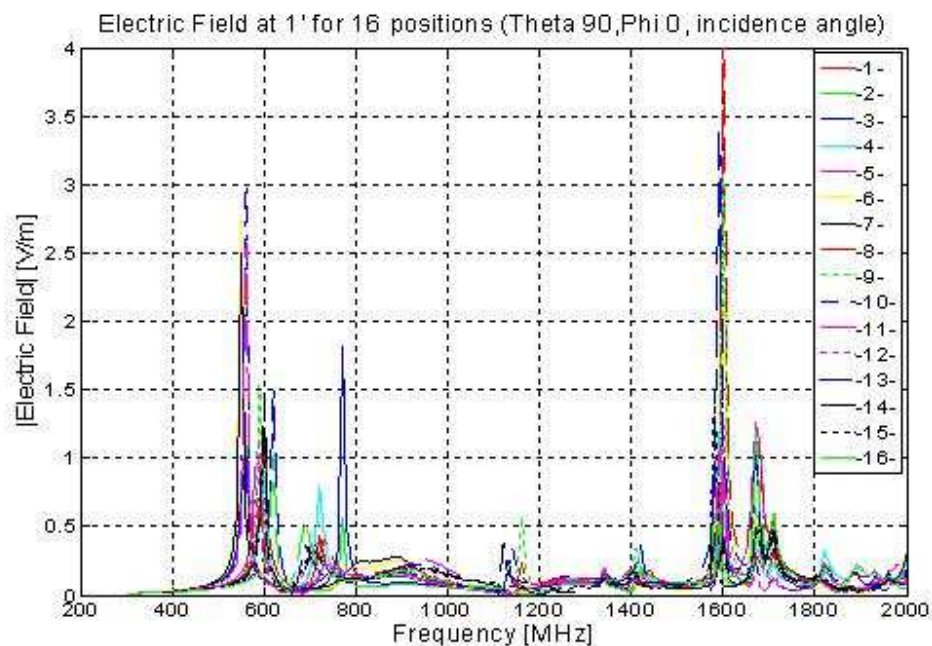


Figure 5.1.4.1. Electric field as a function of frequency at point 1' for 16 wire positions (theta = 90 degrees, phi = 0 degree).

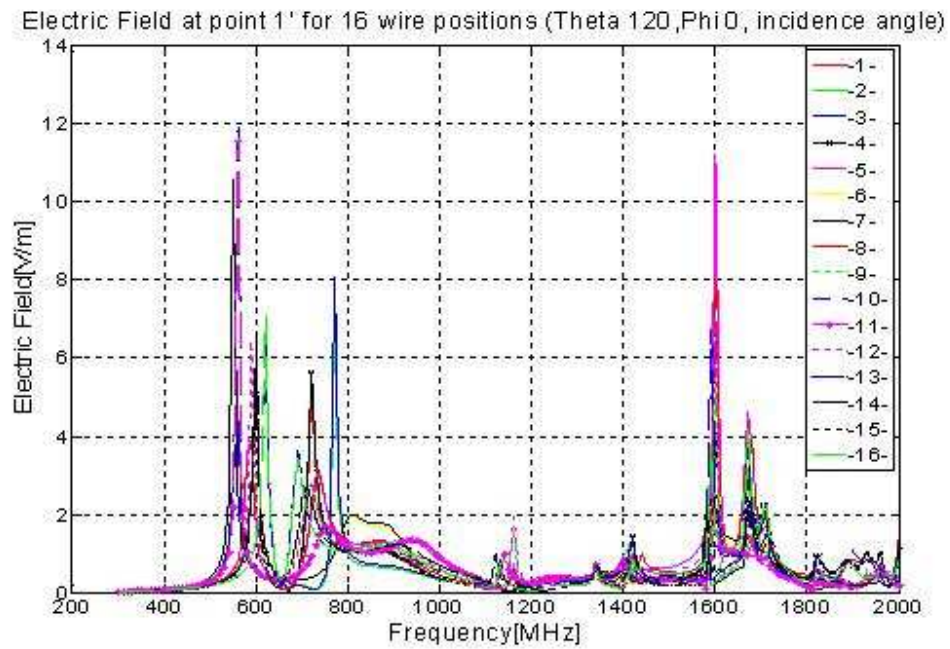


Figure 5.1.4.2. Electric field as a function of frequency at point 1' for 16 wire positions (theta = 120 degrees, phi = 0 degree).

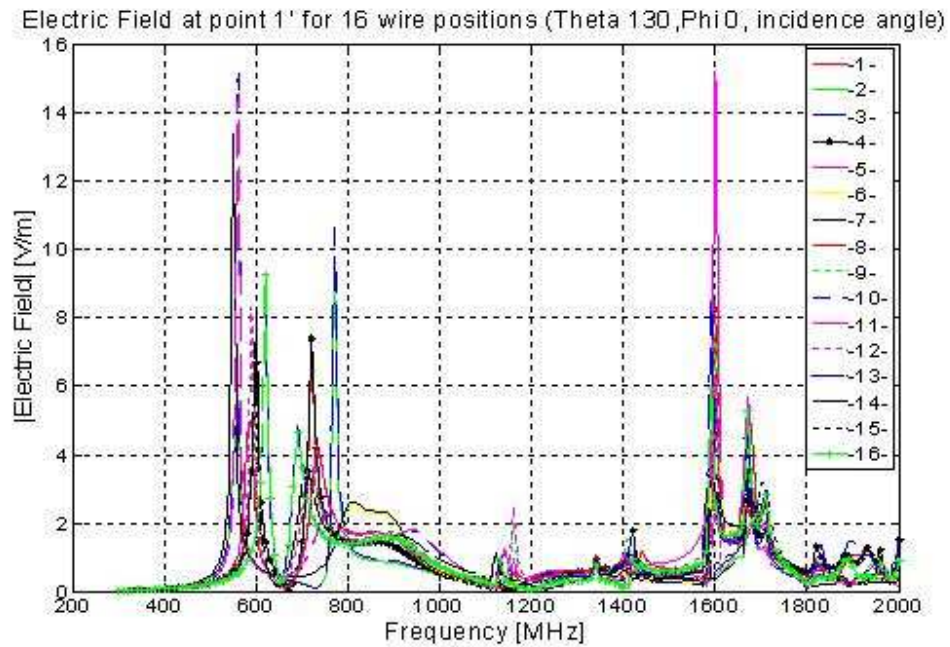


Figure 5.1.4.3. Electric field as a function of frequency at point 1' For 16 wire positions (theta = 130 degrees, phi = 0 degree).

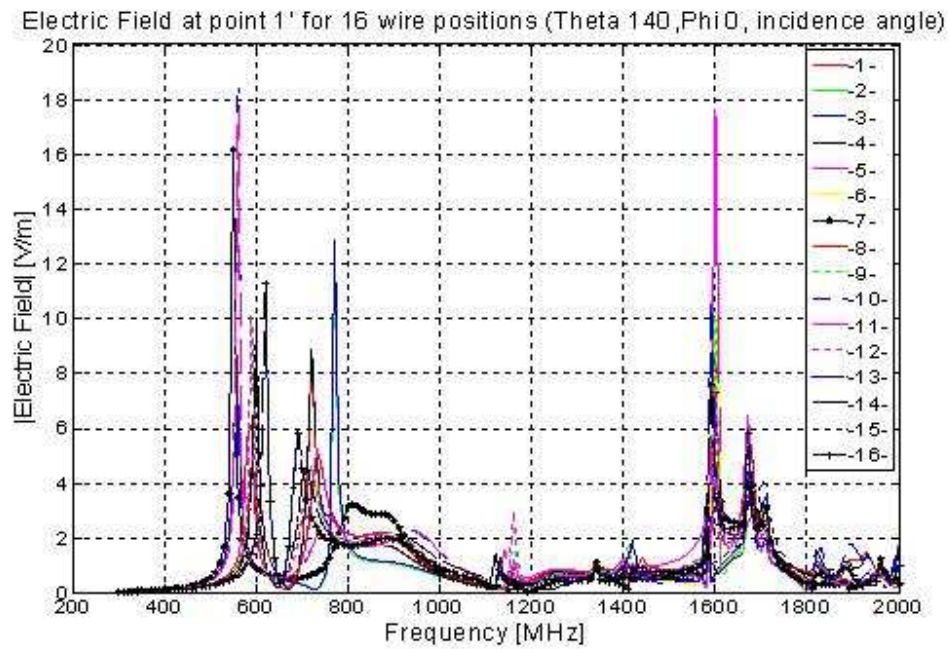


Figure 5.1.4.4. Electric field as a function of frequency at point 1' For 16 wire positions (theta = 120 degrees, phi = 0 degree).

### 5.1.5 Field calculation for different aperture size

In an effort to explain the peak at around 900 MHz which did not coincide with the empty cavity resonant modes, the aperture size is varied for couple of dimensions and the field at position 1' is calculated for a plane wave source at a normal incidence and for a frequency sweep of 300 MHz to 1 GHz

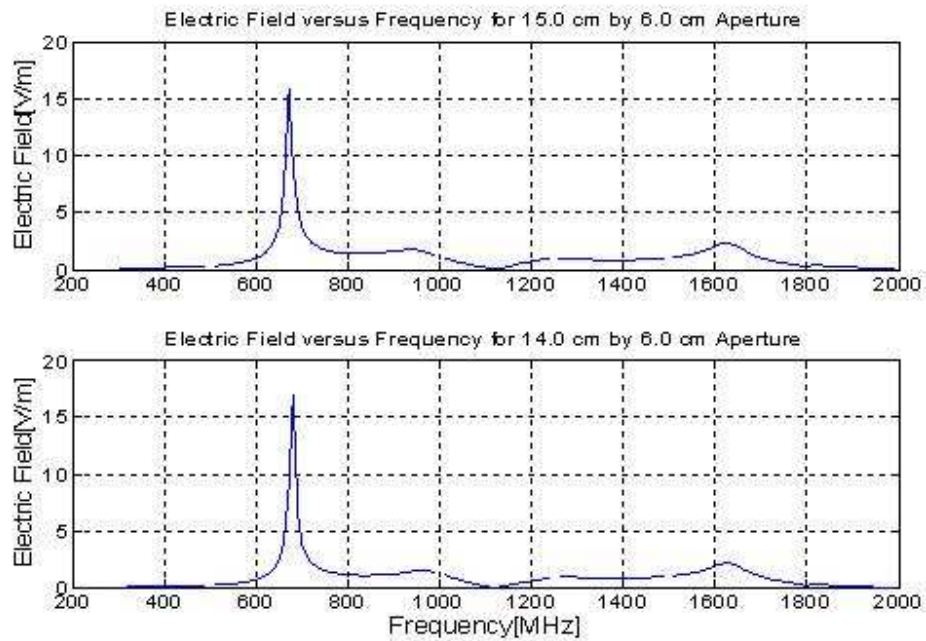


Figure 5.1.5.1. Electric field versus frequency (for aperture size of 15 cm x 6 cm and 14 cm x 6 cm).

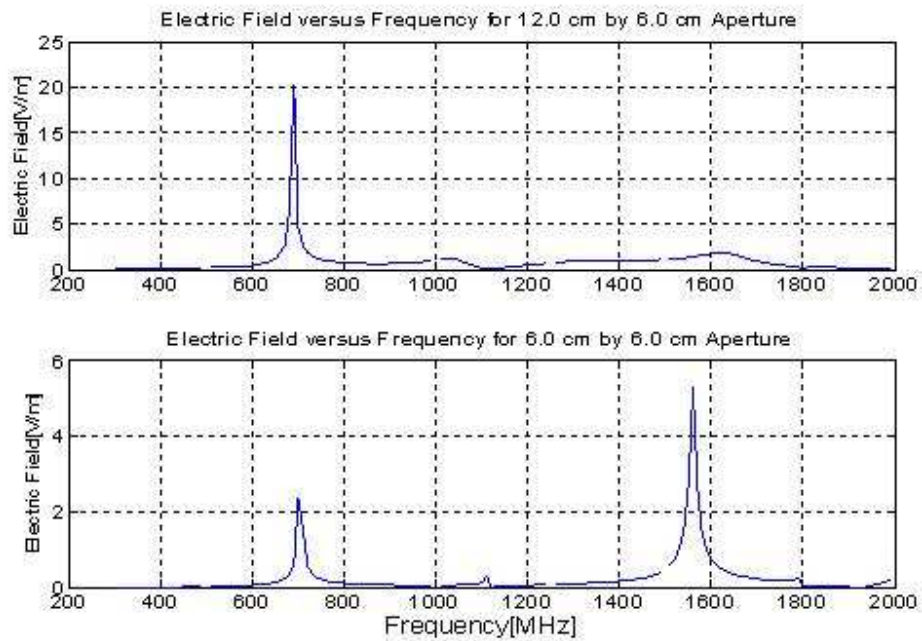


Figure 5.1.5.2. Electric field versus frequency (for aperture size of 12 cm x 6 cm and 6 cm x 6 cm).

As the aperture length is reduced as shown in the Figures 5.1.5.1 to 5.1.5.2 above, we can observe that the peak shifts to the right. We observe that the curve varies significantly as the aperture is changed. For an aperture size of 15 x 6 cm, there is a resonance frequency observed between 900 and 1000 MHz, which was not one of the cavity resonances. The presence of this resonance can be explained by considering the slot resonance at 15 cm slot length, which is 1000 MHz. The slot resonance at 1000 MHz is close to the cavity resonance, and consequently there are high cavity-slot-interactions. As the aperture size is minimized, the resonance at around 900 MHz appears to shift to the right ultimately to one of the cavity resonances just to the right of 1000 MHz. This may also be explained by considering the slot resonances of the smaller slot lengths, as the slot length gets smaller, the slot resonant frequency will be higher resulting less cavity-slot-interactions thus less effect on cavity resonances. The resonant frequencies are 1000 MHz for 15 cm, 1250 MHz for 12 cm, 1875 MHz for 8 cm, 2500 MHz for 6 cm length of the slot [27].

The preliminary study presented in this section gives very limited information about the coupled quantities as it is difficult to consider the effects of every different changing situation. Therefore an extra effort is made to apply a more general description of the electromagnetic environment by using statistical approach. The implementation of random plane wave superposition method and reciprocity are described in the next section.

## **5.2. Statistics of the current in a complex environment represented by superposition of plane waves**

### **5.2.1 MC simulation: Random plane wave approach**

In an effort to analyze the statistics of the current coupled to a wire residing in a complex environment, a random plane wave superposition approach is implemented. 20 plane waves are chosen as incident field source matching Musso's paper [19]. In this simulation, A 10.4 cm long wire is placed vertically on a 50.8 cm x 33.02 cm rectangular ground plane. The parameters of the 20 plane waves,  $N = 20$  are taken from random numbers with uniform distribution. A uniform distribution is also chosen for the phase due to multiple scattering of waves inside the RC environment. Therefore, the azimuth and elevation angles of the plane waves are taken from uniform distribution over the solid angle, the polarization and phase angles are also taken from a uniform distribution with an interval  $[0, 2\pi]$ . A random number generator is used to get the random values from the respective ranges. The current coupled for the 20 plane wave encounter is calculated using FEKO. This calculation is repeated for different number of combinations,  $M$ , by taking the random numbers  $M$  times, where  $M$  is varied as 150, 400 and 1500 representing the corresponding individual current data for different virtual stirrer positions. The number of iterations is increased to obtain a better statistics, especially for the tails. Each plane wave has frequency of 1GHz as it is assumed to accommodate enough number of modes for the required complex environment. The comparison of the cumulative distribution function plots for the simulated current and that of an ideal Rayleigh distribution for different combination of  $M$  are shown in Figures 5.2.1.1.a to 5.2.1.1.c and Figures 5.2.1.2.a to 5.2.1.2.c below.

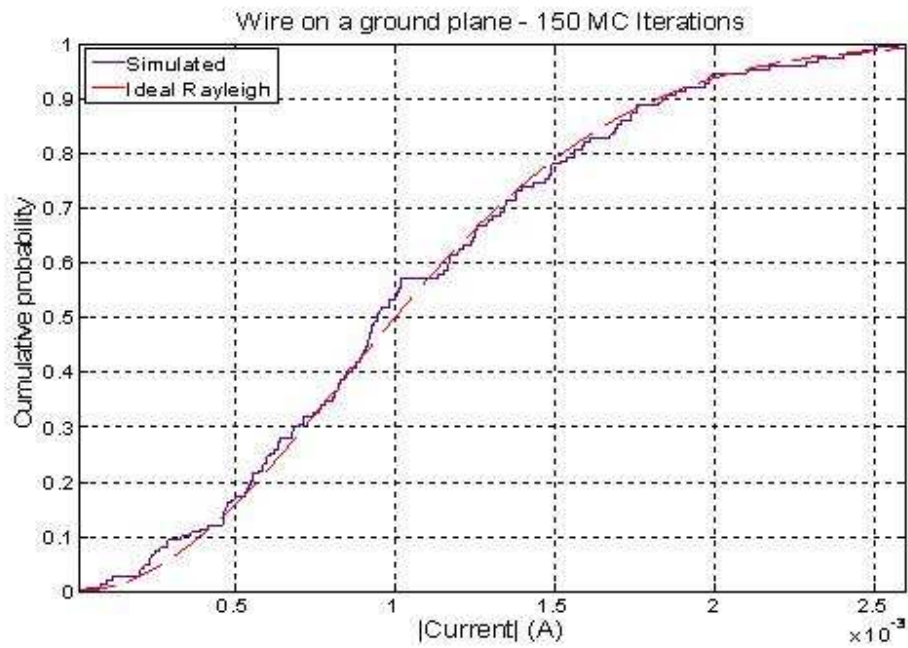


Figure 5.2.1.1.a. Cumulative distribution function of the simulated current induced to the wire on the ground plane for 150 iterations compared with a Rayleigh distribution.

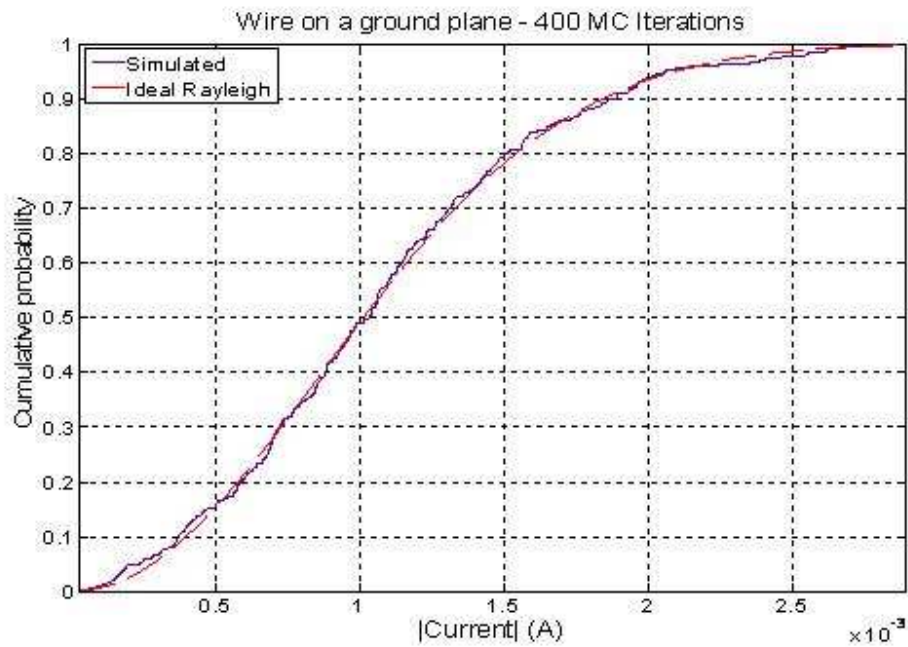


Figure 5.2.1.1.b. Cumulative distribution function of the simulated current induced to the wire on the ground plane for 400 iterations compared with a Rayleigh distribution.

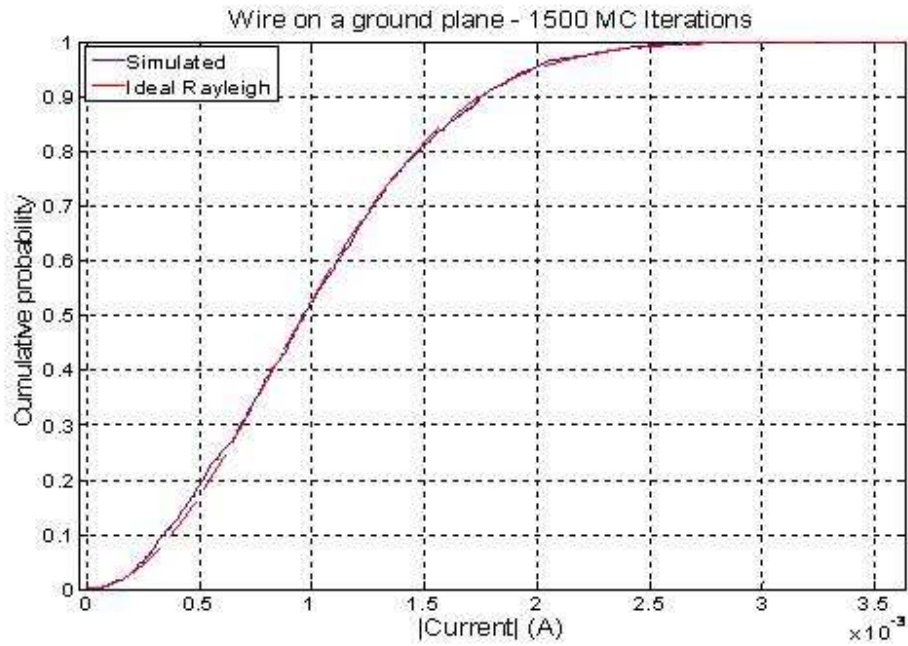


Figure 5.2.1.1.c. Cumulative distribution function of the simulated current induced to the wire on the ground plane for 1500 iterations compared with a Rayleigh distribution.

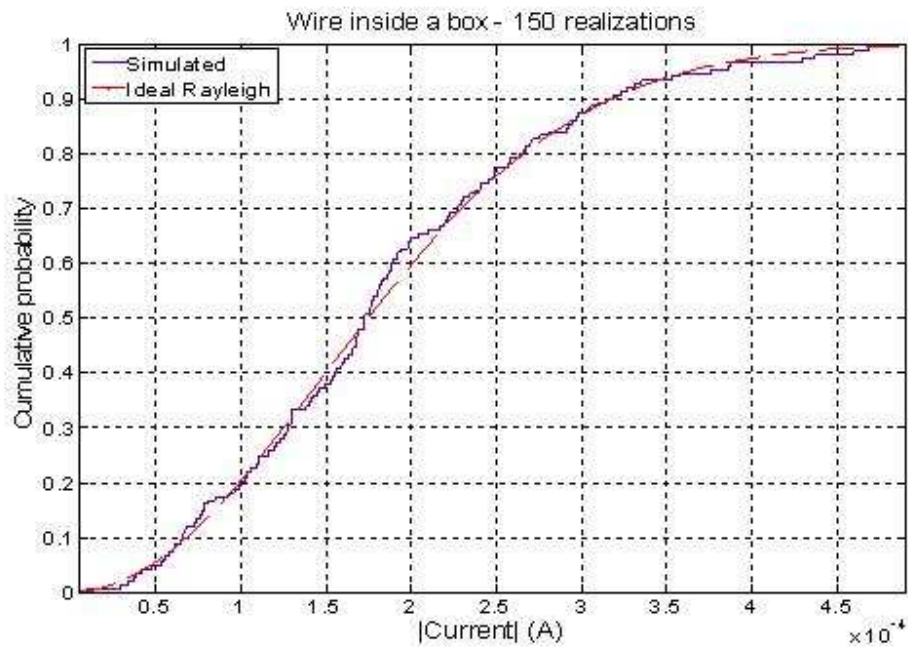


Figure 5.2.1.2.a. Cumulative distribution function of the simulated current induced to the wire on in the box for 150 iterations compared with a Rayleigh distribution (20 plane waves per realization).

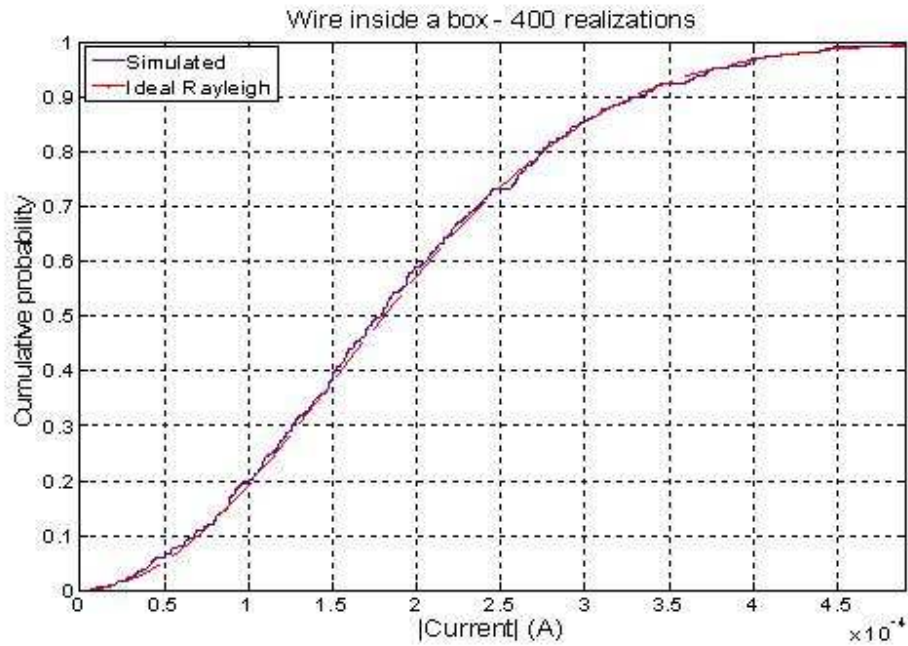


Figure 5.2.1.2.b. Cumulative distribution function of the simulated current induced to the wire in the box for 400 iterations compared with a Rayleigh distribution (20 plane waves per realization).

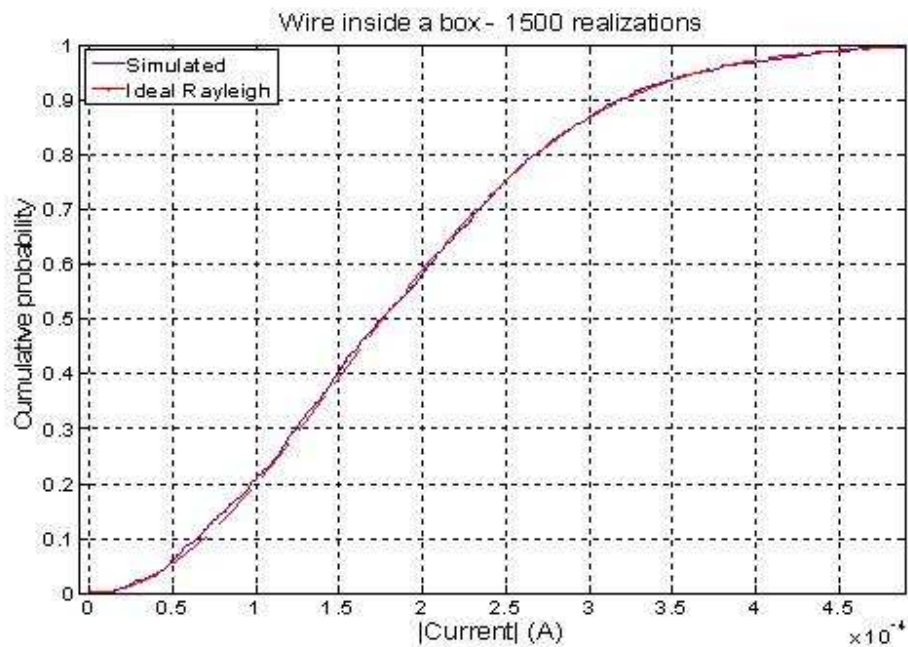


Figure 5.2.1.2.c. Cumulative distribution function of the simulated current induced to the wire in the box for 1500 iterations compared with a Rayleigh distribution (20 plane waves per realization).

The good alignment of theoretical CDF to simulated is an indication to the good agreement of the current statistics which is expected to have a Rayleigh distribution in an ideal RC environment. It can be shown that the comparison gets better as the number of trials increases. It appears that there is a very good alignment between theoretical and simulated CDF plots for 1500 iterations, however the small deviation at the lower tail should be checked. The main concern with this method is the time taken to generate the required data by evaluating the current for each plane wave encounter. Implementing 20 plane waves and for simulation of 1500 different stirrer positions require  $20 \times 1500 = 30,000$  times current evaluations using FEKO. This simulation took 21 minutes. For further comparison of computational time with reciprocity method, 5000 stirrer positions are simulated using 20 plane waves resulting in  $20 \times 5000 = 100,000$  current evaluations. This took 72 minutes which can be greatly reduced using the reciprocity and efficient sampling methods which will be discussed in the next sections.

### **5.2.2 Validation of method for using reciprocity**

In order to have confidence in the simulation methods by which the reciprocity theorem is applied and to use the data collected by the reciprocity approach, investigation is made by comparing the data collected using the forward and reciprocal methods. For a wire on a ground plane with test point at the end segment of the, the forward and reciprocal problems are evaluated for azimuth angle variation from 0 to 180 in 5 degrees steps difference. The current induced at the test point is evaluated. The result is shown in Figure 5.2.2.1 below. Taking sample points at the plots, the ratio of the current induced for the forward problem to the electric field obtained for the reciprocal problem is found

to be the predicted constant value, which is  $1.5 \times 10^{-3}$  for free space and at 1 GHz frequency. The validation is also extended for the wire in the box case latter.

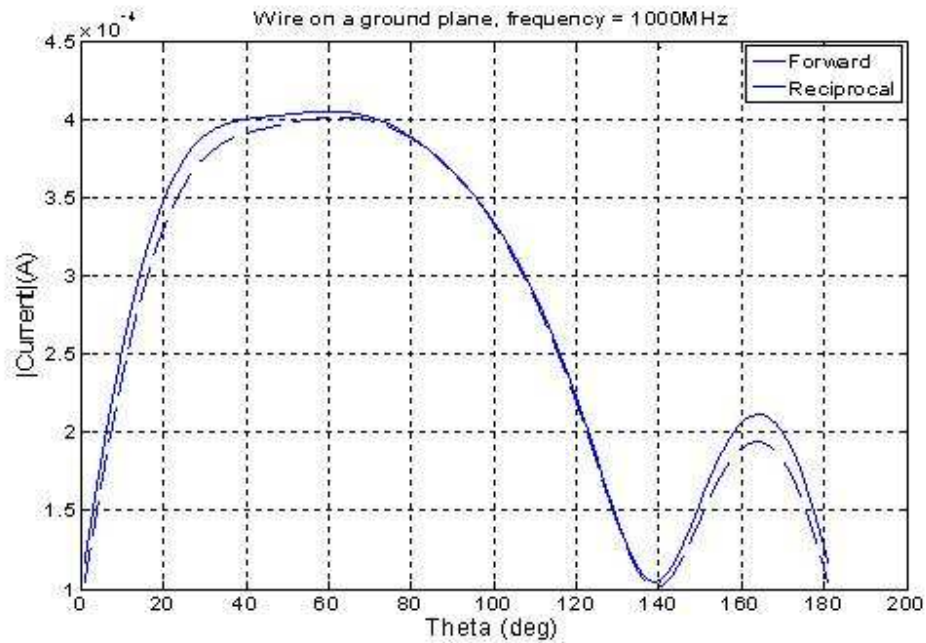


Figure 5.2.2.1. Comparison of forward and reciprocal data for the wire on the ground plane.

In order to apply the proportionality constant to every values and to get the exact value of the current, the far field should be calculated for a radiating source of magnitude  $\frac{4\pi}{k\eta}$  volts. Or this can be achieved by radiating a 1V source and multiplying each field values by  $\frac{4\pi}{k\eta}$  due to the linearity of the system. This method is used in order to further validate the reciprocity for the wire in the box. For this case, an effort is made to consider multiple variations of parameters such as fixing the azimuth angle and frequency and varying the elevation angle, fixing the elevation angle and frequency and varying the

azimuth angle, and finally fixing the elevation and azimuth angles and varying the frequency. After the simulation is run using FEKO, data is collected for the field and current values in a matrix. For the same setup of geometry of wire in the box with aperture used for validation of reciprocity, a far field radiation is evaluated. For a 1V source at the end of the wire and frequency sweep of 800MHz to 2500MHz in 20MHz difference, the far field is evaluated for a single run and for the following angle variations: the elevation angle is varied from 0 to 180 in 10 degrees difference and the azimuth angle is changed from 0 to 360 degrees in 10 degrees difference. Each field evaluation represents the response current of the wire for a plane wave interaction coming from the respective similar directions. In order to get the expected value of current induced on the wire from the field result collected using reciprocal problem, each result should be multiplied by the proportional constant corresponding to the respective frequency, as the constant is dependent on frequency. The data obtain from the FEKO simulation is parsed and is stored in a convenient way using MATLAB. The data is then collected and organized in a matrix in such a way that one can extract the values for a fixed frequency and change in incident angles vertically and for fixed angle and change in frequency horizontally. The detail of the data arrangement is shown in Appendix C. The comparison between the forward and reciprocal results for fixed phi and frequency and varying theta is shown in Figures 5.2.2.1.1 to 5.2.2.1.4, comparison for fixed phi and theta and varying frequency is shown in Figures 5.2.2.2.1 to 5.2.2.1.6, and comparison for fixed theta and frequency and varying phi is shown in the Figures 5.2.2.3.1 to 5.2.2.3.4.

For the comparison of the forward and reciprocal problems shown above, it can be observed that there is no exact match. In order to see the effect of the meshing on the result a finer mesh is implemented using a maximum frequency of 3500 MHz to determine the mesh size. This corresponds to decreasing the mesh size to  $\lambda/42$  from  $\lambda/12$ . The result for the finer mesh is shown in Figure 5.2.2.2 below. It can be seen that a better match is obtained which indicates that increasing the mesh size can be one of the methods for improving the accuracy of the result.

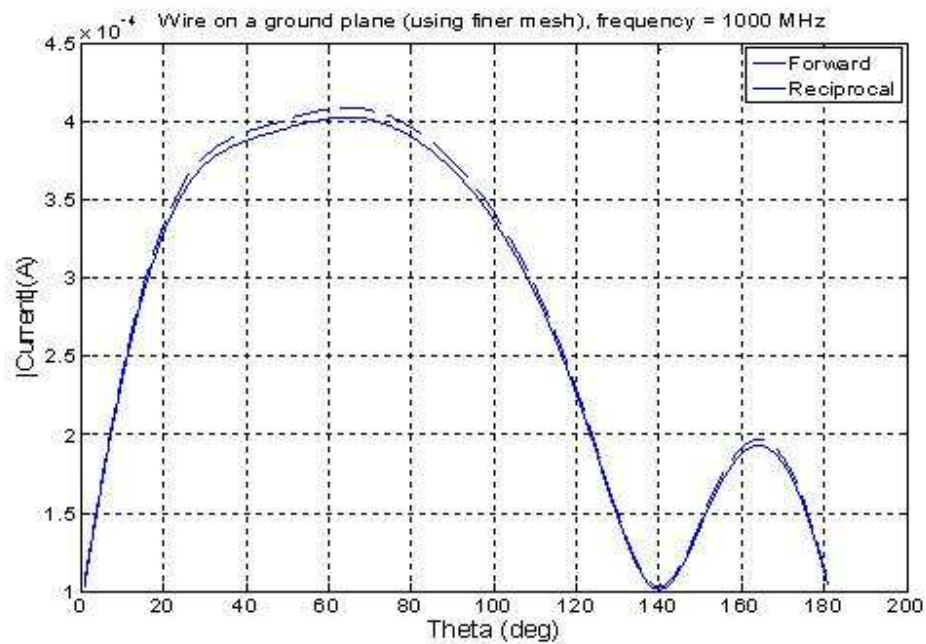
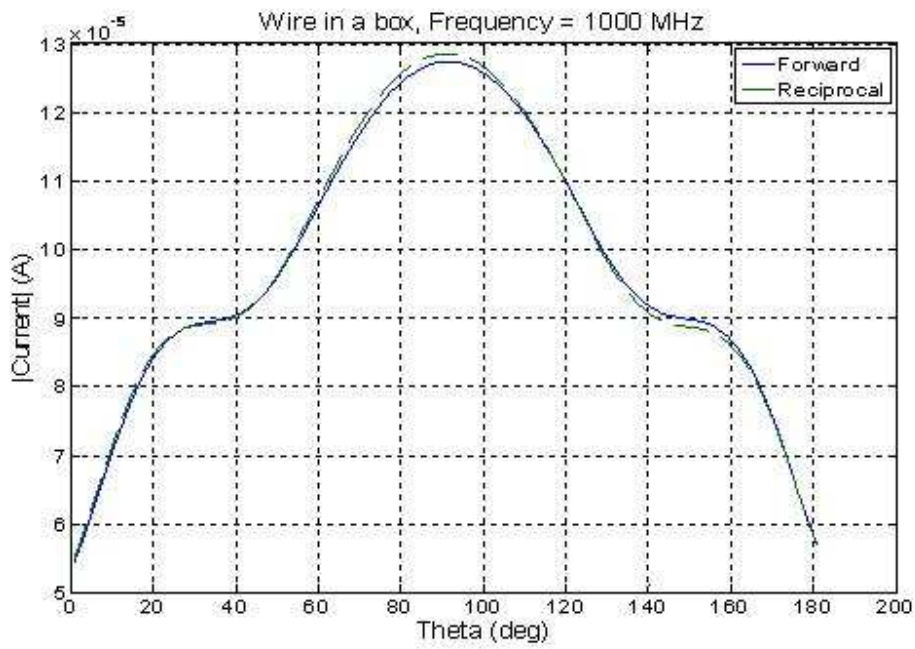


Figure 5.2.2.2. Comparison of forward and reciprocal data for the wire on the ground Plane (For a finer mesh of size  $\lambda/42$ )

### 5.2.2.1. Fixed phi and frequency, change in theta (Moving along the elevation angle)



Figure 5.2.2.1.1. Comparison of forward and reciprocal data for the wire in the box for variation in theta (phi = 90 degrees, Frequency = 800 MHz).



Fig

ure 5.2.2.1.2. Comparison of forward and reciprocal data for the wire in the box for variation in theta ( $\phi = 90$  degrees, Frequency = 1000 MHz).

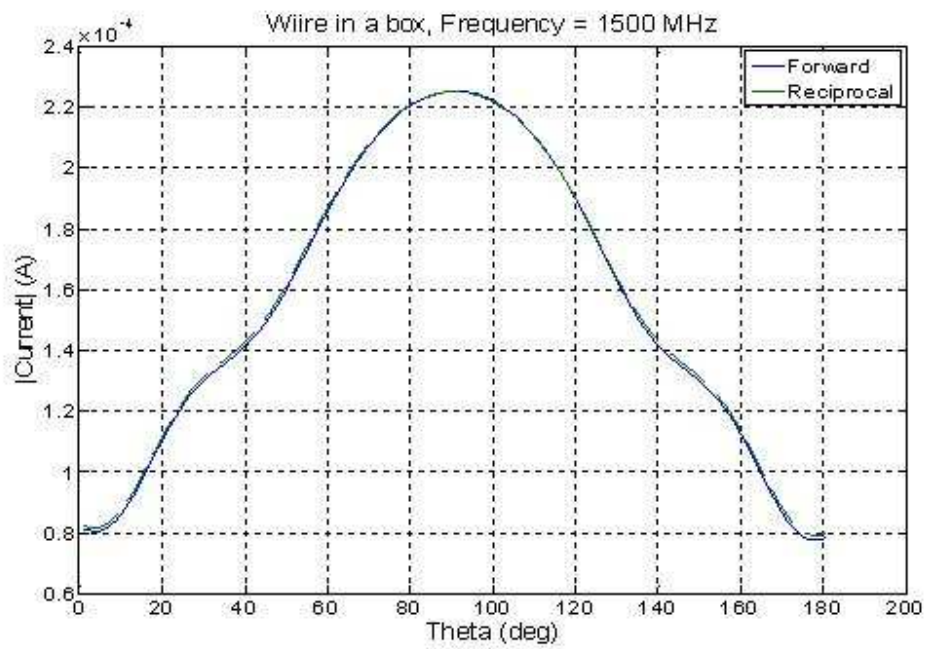


Figure 5.2.2.1.3. Comparison of forward and reciprocal data for the wire in the box for variation in theta ( $\phi = 90$  degrees, Frequency = 1500 MHz).

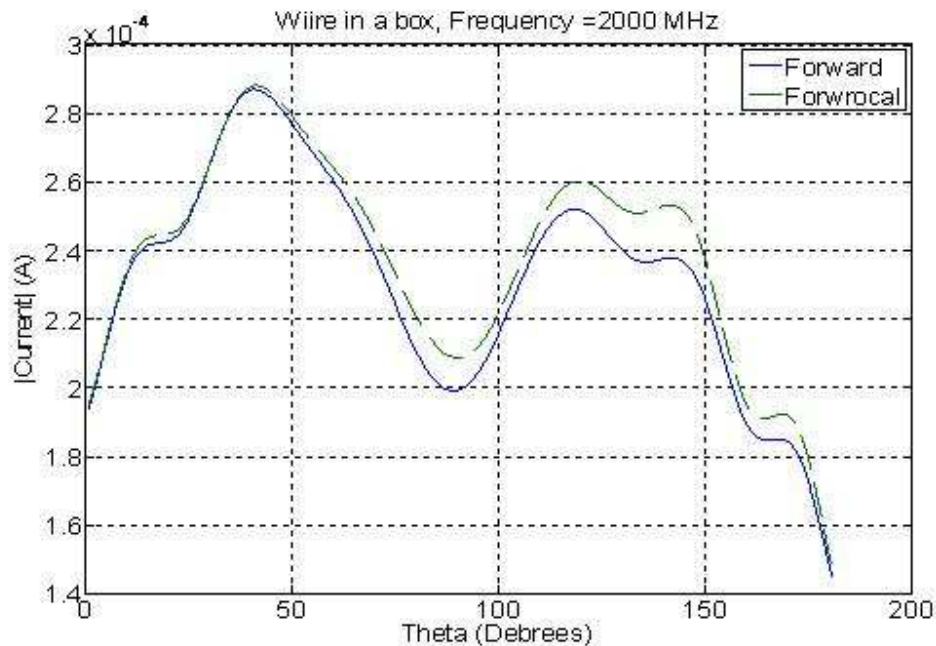


Figure 5.2.2.1.4. Comparison of forward and reciprocal data for the wire in the box for variation in theta ( $\phi = 90$  degrees, Frequency = 2000 MHz).

The comparison between the forward and reciprocal problems for the wire in the box for varying frequency shows a good agreement except for 2000MHz frequency. The dependency on frequency lies mainly due to the meshing of the triangle edge length and segment length of the cavity and loading which is used for solving the current and field values. Since the mesh uses the maximum frequency for meshing all the cavity components, the accuracy of the solution varies for different frequencies. As it is shown, a less accurate comparison is found for 2000 MHz. For this particular plot, a finer mesh is implemented using 2800 MHz as the maximum frequency for the mesh and the corresponding result is shown in the Figure 5.2.2.1.5 below. Even though it is tried to decrease the mesh size by increasing the maximum frequency even more and observe how the accuracy increases, there was a memory usage limitation beyond that frequency.

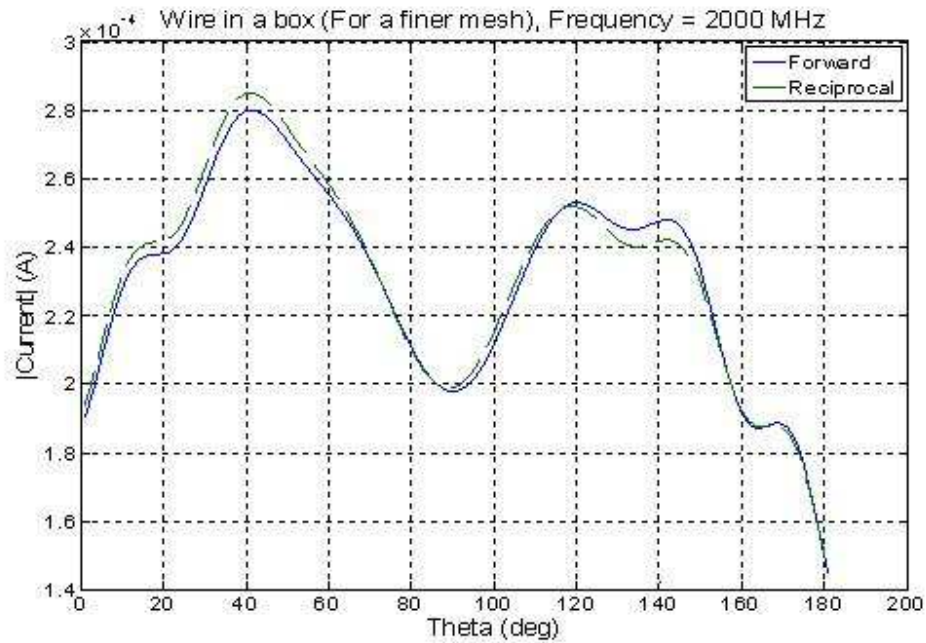


Figure 5.2.2.1.5. Comparison of forward and reciprocal data for the wire in the box for variation in theta, for finer mesh size of  $\lambda/17$  ( $\phi = 90$  degrees, Frequency = 2000 MHz).

From this result shows that the comparison between the forward and reciprocal results improves for a finer mesh size. This improvement is also demonstrated for other simulations in the next sections.

**5.2.2.2. Fixed phi and theta, change in frequency (Changing the frequency and changing steps along the elevation angle)**

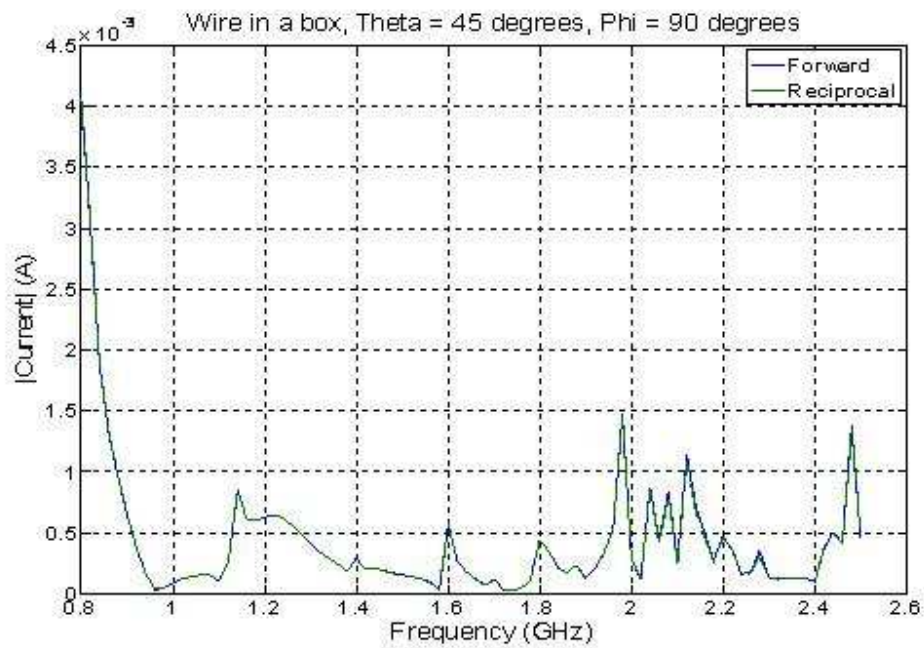


Figure 5.2.2.2.1. Comparison of forward and reciprocal data for the wire in the box for variation in frequency (theta = 45 degrees, phi = 90 degrees).

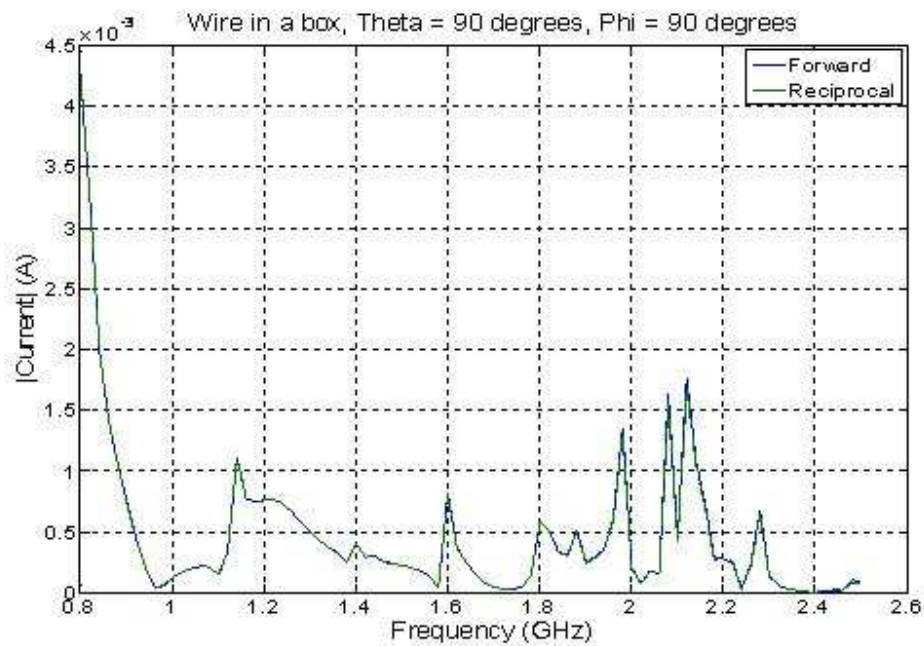


Figure 5.2.2.2.2. Comparison of forward and reciprocal data for the wire in the box for variation in frequency (theta = 90 degrees, phi = 90 degrees).

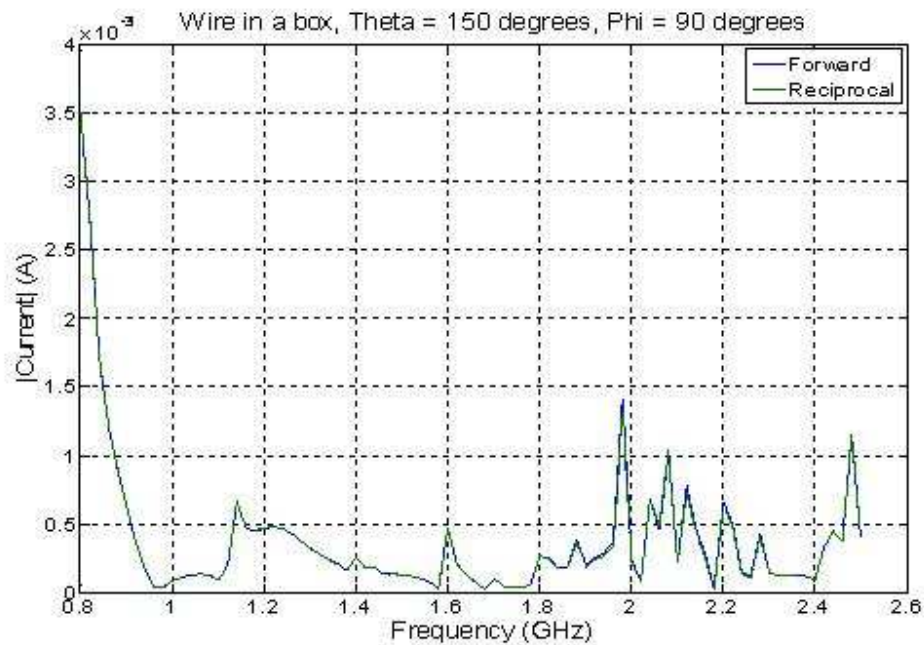


Figure 5.2.2.2.3. Comparison of forward and reciprocal data for the wire in the box for variation in frequency (theta = 150 degrees, phi = 90 degrees).

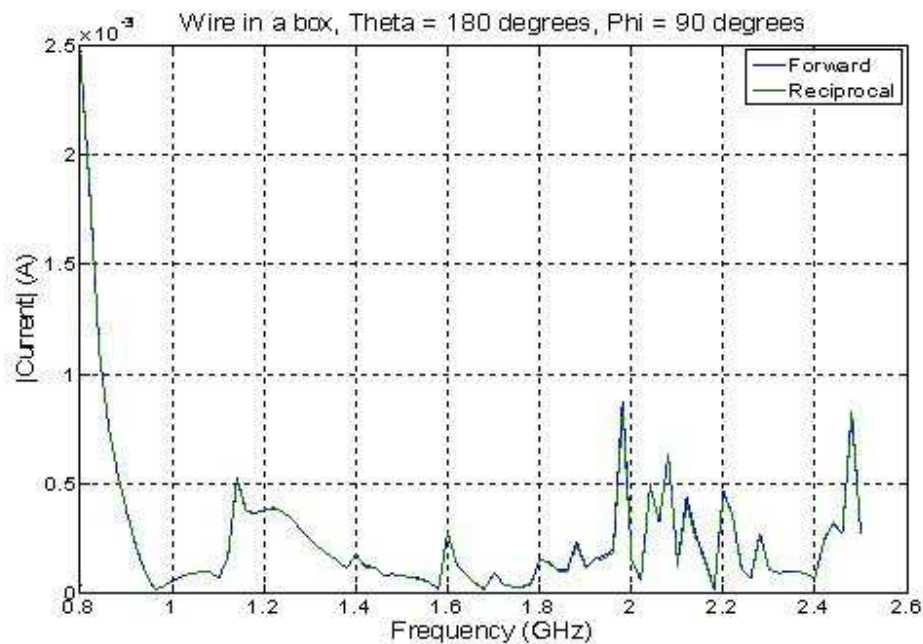


Figure 5.2.2.2.4. Comparison of forward and reciprocal data for the wire in the box for variation in frequency (theta = 180 degrees, phi = 90 degrees).

As it is shown in the Figures 5.2.2.2.1 to 5.2.2.2.4 above, by fixing phi at 90 degrees, theta is varied for some angles 45, 90, 150 and 180 degrees which mean rotating the incidence angle along the elevation angle. As it is evident from the plots, there is a good agreement between the forward and reciprocal values. It should be noted that the comparison between the forward and the reciprocal values should be made with respect to the corresponding components of the field radiation and the incidence plane waves. In this simulation the comparison is made with the theta component of the radiation field for a theta component of plane wave incidence. In order to observe the result for other angle variations, the comparison is repeated for values along the azimuth angle and the result is shown in the next section.

**5.2.2.3. Fixed phi and theta, change in frequency (Changing the frequency and changing steps along the azimuth angle)**

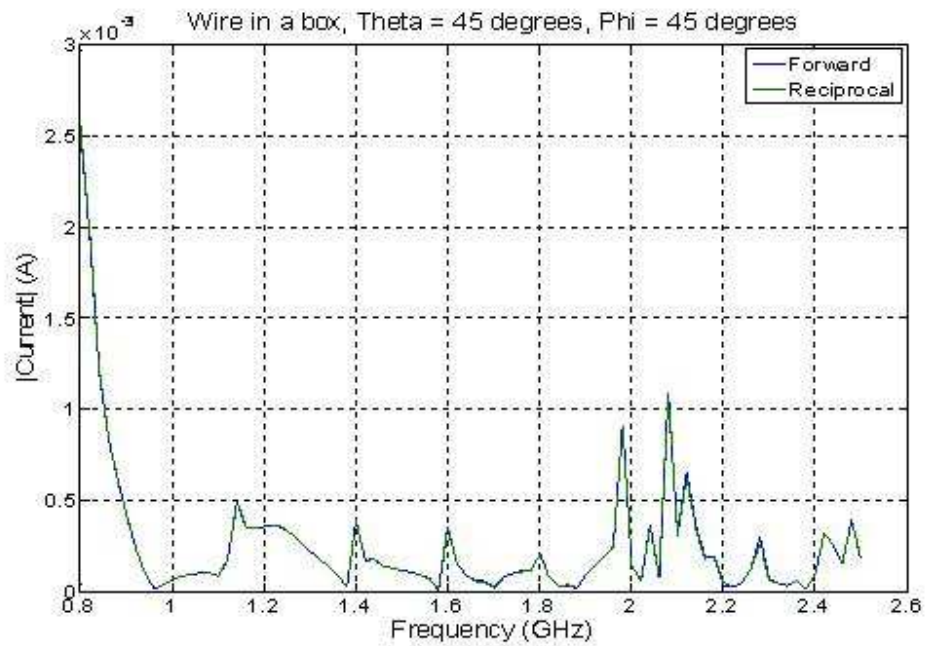


Figure 5.2.2.2.5. Comparison of forward and reciprocal data for the wire in the box for variation in frequency (theta = 45 degrees, phi = 45 degrees).

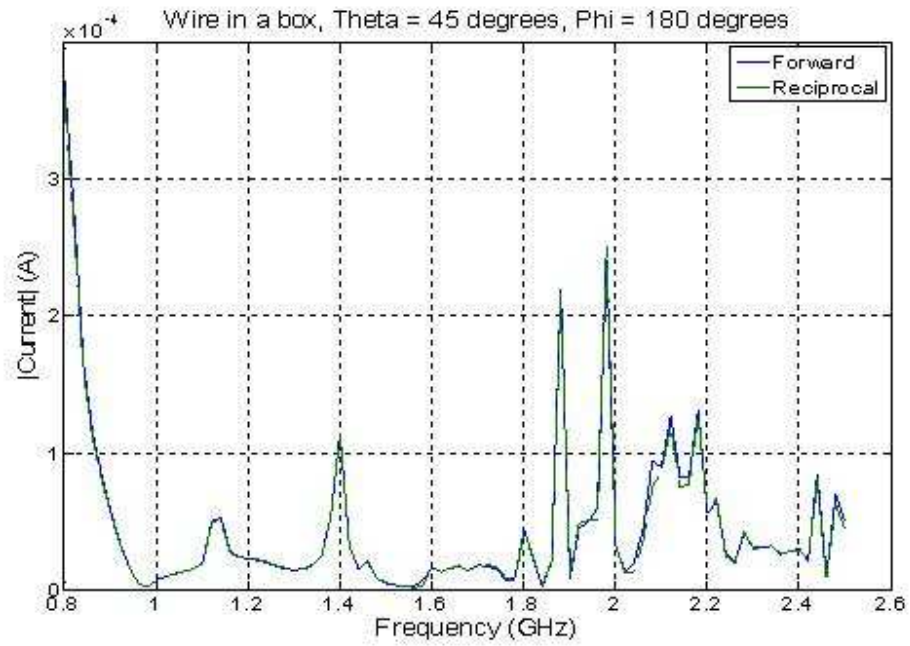


Figure 5.2.2.2.6. Comparison of forward and reciprocal data for the wire in the box for variation in frequency (theta = 45 degrees, phi = 180 degrees).

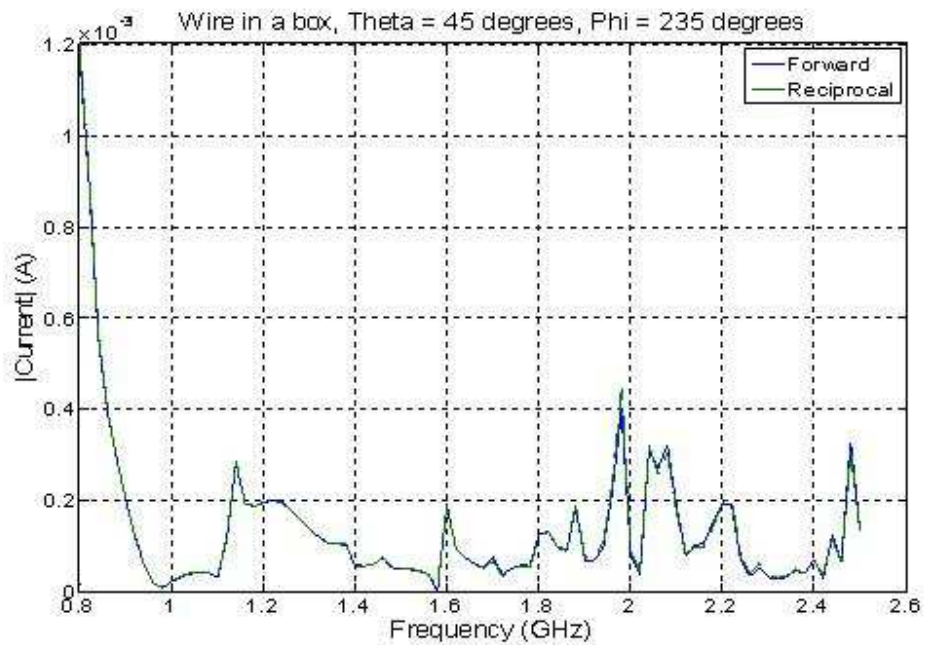


Figure 5.2.2.2.7. Comparison of forward and reciprocal data for the wire in the box for variation in frequency (theta = 45 degrees, phi = 235 degrees).

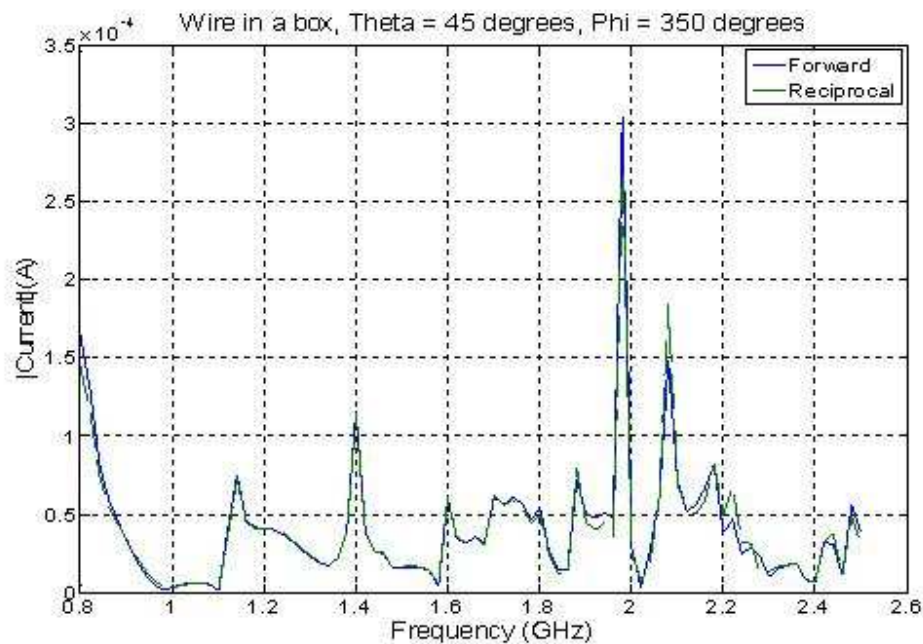


Figure 5.2.2.2.8. Comparison of forward and reciprocal data for the wire in the box for variation in frequency (theta = 45 degrees, phi = 350 degrees).

An observation is made for variation of phi to different values, i.e. 45, 180, 235 and 350 degrees by fixing theta at 45 degrees as shown in the Figures 5.2.2.2.5 to 5.2.2.2.8 above. This is the same as rotating the sample points along the azimuth angle. From the result shown, it can be observed that there is a good match between the forward and reciprocal comparisons except some deviations at some frequencies. There is a 4 dB difference at frequency of 2.08 GHz. However this deviation is expected to decrease if the mesh is decreased from the  $\lambda/10$  value. This improvement in accuracy by using a finer mesh is demonstrated in the next section for a simulation with fixed frequency. For this current set up, we are limited by the memory to make the mesh finer. The next comparison is made by fixing frequency and theta and varying phi from 0 to 360 degrees. The result for this comparison is shown in figures 5.2.2.3.1 to 5.2.2.3.4 below.

#### 5.2.2.4. Fixed theta and frequency, change in phi (Moving along the azimuth angle)

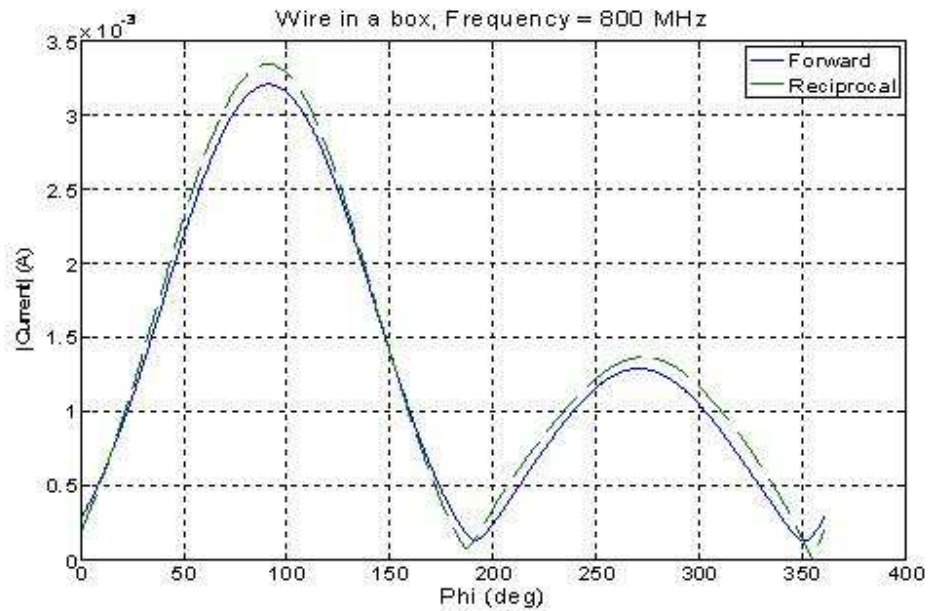


Figure 5.2.2.3.1. Comparison of forward and reciprocal data for the wire in the box for variation in phi (theta = 45 degrees, Frequency = 800 MHz).

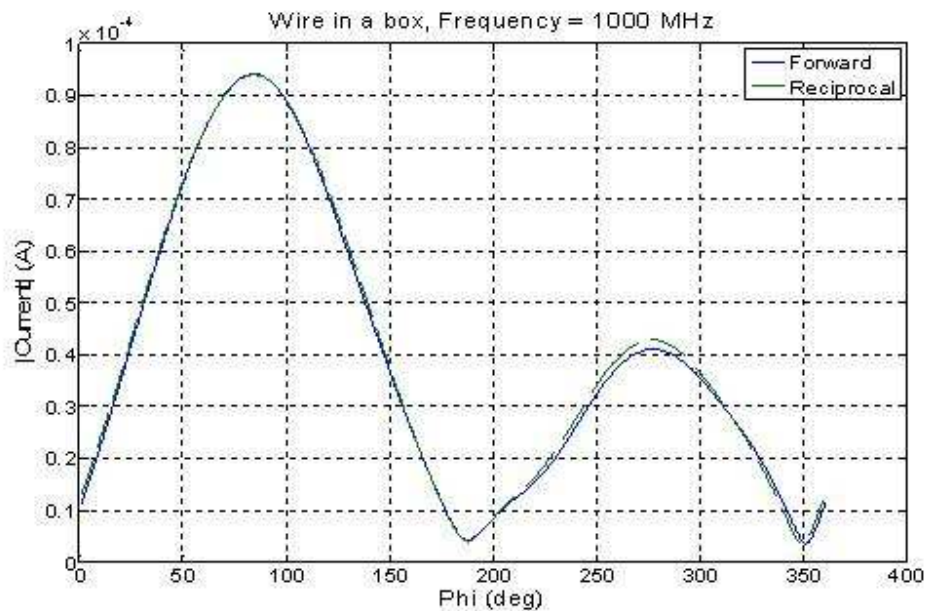


Figure 5.2.2.3.2. Comparison of forward and reciprocal data for the wire in the box for variation in phi (theta = 45 degrees, Frequency = 1000 MHz).

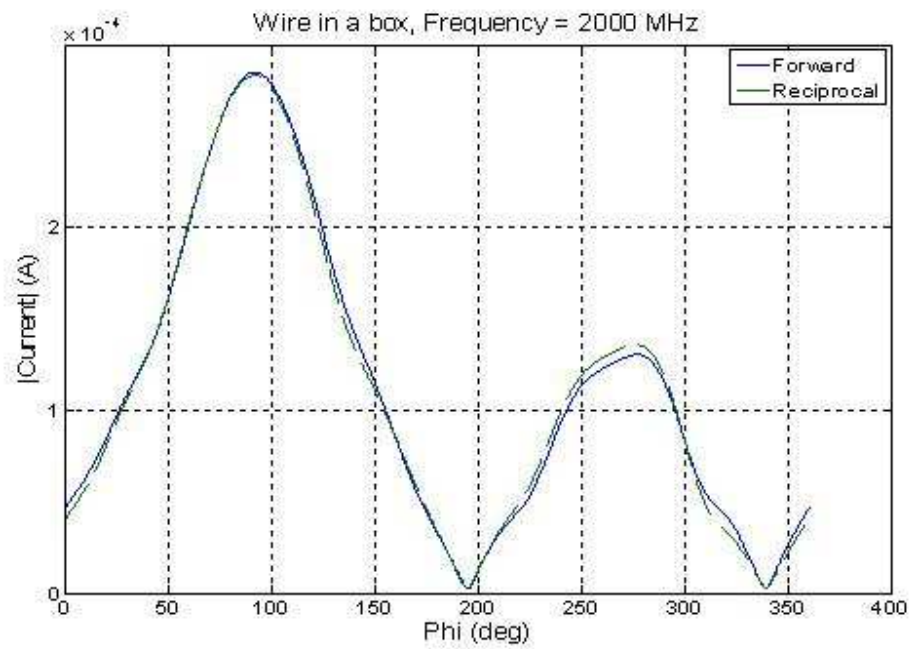


Figure 5.2.2.3.3. Comparison of forward and reciprocal data for the wire in the box for variation in phi (theta = 45 degrees, Frequency = 2000 MHz).

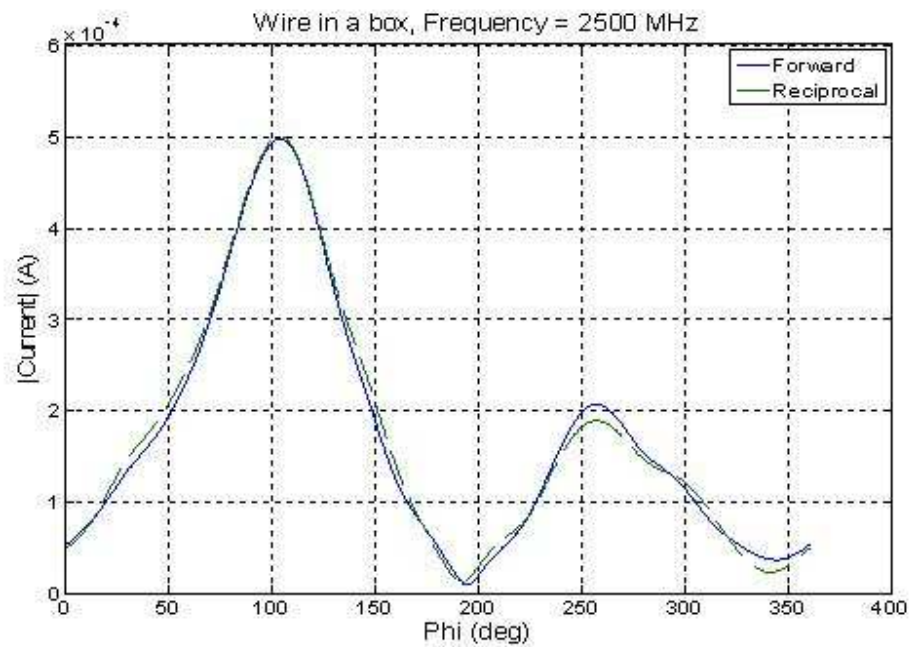


Figure 5.2.2.3.4. Comparison of forward and reciprocal data for the wire in the box for variation in phi (theta = 45 degrees, Frequency = 2500 MHz).

From the results above, it can be observed that there is still an agreement between the forward and reciprocal values for the specified variation of angle. However there are some deviations at some angles, the maximum being a 3.8 dB difference which is shown on Figure 5.2.2.3.4 at phi angle of 91 degrees. To explain this deviation this result is simulated again using a finer mesh and the result is shown in Figure 5.2.2.3.5 below. When the mesh is decreased we can observe a good improvement in accuracy. From this result we can suggest that the improvement of the mesh size can affect the accuracy of all the other results.

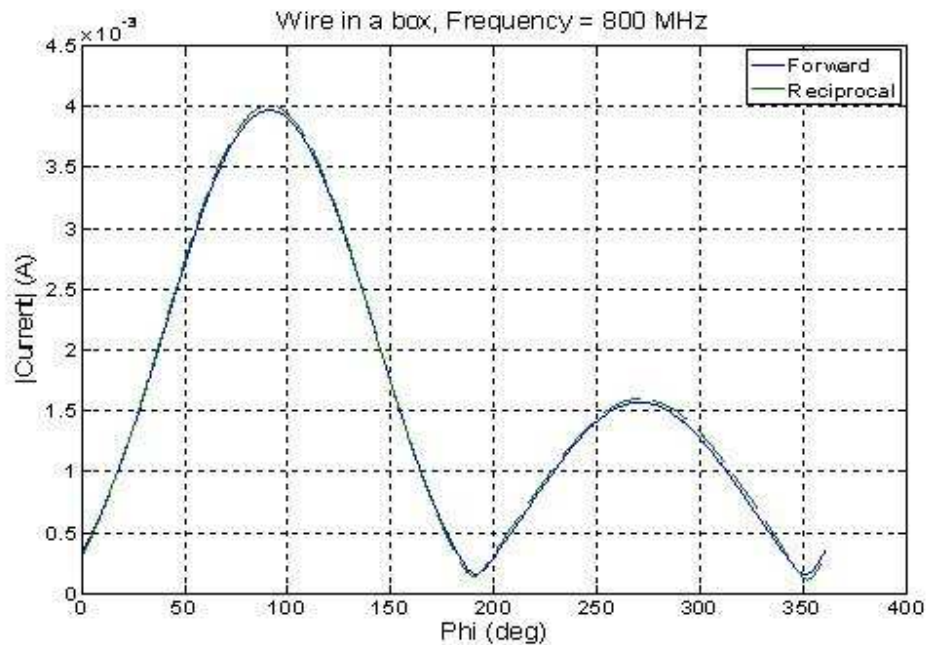


Figure 5.2.2.3.5. Comparison of forward and reciprocal data for the wire in the box for variation in phi, ( $\theta = 45$  degrees, Frequency = 800 MHz) for a finer mesh using frequency = 2000 MHz.

### 5.2.3 Statistics of reciprocal field data

#### 5.2.3.1 Summation of reciprocal fields

The ultimate goal of using reciprocity is in order to accomplish the plane wave superposition representation of RC with less computational overload. According to superposition representation of RC, the response of an EUT to fields for a specific RC stirrer paddle position is represented by the sum of responses to some individual random plane waves. In this work, an attempt to implement the summation of the fields, hence the response currents, is made using the reciprocal field values. In order to verify the superposition of field values from the reciprocal calculation can be used in place of superposition of currents, a comparison is made between the summation of currents from the forward problem and summation of fields from the reciprocal problem. The proper constant is multiplied to the field magnitudes after the summation is accomplished component by component. The same EUT, which is the wire in the rectangular box, is used for this purpose. The current induced on the wire is calculated for a plane wave incidence of magnitude 1V/m and 800 MHz frequency source. The incidence angle is changed by varying theta from 0 to 180 degrees in 1 degrees difference and fixing phi at 90 degrees. In another simulation the reciprocal field is found by putting a 1v source at the lower end of the wire and evaluating the far field values at the same angle variation as the incidence plane wave in the forward problem. The summation for the first case is accomplished by taking five current values from the total of 181 data and then taking the next five values and so on. . The summation for the later case is accomplished by taking the far field values and summing component by component ( $E_\theta$  and  $E_\phi$ ) by the same way. The result of the two comparisons is shown in the Figure 5.2.3.1.a-b below. In order to

further notice the superposition, the summation is repeated by taking 10 consecutive values as shown in Figure 5.2.3.2.a-b which shows an increase in magnitude as more samples are taken. The process is shown for frequency of 800 MHz and 1000 MHz. The result shows a very close similarity between the two summations and indicates that only the far field values can be used to manipulate the data in order to get superposition values. The MATLAB procedure for taking the random values from the FEKO calculated output data and summation of current and field values component by component is shown in Appendix D and E respectively.

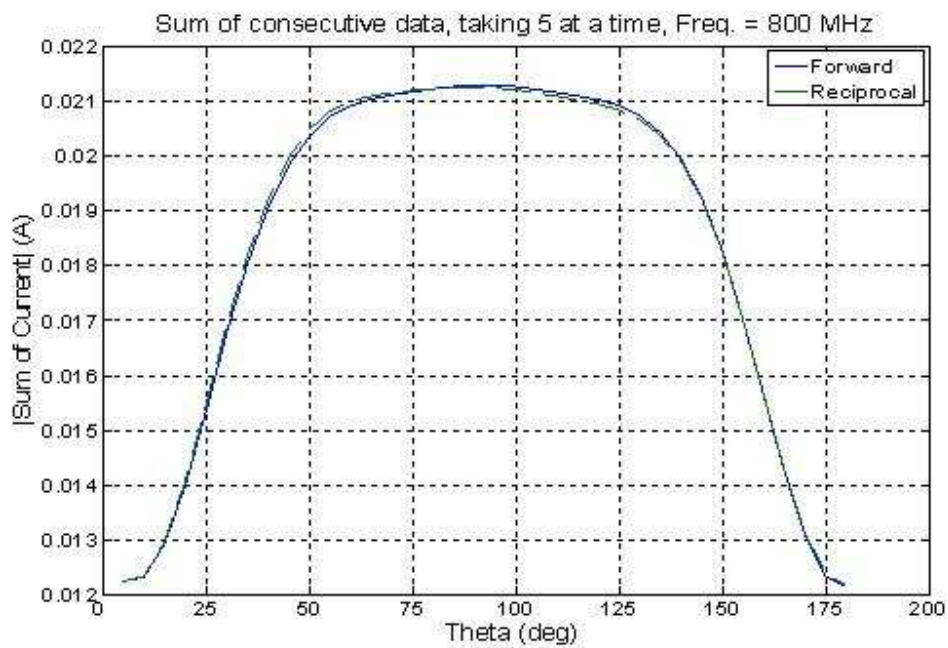


Figure 5.2.3.1.1. Sum of far field data taking 5 consecutive values at a time for change of  $\theta$  from 0 to 180 degrees in 1 degrees variation, at frequency = 800 MHz

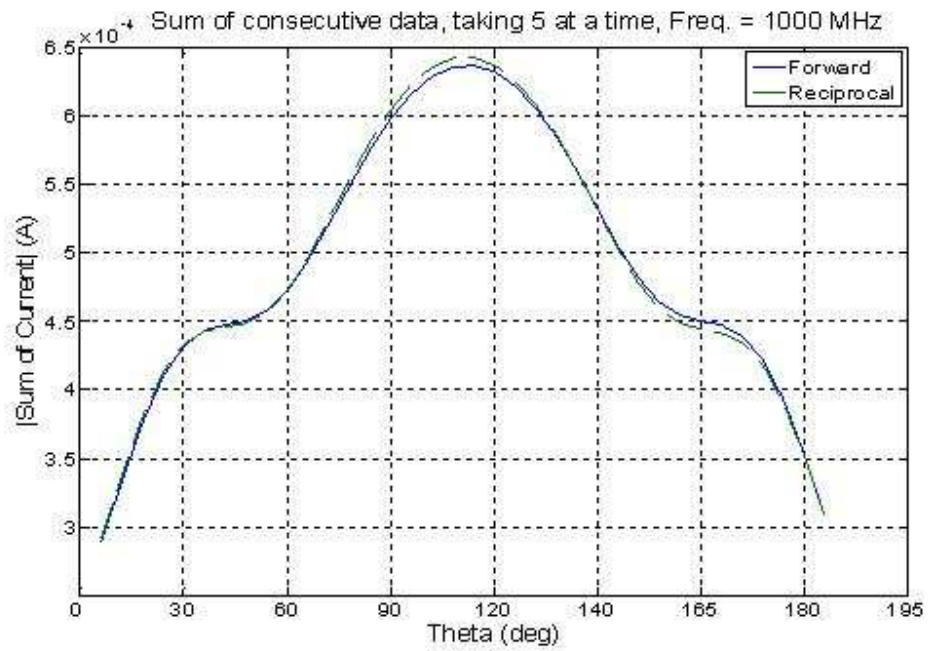


Figure 5.2.3.1.2. Sum of far field data taking 5 consecutive values at a time for change of  $\theta$  from 0 to 180 degrees in 1 degrees variation, at frequency = 1000 MHz

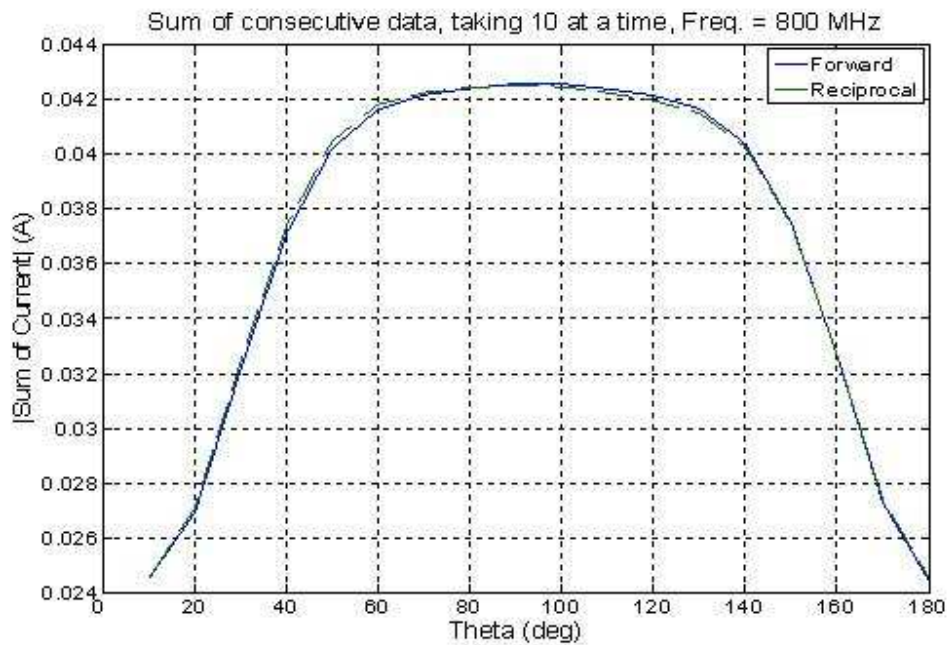


Figure 5.2.3.1.3. Sum of far field data taking 10 consecutive values at a time for change of  $\theta$  from 0 to 180 degrees in 1 degrees variation, at frequency = 800 MHz

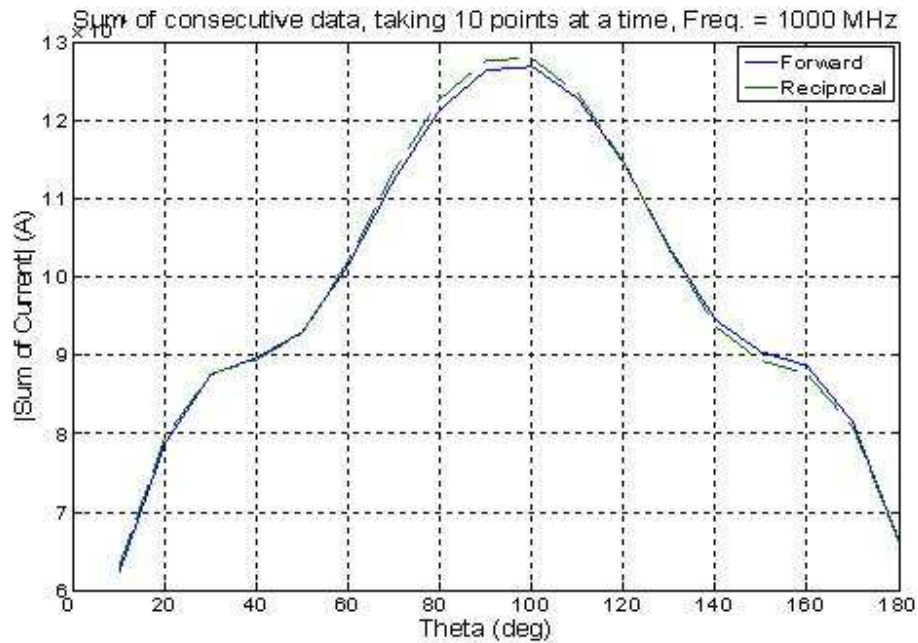


Figure 5.2.3.1.4. Sum of far field data taking 10 consecutive values at a time for change of  $\theta$  from 0 to 180 degrees in 1 degrees variation, at frequency = 1000 MHz

Even though there are suspicious comparison results between the reciprocal and forward problem results for particular frequencies and angle of incidences, which needs to be examined in detail, we can observe an acceptable alignment between the two reverse problems for statistical investigations. Therefore a reciprocal data which is far field evaluations for a given source at the EUT can be used instead of calculating current coupled to the EUT due to a varying source from the respective directions. Using the reciprocity method is a more efficient method as it reduces the computational time by decreasing the number of computations required. In the following sections, the statistics of the current data which is collected using the reciprocity method will be investigated using the efficient methods of sampling.

### 5.2.3.2 Accurate uniform sampling of the reciprocal field

It is known mathematically that specifying the angles of incidences from uniform distribution in  $\theta \in [0, 2\pi]$  and  $\phi \in [0, \pi]$  is not a very accurate method of sampling the angles uniformly on a sphere. This is because the area element  $d\Omega = \sin\phi d\theta d\phi$  is a function of  $\phi$ , and picking angles uniformly from  $\theta \in [0, 2\pi]$  and  $\phi \in [0, \pi]$  respectively results in points more concentrated at the poles [46]. In order to get random field realizations from a uniform incidence sampling, the following procedures are implemented:

- a. Random uniform points are picked for  $\theta$  from 0 to  $2\pi$  by multiplying  $2\pi$  with a uniform random variable  $u$  on (0, 1), i.e.  $\theta = 2\pi u$ .
- b. Random points are picked for  $\phi$  according to the equation  $\phi = \cos^{-1}(2v - 1)$ , where  $v$  is another random variable on (0, 1).

In this thesis, the accurate sampling over a sphere is used to evaluate the current coupling based on reciprocal far field values sampled at the specified points. 100,000 random sample points are generated for the spherical coordinates  $\theta$  and  $\phi$  using a MATLAB code. The pattern from the data is imported to FEKO preprocessor to evaluate far fields at the given random directions. The field is evaluated for a 1V source of 1000 MHz, at the end segment of the 10.4 cm wire inside the 30 cm x 12 cm x 30 cm box. The current response to the random plane waves is evaluated using reciprocity from the field calculations. The response to the two orthogonal, unity magnitude field components  $E_\theta$  and  $E_\phi$  are separately calculated applying reciprocity to each component. In order to

account for the random polarization, polarization angles  $\psi$  are generated from a uniform random distribution in  $[0, 2\pi]$ . Once the current responses to the two orthogonal, unity magnitude field components  $E_\theta$  and  $E_\phi$  are found, the response to a plane wave from the same direction but with a random polarization is found from Equation (5.2.3.2.1) below. The random phase is also added by generating random phase angles  $\varphi$  from uniform random distribution in  $[0, 2\pi]$  as shown in Equation (5.2.3.2.2).

$$I_{\_randPol} = I_\theta * \cos(\psi) + I_\phi * \sin(\psi) \quad (5.2.3.2.1)$$

where  $I_{\_randPol}$  is the current response when the random polarization is included,  $I_\theta$  is the response to  $E_\theta$ , and  $I_\phi$  is the response to  $E_\phi$  and  $\psi$  is the polarization angle.

$$I_{\_randPol \& Phase} = I_{\_randPol} * e^{j\varphi} \quad (5.2.3.2.2)$$

where  $I_{\_randPol \& Phase}$  is the current response when both random polarization and random phase are considered, and  $\varphi$  is the phase angle.

From the 100,000 random current data collected in the above method, summation of currents is accomplished by taking 50 samples at a time (which represents number of plane waves to be added or incident per one stirrer position) and iterating 150, 400, and 1500 times (representing the number of stirrer positions).

The resulting CDF plots for the current evaluations calculated from the reciprocal field values by taking 50 plane waves and iterating 150, 400 and 1500 times are shown in the Figures 5.2.3.3.1 to 5.2.3.3.3 respectively. From the comparison of the three plots we can observe that the statistics gets better as more number of realizations is considered.

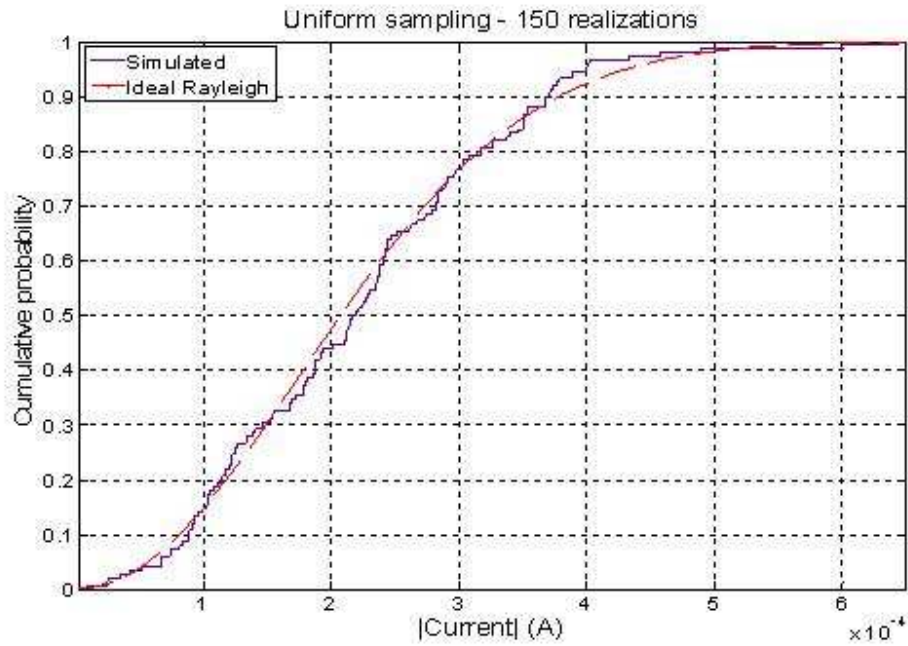


Figure 5.2.3.2.1. Cumulative distribution function of the simulated current induced to the wire on in the box for 150 realizations compared with a Rayleigh distribution (50 plane waves per realization).

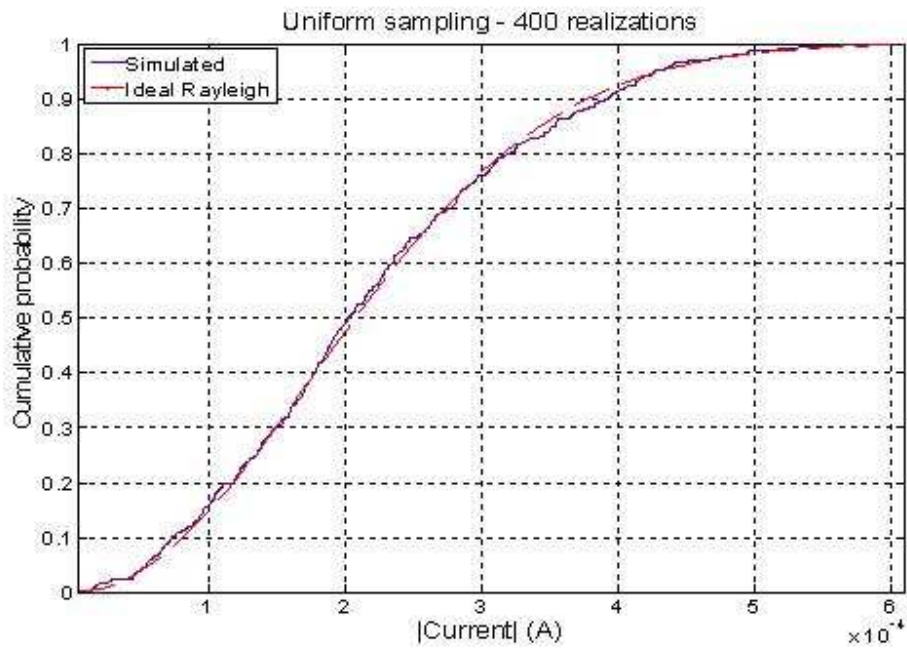


Figure 5.2.3.2.2. Cumulative distribution function of the simulated current induced to the wire on in the box for 400 realizations compared with a Rayleigh distribution (50 plane waves per realization)

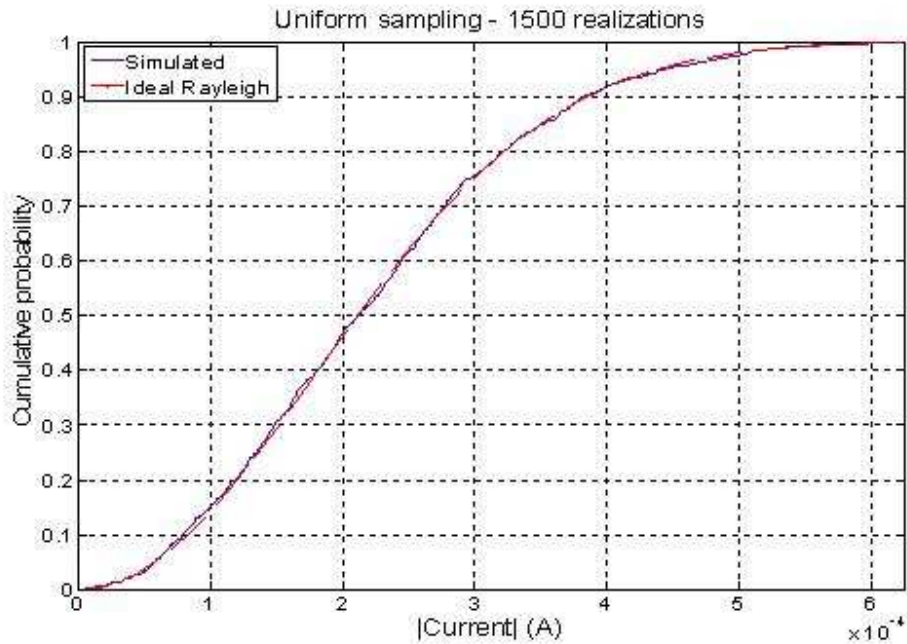


Figure 5.2.3.2.3. Cumulative distribution function of the simulated current induced to the wire on in the box for 1500 realizations compared with a Rayleigh distribution (50 plane waves per realization).

The above result shows that the accurate random sampling method gives a good statistics for 50 plane waves approaching Rayleigh distribution for the current magnitude. The time taken by the FEKO simulation to evaluate the field points at the 100,000 sample points is only 2 minutes. The rest of the computational time is taken by the MATLAB code to take this data and change it to current values, which is very few seconds. This computational time is very much less compared to that of the MC simulation which was evaluated directly by evaluation of current response for each plane wave incidence, which requires 100,000 separate computations. As it is shown from the above result, the uniform sampling method depends on large number of samples for accurate representation of the statistics; moreover this sampling method does not suggest the exact number of plane waves required that could be enough for the accurate statistics to be

achieved. On the other hand, another sampling method, Legendre/uniform sampling is investigated in order to further reduce the computational time by obtaining the exact number of plane waves required to achieve the required statistics for the current. Legendre/uniform sampling is validated and implemented for the evaluation of the current statistics.

### 5.2.3.3 Validation of Legendre/uniform sampling for the wire in the box

According to the Legendre/uniform sampling, the magnitude of the plane waves is made random for fixed incidence angles instead of varying the field parameters such as incidence angle, phase and polarization [45]. The elevation and azimuth angles are sampled according to the spectral sampling theory. The elevation angle ( $\theta$ ) is sampled by specifying  $\cos \theta_l$  at the  $l$ th zero of the Legendre polynomial  $P_L(\cos \theta)$ , the azimuth angle ( $\phi$ ) is sampled uniformly at  $2L$  points within  $[0, 2\pi]$  interval.  $L$  is determined from the special bandwidth of the field that allows enough samples to be sampled and it is given by  $L \geq kD/2$ . For a non ideal bandlimited field environment,  $L \geq k(D + \lambda)/2$ , where  $D$  is the largest dimension of the cavity and  $\lambda$  is the wavelength.

The discretized form of representation of electric field in an ideal reverberation chamber using the integral of a uniform plane wave spectrum using the spectral sampling theory is:

$$\vec{E}(\vec{r}) = \sum_{l=1}^L \sum_{m=1}^{2L} F_{lm} \exp(j\vec{k}_{lm} \cdot \vec{r}) \quad (5.2.3.4.1)$$

$$\vec{F}_{lm} = \vec{a}_\alpha F_{lm,\alpha} + \vec{a}_\beta F_{lm,\beta} \quad (5.2.3.4.2)$$

The real and imaginary components of  $F_{lm,\alpha}$  and  $F_{lm,\beta}$  are generated from normal distribution,  $N(0, w_l E_o^2 / 16L)$ , where  $w_l$  is the Gaussian-Legendre quadrature weighting factor associated with each Legendre polynomial zeros.

In this present work, the Legendre/uniform sampling is used to validate the method and evaluate the current response to the wire at position 7 in the 30cm x 12cm x 30cm box. For this dimension of cavity and source frequency of 1000MHz, L equals to 8. This method is validated using FEKO and MATLAB simulations. The response is evaluated using FEKO simulation and the summation is performed using MATLAB code.

A response for  $2L^2 = 128$  plane waves (or  $4L^2$  orthogonally polarized waves) is evaluated using reciprocity by evaluating field values at the 128 plane wave incidence angles sampled according to the spectral sampling theory.

The induced current is given by

$$I = \sum_{l=1}^L \sum_{m=1}^{2L} \{F_{lm,\alpha} I_{lm,\alpha} + F_{lm,\beta} I_{lm,\beta}\} \quad (5.2.3.4.3)$$

where  $I_{lm,\alpha}$  is current induced due to  $E_\theta$  and  $I_{lm,\beta}$  is current induced due to  $E_\phi$ .

After the current response for each orthogonal components is evaluated, the total current at one independent event is obtained by multiplying each current component with the random complex magnitudes for the given summation limits. The response to independent field realizations is found by repeating the summation for different iterations M. The numbers of realizations implemented in this work are 150, 400 and 1500. The results for these three cases of iterations are shown in figures 5.2.3.4.1 to 5.2.3.4.2 below.

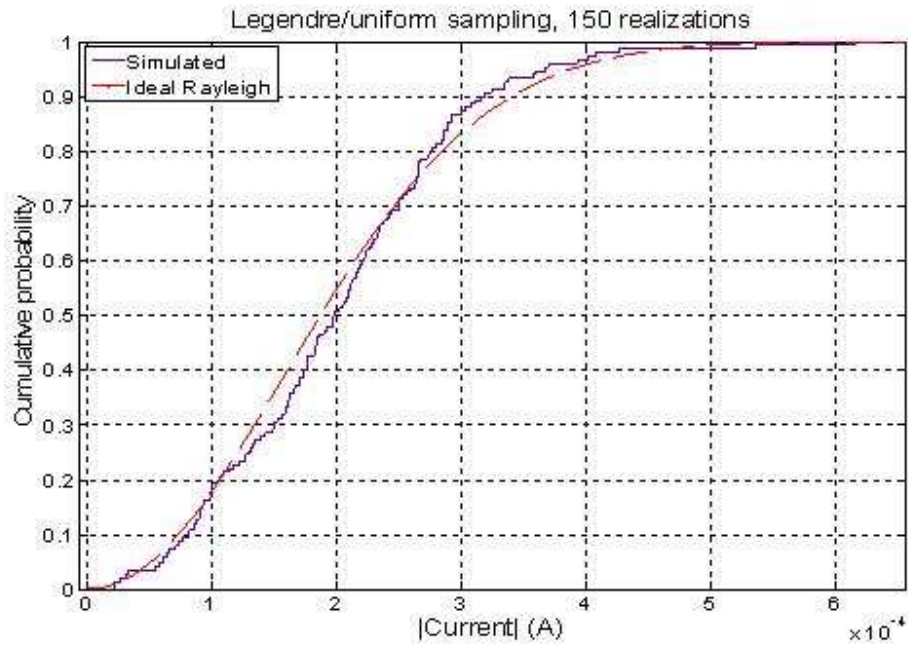


Figure 5.2.3.3.1. Cumulative distribution function of the simulated current induced to the wire on in the box for 150 field realizations compared with a Rayleigh distribution.

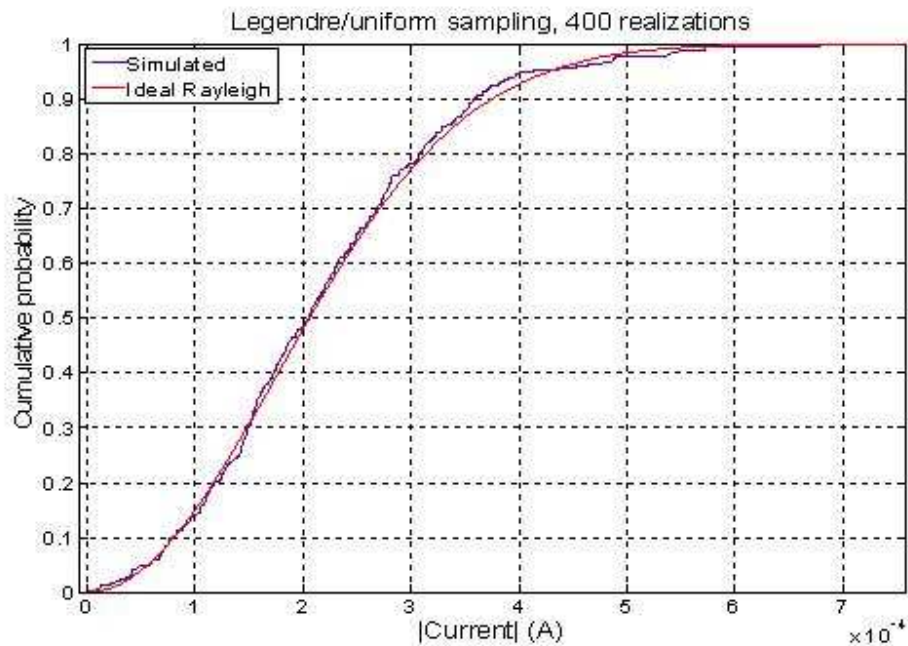


Figure 5.2.3.4.2. Cumulative distribution function of the simulated current induced to the wire on in the box for 400 field realizations compared with a Rayleigh distribution.

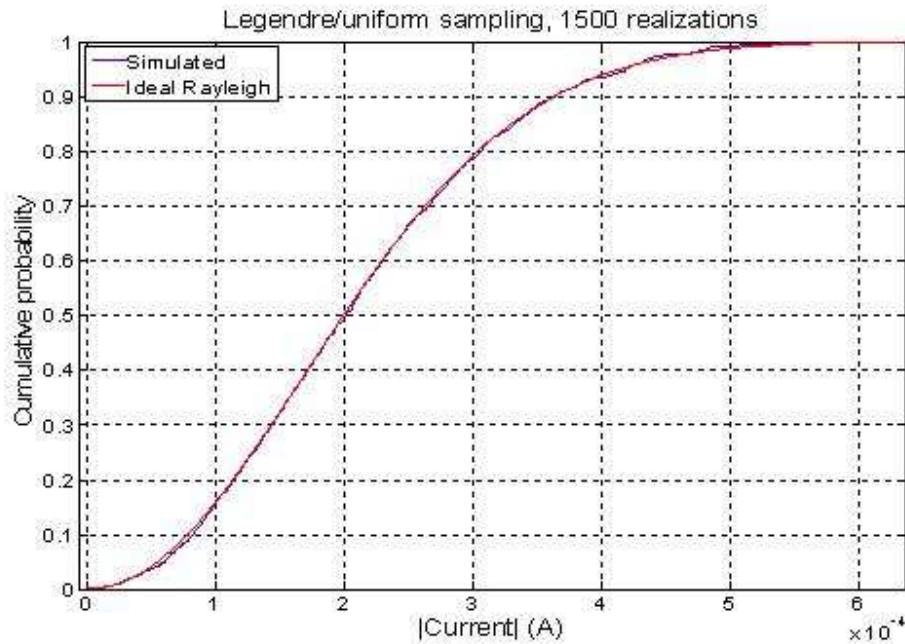


Figure 5.2.3.3.3. Cumulative distribution function of the simulated current induced to the wire on in the box for 1500 field realizations compared with a Rayleigh distribution.

As it is shown above, the results give good agreement with an ideal Rayleigh distribution which is expected for an ideal reverberation chamber environment. The computational time to evaluate the far field for the 128 plane waves is only 6 seconds. The time taken by MATLAB for generating random numbers and performing the superposition varies based on the number of iterations, the strength of the random number generator and the computer performance. Running the code on a 2 GHz RAM, windows Pentium, Dual CPU computer the time taken for the 1000 iterations is half a minute which gives a total computational time of less than a minute. This means a total of less than a minute is taken for  $128 \times 1000 = 128,000$  current computations. Using Legendre/uniform sampling method, a very large number of computations can be achieved depending on the performance of the random number generators. As the number of iterations increases the

computational time increases depending on the computer performance. For 10,000 computations the MATLAB processing time on the same machine is approximately 3 minutes. One of the advantages of the Legendre/uniform sampling over random sampling is that since the complex magnitudes of the fields are taken from a normal distribution, the distribution of the components of the responses to the superposition of the plane waves is normal irrespective of the number of plane waves added, which results a Rayleigh distribution for the magnitudes. Whereas the distribution of the response of a superposition of plane waves for the random sampling depends on the number of plane waves taken to satisfy the central limit theorem.

The comparison of the computational time for the three methods is summarized in the table below.

<b>Computational methods</b>	<b>Computations Required</b>	<b>Time taken for EM Computations (Seconds)</b>	<b>Time taken for Random Number generation (Seconds)</b>	<b>Time taken for random current realizations and linear combinations (Second)</b>	<b>Total Time (Seconds)</b>
MC simulation with direct current evaluation	-100,000 EM computations (current calculations) -1500 random current realizations	4319	2	1	4322
Accurate uniform sampling	-100,000 EM computations (field calculations) -1500 random current realizations	120	2	1	123
Legendre/ uniform sampling	-128 EM computations (field calculations) -Linear combinations -1500 random current realizations	6	2	25	33

## CHAPTER VI

### CONCLUSIONS AND FUTURE WORK

A preliminary analysis was conducted by changing field parameters such as variation of incidence angles and the frequency of the source, and a change of structure by varying the position of wire and aperture size. Observation of the effect of change of the parameters on the current coupling to a wire inside an overmoded enclosure was able to provide an indication to how the field and current coupling in the enclosure were affected due to changes in the external field source. The maximum field coupling frequencies were observed by comparing the field peak values with the empty cavity modes showing a direct relation. The effect of relocation of the wire was also observed showing only a slight disturbance for the wire movement of the wire to different locations inside the cavity. The investigation of the field coupled to the cavity for different aperture sizes suggested a significant effect of slot-cavity resonance interactions. However the methods of evaluation of the current coupling in a complex environment using the preliminary study presented in this thesis will be inefficient as it is difficult to investigate every possible changing situation. If the intention is to represent the real changing environment, representing every situation individually will be impractical without significant attention to the efficiency of the approach.

A more general description of the electromagnetic environment is made by using a statistical approach. Efficient methods are implemented for evaluating the current coupled to the wire due to the stochastic field environment in the box. One of the optimization methods, using reciprocity and the commercial software FEKO, is investigated for its accuracy. In order to validate the software and the codes for using the reciprocity approach and to reduce computational time, a comparison of the forward and reciprocal problems is made. The comparison is made by varying the following parameters; by fixing frequency and rotating the incidence angle along the elevation angle and also azimuth angle, fixing the azimuth angle and changing frequency for some values of elevation angles, fixing the elevation angle and changing the frequency for some azimuth angles. Good agreement is obtained for the comparisons except a few deviations at some frequencies and incidence angles. The 3.8 dB deviation between the forward and reciprocal values at 91 degrees of phi found for fixed frequency of 800 MHz and theta 45 degrees and variation of phi from 0 to 360 degrees (Figure 5.2.2.3.4) is greatly improved to less than 2 dB by using a finer mesh size of  $\lambda/19$ . This improvement is an indication that other results could be improved if the mesh size is decreased. For the comparisons with change in frequency from 800 MHz to 2500 MHz, it was difficult to use a finer mesh. The memory allocation for the matrix to evaluate the calculation by FEKO was a limitation to decrease the mesh further. Therefore the software should be optimized for better meshing flexibility. From the comparison results, it can be concluded that the data collected using the reciprocal method can be used for statistical analysis.

All the three methods implemented to represent a stochastic field environment (direct current evaluation, accurate uniform sampling and Legendre/uniform sampling) indicate good agreement between the simulated and theoretical CDF which is expected to be Rayleigh distributed as in an ideal RC environment. However there are some basic differences between the three methods with respect to the accuracy of the results obtained and the computational time required.

It is shown that the random sampling method results in better statistics as the number of iterations increases. However the Legendre/uniform sampling insures a Rayleigh distribution for current even for few numbers of plane waves and iterations by taking field components from normal distributions with zero mean. Moreover the Legendre/uniform sampling allows determination of the number of plane waves required therefore avoiding additional unnecessary computations.

Computationally, there is a large time reduction using reciprocity and implementing the accurate sampling method. The 72 minutes taken by FEKO in order to evaluate current coupling to a wire in a box for 100,000 computations was reduced to 2 minutes to sample the field points at 100,000 field points. This time reduction can be of great help to further investigate the statistical approach of current evaluation in a stochastic environment. This time is further reduced using Legendre/ uniform to less than a minute to sample the field points at the determined few sample points and linear superposition of random components resulting in a total of 128,000 computations.

## **Future Work**

More detailed analysis of the change of parameters is needed in order to identify the impact of individual field parameters on the coupling problems. By optimizing FEKO software to run changing different parameters in batch and by performing detailed observation, identification of the variables that contribute the most to the random variation could be identified. Optimization of FEKO is also required for better meshing hence better accuracy of results, especially for large frequencies.

After the required data is collected, further statistical investigation should be made in order to further investigate the difference between the different statistical methods. This includes observation of the representation of the tails of the distributions in order to determine if the maximum values are correctly represented. This is important because the maximum values of current are the most important components for susceptibility studies.

## REFERENCES

- [1] R. Holland and R. H. St John, "Em pickup and scattering by a wire," *IEEE Trans. Electromagn. Compat.*, vol. 42, pp. 461-469, Nov 2000.
- [2] L. Paletta, "Susceptibility analysis of wiring in a complex system combining a 3-d solver and a transmission-line network simulation," *IEEE Trans. Electromagn. Compat.*, vol. 44, pp. 309-317, May 2002.
- [3] C. F. Bunting and S. P. Yu, "Field penetration in a rectangular box using numerical techniques: An effort to obtain statistical shielding effectiveness," *IEEE Trans. Electromagn. Compat.*, vol. 46, pp. 160-168, May 2004.
- [4] G. Gradoni, "Numerical and experimental analysis of the field to enclosure coupling in reverberation chamber and comparison with anechoic chamber," *IEEE Trans. Electromagn. Compat.*, vol. 48, pp. 203-211, Feb 2006.
- [5] X. N. Ye, "High-performance inter-pcb connectors: Analysis of emi characteristics," *IEEE Trans. Electromagn. Compat.*, vol. 44, pp. 165-174, Feb 2002.
- [6] R. Araneo and G. Lovat, "Fast mom analysis of the shielding effectiveness of rectangular enclosures with apertures, metal plates, and conducting objects," *IEEE Trans.*

*Electromagn. Compat.*, vol. 51, pp. 274-283, May 2009.

- [7] E. S. S. Siah, K.; Volakis, J.L.; Liepa, V., "Em coupling and suppression through slots into lossless overmoded cavities using the multilevel fast multipole algorithm," *Proc. IEEE Int. Symp Electromagn. Compat.*, vol. 1, pp. 161 - 166, 2002.
- [8] P. Corona, "Reverberating chambers as sources of stochastic electromagnetic fields," *IEEE Trans. Electromagn. Compat.*, vol. 38, pp. 348-356, Aug 1996.
- [9] M. Magdowski, "Coupling of stochastic electromagnetic fields to a transmission line in a reverberation chamber," *IEEE Trans. Electromagn. Compat.*, vol. 53, pp. 308-317, May 2011.
- [10] P. Corona, "Performance and analysis of a reverberating enclosure with variable geometry," *IEEE Trans. Electromagn. Compat.*, vol. 22, pp. 2-5, 1980.
- [11] P. Corona, "Reverberation-chamber research - then and now: A review of early work and comparison with current understanding," *IEEE Trans. Electromagn. Compat.*, vol. 44, pp. 87-94, Feb 2002.
- [12] C. F. Bunting, "Statistical characterization and the simulation of a reverberation chamber using finite-element techniques," *IEEE Trans. Electromagn. Compat.*, vol. 44, pp. 214-221, Feb 2002.
- [13] P. Bonnet, "FDTD modelling of reverberation chamber," *Electron. Lett.*, vol. 41, pp. 1101-1102, Sep 2005.

- [14] D. Fedeli, "Accurate analysis of reverberation field penetration into an equipment-level enclosure," *IEEE Trans. Electromagn. Compat.*, vol. 51, pp. 170-180, May 2009.
- [15] D. Weinzierl, "Simulation of a mode stirred chamber excited by wires using the tlm method," *Compel-Int. J. Comp. Math. Electr. Electron. Eng.*, vol. 22, pp. 770-778, 2003.
- [16] U. Carlberg, "Numerical study of position stirring and frequency stirring in a loaded reverberation chamber," *IEEE Trans. Electromagn. Compat.*, vol. 51, pp. 12-17, Feb 2009.
- [17] D. A. Hill, "Electronic-mode stirring for reverberation chambers," *IEEE Trans. Electromagn. Compat.*, vol. 36, pp. 294-299, Nov 1994.
- [18] D. A. Hill, "Plane wave integral representation for fields in reverberation chambers," *IEEE Trans. Electromagn. Compat.*, vol. 40, pp. 209-217, Aug 1998.
- [19] V. B. L.Musso, F. Canavero, and B. Demoulin, "A plane wave monte carlo simulation method for reverberation chambers," *Proc. EMC Europe 2002, Int. Symp. Electromagnetic Compatibility*, vol. 1, pp. 45-50S, 2002.
- [20] D. A. Hill, "Reciprocity in reverberation chamber measurements," *IEEE Trans. Electromagn. Compat.*, vol. 45, pp. 117-119, Feb 2003.
- [21] R. S. Langley, "A reciprocity approach for computing the response of wiring systems to diffuse electromagnetic fields," *IEEE Trans. Electromagn. Compat.*, vol. 52, pp. 1041-1055, Nov 2010.

- [22] Z. A. Khan, "Shielding effectiveness of metallic enclosures at oblique and arbitrary polarizations," *IEEE Trans. Electromagn. Compat.*, vol. 47, pp. 112-122, Feb 2005.
- [23] B. Audone and M. Balma, "Shielding effectiveness of apertures in rectangular cavities," *IEEE Trans. Electromagn. Compat.*, vol. 31, pp. 102-106, Feb 1989.
- [24] G. Manara, "Electromagnetic penetration and coupling to wires through apertures of arbitrary shape," *IEEE Trans. Electromagn. Compat.*, vol. 40, pp. 391-396, Nov 1998.
- [25] K. Y. Kabalan, "Electromagnetic coupling to conducting objects behind apertures in a conducting body," *Radio Science*, vol. 32, pp. 881-898, May-Jun 1997.
- [26] G. Manara, "Electromagnetic coupling to wires through arbitrarily shaped apertures in infinite conducting screens," *Microw. Opt. Technol. Lett.*, vol. 13, pp. 42-44, Sep 1996.
- [27] E. S. Siah, "Coupling studies and shielding techniques for electromagnetic penetration through apertures on complex cavities and vehicular platforms," *IEEE Trans. Electromagn. Compat.*, vol. 45, pp. 245-257, May 2003.
- [28] D. A. Hill, "Aperture coupling to a coaxial air line - theory and experiment," *IEEE Trans. Electromagn. Compat.*, vol. 35, pp. 69-74, Feb 1993.
- [29] D. A. Hill, "Aperture excitation of electrically large, lossy cavities," *IEEE Trans. Electromagn. Compat.*, vol. 36, pp. 169-178, Aug 1994.
- [30] C. F. Bunting, "A two-dimensional finite-element analysis of reverberation chambers,"

- IEEE Trans. Electromagn. Compat.*, vol. 41, pp. 280-289, Nov 1999.
- [31] D. A. Hill, "Linear dipole response in a reverberation chamber," *IEEE Trans. Electromagn. Compat.*, vol. 41, pp. 365-368, Nov 1999.
- [32] I. Junqua, "Field-to-wire coupling in an electrically large cavity: A semianalytic solution," *IEEE Trans. Electromagn. Compat.*, vol. 52, pp. 1034-1040, Nov 2010.
- [33] C. L. Holloway, "Use of reverberation chambers to determine the shielding effectiveness of physically small, electrically large enclosures and cavities," *IEEE Trans. Electromagn. Compat.*, vol. 50, pp. 770-782, Nov 2008.
- [34] Q. G. Wang, "On the shielding effectiveness of small-dimension enclosures using a reverberation chamber," *IEEE Trans. Electromagn. Compat.*, vol. 53, pp. 562-569, Aug 2011.
- [35] M.B.Slocum, "Electromagnetic environment characterization of below-deck spaces in ships " *IEEE Intern. Symp. on Electromagn. Compat.*, pp. 1-6, 2008.
- [36] S. P. F.Moglie, "Modeling of the reverberation chamber method for the wire-mesh shielding performance evaluation " *IEEE Intern. Symp. on Electromagn. Compat.*, pp. 1-5, 2007.
- [37] F. Moglie, "Modeling of the reverberation chamber method for determining the shielding properties of a coaxial cable " *IEEE Intern. Symp. on Electromagn. Compat.*, vol. 50, pp. 246-251, 2008.

- [38] D. A. Hill and J. M. Ladbury, "Spatial-correlation functions of fields and energy density in a reverberation chamber," *IEEE Trans. Electromagn. Compat.*, vol. 44, pp. 95-101, Feb 2002.
- [39] T. H. Lehman, "A statistical theory of electromagnetic fields in complex cavities," *Interaction Notes, Note 494*, 1993.
- [40] D. A. Hill, "Spatial correlation-function for fields in a reverberation chamber," *IEEE Trans. Electromagn. Compat.*, vol. 37, pp. 138-138, Feb 1995.
- [41] M. Magdowski and D. A. Hill, "Boundary fields in reverberation chambers " *IEEE Trans. Electromagn. Compat.*, vol. 51, pp. 420-421, May 2009.
- [42] J. G. Kostas and B. Boverie, "Statistical-model for a mode-stirred chamber," *IEEE Trans. Electromagn. Compat.*, vol. 33, pp. 366-370, Nov 1991.
- [43] F. Moglie and A. P. Pastore, "FDTD analysis of plane wave superposition to simulate susceptibility tests in reverberation chambers," *IEEE Trans. Electromagn. Compat.*, vol. 48, pp. 195-202, Feb 2006.
- [44] J. C. West, C.F. Bunting, and V. Rajamani, "Optimal plane-wave representation of random fields in a reverberation chamber," in *proceedings of the 2011 IEEE International Symposium on Electromagnetic Compatibility*, 14-19 August, Long Beach, CA, 2011, accepted for publication.
- [45] J. C. West, C.F. Bunting, and V. Rajamani, "Accurate and efficient numerical

simulation of the random environment within an ideal reverberation chamber,”  
*IEEE Trans. Electromagn. Compat.*, Accepted by *IEEE Trans. Electromagnetic  
Compatibility*, Aug. 2011

- [46] E. Weisstein. “Sphere Point Picking.” Internet:  
<http://mathworld.wolfram.com/SpherePointPicking.html>, Nov. 29, 2011 [Nov. 30,  
2011].

## APPENDIX A

### FIELD POINTS AND WIRE POSITIONS WITH RESPECT TO THE DEFINED COORDINATES

The exact values of the field and current calculation points inside the Box with respect to the defined coordinate are described as follows:

FP = Field monitor Position in cm

WP = Wire Position in cm

Field Points:

Position Label	x-coordinate	y-coordinate	z-coordinate
FP (1')	0	0	15
FP (2')	12	0	27

Wire Positions:

Position Label	x-coordinate	y-coordinate	z-coordinate
WP (1)	9	-6	6
WP (2)	3	-6	6
WP (3)	-3	-6	6
WP (4)	-9	-6	6
WP (5)	9	-6	12
WP (6)	3	-6	12
WP (7)	-3	-6	12
WP (8)	-9	-6	12
WP (9)	9	-6	18
WP (10)	3	-6	18
WP (11)	-3	-6	18
WP (12)	-9	-6	18
WP (13)	9	-6	24
WP (14)	3	-6	24
WP (15)	-3	-6	24
WP (16)	-9	-6	24

## APPENDIX B

### PREFEKO INPUT FILE TO INPUT A RANDOM PLANE WAVE

The FEKO Pre Processing input file which evaluates responses for 20 plane waves input of incidence angles theta and phi drawn from a file containing random uniform values from interval [ 0 180] and [0 360] respectively and repeating the process for #num times.

```
** PREFEKO input file generated by CADFEKO version 5.0.124623
```

```
** Work in cm
```

```
SF: 1 : : : : 0.01
```

```
** Import mesh model
```

```
IN 8 31 "StatistFeko111222.cfm"
```

```
** End of geometry
```

```
EG: 1 : 0 : 0 : : : 1e-06 : 1 : 1 : : 0 : 0 : 0 : 1
```

```
#num=150 ** Number of times the sum of plane waves taken (no of stirrer positions)
```

```
!!for #i = 1 to #num
```

```
#theta1=FILEREAD("matrixtheta", #i, 1)
```

```
#phi1=FILEREAD("matrixphi", #i, 1)
```

```
#polar1=FILEREAD("matrixpolar", #i, 1)
```

#phase1=FILEREAD("matrixphase", #i, 1)

\*\* Set frequency

FR: : : : : 1000000000

\*\* Sources

A0	0	1	1	1	#phase1	#theta1	#phi1	#polar1	0	0	0	** PlaneWaveSource1
A0	1	1	1	1	#phase2	#theta2	#phi2	#polar2	0	0	0	** PlaneWaveSource2
A0	1	1	1	1	#phase3	#theta3	#phi3	#polar3	0	0	0	** PlaneWaveSource3
A0	1	1	1	1	#phase4	#theta4	#phi4	#polar4	0	0	0	** PlaneWaveSource4
A0	1	1	1	1	#phase5	#theta5	#phi5	#polar5	0	0	0	** PlaneWaveSource5
A0	1	1	1	1	#phase6	#theta6	#phi6	#polar6	0	0	0	** PlaneWaveSource6
A0	1	1	1	1	#phase7	#theta7	#phi7	#polar7	0	0	0	** PlaneWaveSource7
A0	1	1	1	1	#phase8	#theta8	#phi8	#polar8	0	0	0	** PlaneWaveSource8
A0	1	1	1	1	#phase9	#theta9	#phi9	#polar9	0	0	0	** PlaneWaveSource9
A0	1	1	1	1	#phase10	#theta10	#phi10	#polar10	0	0	0	** PlaneWaveSource10
A0	1	1	1	1	#phase11	#theta11	#phi11	#polar11	0	0	0	** PlaneWaveSource11
A0	1	1	1	1	#phase12	#theta12	#phi12	#polar12	0	0	0	** PlaneWaveSource12
A0	1	1	1	1	#phase13	#theta13	#phi13	#polar13	0	0	0	** PlaneWaveSource13
A0	1	1	1	1	#phase14	#theta14	#phi14	#polar14	0	0	0	** PlaneWaveSource14
A0	1	1	1	1	#phase15	#theta15	#phi15	#polar15	0	0	0	** PlaneWaveSource15
A0	1	1	1	1	#phase16	#theta16	#phi16	#polar16	0	0	0	** PlaneWaveSource16
A0	1	1	1	1	#phase17	#theta17	#phi17	#polar17	0	0	0	** PlaneWaveSource17
A0	1	1	1	1	#phase18	#theta18	#phi18	#polar18	0	0	0	** PlaneWaveSource18
A0	1	1	1	1	#phase19	#theta19	#phi19	#polar19	0	0	0	** PlaneWaveSource19
A0	1	1	1	1	#phase20	#theta20	#phi20	#polar20	0	0	0	** PlaneWaveSource20

\*\* Total source power

\*\* use defaults

\*\* Requested output

DA: : : : 1

OS: 3 \*\* Currents1

!!next

\*\* End of file

EN

\*\* CADFEKO Checksum: 7aa0b6172db724dbac9ac25995e355aa

**APPENDIX C**  
**DATA ARRANGEMENT**

a) For a fixed  $\phi$ , varying  $\theta$  and frequency sweep

$$\left[ \begin{array}{l} I_R^{f(1)}(\theta_1, \phi_1) \dots I_R^{f(2)}(\theta_1, \phi_1) \dots I_R^{f(3)}(\theta_1, \phi_1) \dots \dots \dots I_R^{f(N)}(\theta_1, \phi_1) \\ I_R^{f(1)}(\theta_2, \phi_1) \dots I_R^{f(2)}(\theta_2, \phi_1) \dots I_R^{f(3)}(\theta_2, \phi_1) \dots \dots \dots I_R^{f(N)}(\theta_2, \phi_1) \\ I_R^{f(1)}(\theta_3, \phi_1) \dots I_R^{f(2)}(\theta_3, \phi_1) \dots I_R^{f(3)}(\theta_3, \phi_1) \dots \dots \dots I_R^{f(N)}(\theta_3, \phi_1) \\ \cdot \\ \cdot \\ \cdot \\ \cdot \\ \cdot \\ I_R^{f(1)}(\theta_M, \phi_1) \dots I_R^{f(2)}(\theta_M, \phi_1) \dots I_R^{f(3)}(\theta_M, \phi_1) \dots \dots \dots I_R^{f(N)}(\theta_M, \phi_1) \end{array} \right]$$

This is repeated for others selected  $\phi$ .

b) For a fixed  $\theta$ , varying  $\phi$  and frequency sweep

$$\begin{bmatrix}
I_R^{f(1)}(\phi_1, \theta_1) \dots I_R^{f(2)}(\phi_1, \theta_1) \dots I_R^{f(3)}(\phi_1, \theta_1) \dots \dots \dots I_R^{f(N)}(\phi_1, \theta_1) \\
I_R^{f(1)}(\phi_2, \theta_1) \dots I_R^{f(2)}(\phi_2, \theta_1) \dots I_R^{f(3)}(\phi_2, \theta_1) \dots \dots \dots I_R^{f(N)}(\phi_2, \theta_1) \\
I_R^{f(1)}(\phi_3, \theta_1) \dots I_R^{f(2)}(\phi_3, \theta_1) \dots I_R^{f(3)}(\phi_3, \theta_1) \dots \dots \dots I_R^{f(N)}(\phi_3, \theta_1) \\
\cdot \\
\cdot \\
\cdot \\
\cdot \\
\cdot \\
I_R^{f(1)}(\phi_L, \theta_1) \dots I_R^{f(2)}(\phi_L, \theta_1) \dots I_R^{f(3)}(\phi_L, \theta_1) \dots \dots \dots I_R^{f(N)}(\phi_L, \theta_1)
\end{bmatrix}$$

This is repeated for other selected  $\theta$ .

## APPENDIX D

### SUMMATION OF CURRENT

%This code extracts the real and imaginary components of current values from the .OS file of FEKO output and sums required amount at a time for specified times.

```
[a3,b3] = textread('wire in a box for reciprocity_ forward_prob_Phi_90_Th_0180_800M-2500M.os','%*d%*s%*s%*s%*s%*15s%*1s%*16s%*s%*15s%*1s%*16s%*2s%15s%*2s%15s%*[\n]'); %Read current from .OS file of FEKO
```

```
format short eng
```

```
IW2real144=[];
```

```
IW2imag144=[];
```

```
IW2mag144=[];
```

```
m3=cell2mat(a3);
```

```
n3=cell2mat(b3);
```

```
aa3=str2num(m3);
```

```
bb3=str2num(n3);
```

```
for i=0:6335 %this can filter data till freq 1500M. If you want till 2500M, do  
181*85.....85= (2500-800)/20
```

```
x=i*11+11;
```

```
current2real144=aa3(x, 1);
```

```
IW2real144= [IW2real144 current2real144]; %put the real component of current in a  
matrix
```

```
current2imag144=bb3(x, 1);
```

```
IW2imag144= [IW2imag144 current2imag144]; %put the imaginary component of  
current in a matrix
```

```
end
```

```
Iw2rREAL=[];
```

```
Iw2rIMAG=[];
```

```
%TAKING DATA OF FREQUENCY 1000M, WHICH IS THE START OF 181*10 th  
of the whole data which is the value of (181*10*11)+11 of .OS file on excel number
```

```
% for 820M ...m=(181*1)+n;
```

```
% for 840M ...m=(181*2)+n;
```

```
% for 860M ...m=(181*3)+n; ..etc.
```

```
for n=1:181
```

```
m=(181*10)+n; % for 1000M ...m=(181*10)+n; m=(181*20)+n; % for 1200M  
...m=(181*20)+n; % Representing different frequencies.
```

```
Iw2rreal = IW2real144 (m); %Extracting the real component of current for different  
frequencies.
```

```
Iw2iimag = IW2imag144 (m); %Extracting the imaginary comp of current for different  
frequencies.
```

```
Iw2rREAL = [Iw2rREAL Iw2rreal]; %Putting it in a matrix
```

```
Iw2rIMAG = [Iw2rIMAG Iw2iimag]; %Putting it in a matrix
```

```
end
```

```

Iw2rREAL
Iw2rIMAG
IW2real = Iw2rREAL';
IW2imag = Iw2rIMAG';
CurrRealImag = [ IW2real IW2imag ]

sumrreal =[];
sumiimag =[];
Totmag = [];
sumRealll = [];
sumiimaggg = [];
TotmagCurr=[];

% Adding values N times....taking N each time and the next N etc.
M = 36; % When taking 5 points at a time we will have 36 data

N = 5; %For taking 5 points at a time

for j = 1:M

    for k = ((j-1)*N+1):(j)*N

        SampReal = CurrRealImag(k,1);
        SampImag = CurrRealImag(k,2);
    SamReall= [SamReall SampReal ];
    SamImagg= [SamImagg SampImag ];
    End

```

```

sumReal = sum(SamReall); %Summing the real components
sumImag = sum(SamImagg); %Summing the imaginary components

magg(j) = sqrt((sumReal)^2+( sumImag)^2); %Magnititude of the current values

SamReall = 0;
SamImagg = 0;

end

TotmagCurr = [TotmagCurr magg];
TotmagCurr
Save ReciprocityCurrentForwTot1200_5Points TotmagCurr -ascii ); %Save the data

```

## APPEDIX E

### SUMMATION OF FIELD

%This code extracts the phase and magnitude of each components of field values (E-theta and E-Phi) and sums required amount at a time for specified times.

```
field_recip_data = [];
```

```
format short eng
```

```
field_recip_data44 = xlsread('RecipField_th0-180_ph0-360_1000.xls'); %Read the reciprocal field values
```

```
field_recip_data = [field_recip_data field_recip_data44]; %Put it in a matrix
```

```
MagRecCurr = 0;
```

```
Theta = field_recip_data(:, 1); %Theta variation
```

```
Phi = field_recip_data(:, 2) %Phi variation
```

```
magEtheta = field_recip_data(:, 3); %Magnitude of E-theta
```

```
phaseEtheta = field_recip_data(:, 4); %Phase of E-theta
```

```
magEphi = field_recip_data(:, 5); %Magnitude of E-phi
```

```
phaseEphi = field_recip_data(:, 6); %Phase of E-phi
```

```

realofEthetaData = [];

imagofEthetaData = [];

realofEphiData = [];

imagofEphiData = [];

for i= 1:703    %Extracting the values from 703 set of field data found from parsing
FEKO .OUT file

radanglEtheta(i) = (phaseEtheta(i))*pi/180; %Changing the degrees to radians for phase
angle of E-theta

radanglEphi(i) = (phaseEphi(i))*pi/180; %Changing the degrees to radians for phase
angle of E-phi

realofEtheta(i) = magEtheta(i) * cos(radanglEtheta(i)); %Calculating real component of
E-theta

imagofEtheta(i) = magEtheta(i) * sin(radanglEtheta(i)); %Calculating imaginary
component of E-theta

realofEphi(i) = magEphi(i) * cos(radanglEphi(i)); %Calculating real component of E-phi

imagofEphi(i) = magEphi(i) * sin(radanglEphi(i)); %Calculating imaginary component
of E-phi

end

realofEthetaData = [realofEthetaData realofEtheta] %Putting it in a matrix
imagofEthetaData = [imagofEthetaData imagofEtheta] %Putting it in a matrix
realofEphiData = [realofEphiData realofEphi] %Putting it in a matrix
imagofEphiData = [imagofEphiData imagofEphi] %Putting it in a matrix

```

```

realofEthetaData1 = realofEthetaData';
imagofEthetaData1 = imagofEthetaData';
realofEphiData1 = realofEphiData';
imagofEphiData1 = imagofEphiData';

RandomFieldComp = [realofEthetaData1 imagofEthetaData1 realofEphiData1
imagofEphiData1];

    % To take random number of fields at a time from the whole

N = 400    %number of times we want to take randomly../No of stirrer rotations

for j = 1:N

f= 50    %number of plane waves we want to add / No of waves we add w.r.t reciprocity

% current_real_and_imag is the whole matrix containing fields we want some of
% it to add

b = size(RandomFieldComp, 1)

rowIndex = ceil(b*rand(f,1)); % rand(f,1) gives f random fraction numbers between 0
and 1 and the ceil function approximates

    % (b*rand(f,1)) into integers so that we
    % get an index which is a random number
    % between 1 and size of the whole data

chosenRows = RandomFieldComp(rowIndex, :);

```

```

% TO EVALUATE SUM OF FIELD FOR RANDOM COMBINATION

% COMBINE THESE FOUR COLUMN MATRICES FOR EACH ANGLES AND

% FROM THERE VALUES OF FIELDS TAKE RANDOM VALUES (RANDOM
INCIDENCE)

% LETS SAY WE HAVE 38 VALUES/ RANDOM ANGLES AND WE HAVE A
MATRIX OF FOUR

% COLUMNS AND 38 RANDOMLY CHOSEN ANGLE WITH THEIR
RESPECTIVE

% realofEthetaData, imagofEthetaData, realofEphiData, imagofEphiData

% IN ONE MATRIX....SUM FUNCTION SUMS VALUES IN EACH COLUMN
TOGETHER

% say the matrix is called RandomFieldComp

% RandomFieldComp = [realofEthetaData imagofEthetaData realofEphiData
imagofEphiData];

% LETS SAY FOR NOW THE RANDOM TOOK ALL THE VALUES, ALL ANGLES

sumofEachFieldComp = sum (chosenRows)

magEtheta = sqrt(( sumofEachFieldComp(1) )^2+( sumofEachFieldComp(2))^2);
magEphi = sqrt(( sumofEachFieldComp(3) )^2+( sumofEachFieldComp(4))^2);
otalMagField(j) = sqrt(( magEtheta )^2+( magEphi)^2);

% TO FIND MAG OF Recip CURRENT FROM THE FIELD, MULTIPLY BY THE
CONSTANT for

% frequency 800

```

```

% Freqfactor = 5/(pi*800);

Freqfactor = 5/(pi*1000) %Proportionality constant to change field values to reciprocal
current

% Freqfactor = 5/(pi*2000)

MagReciprocalCurrent(j) = TotalMagField(j) * Freqfactor; %Magnitude of the
reciprocal current which is evaluated from the reciprocal field by multiplying every field
values with the constant.

AvgMagReciprocalCurrent(j) = MagReciprocalCurrent(j)/f;

end

MagRecCurr = [];

AvgMagRecCurr =[];

MagRecCurr = [MagRecCurr MagReciprocalCurrent];

AvgMagRecCurr = [AvgMagRecCurr AvgMagReciprocalCurrent];

```

## APPENDIX F

### PREFEKO INPUT FILE TO INPUT RANDOM SAMPLE LOCATIONS FROM EXTERNAL FILE

\*\* PREFEKO input file to specify the field evaluation points from external file.

\*\* Work in cm

SF: 1 : : : : 0.01

\*\* PreFEKO program to import far field random points from external data

\*\* Import mesh model

IN 8 31 "Freq\_1000\_Th&Phi\_100000RandomSamples.cfm"

\*\* End of geometry

EG: 1 : 0 : 0 : : : 1e-06 : 1 : 1 : : 0 : 0 : 0 : 1

\*\* Set frequency

FR: : : : : 1000000000

\*\* Sources

A1: 0 : Union2.Wire1059.Port1 : 0 : : : 1 : 0 \*\* VoltageSource1

\*\* Total source power

\*\* use defaults

```

** Requested output

DA: : : : 1

** Far fields: FarField1

DA: : : 1 : : : : 0

OF: 1 : 0 : : : : 0 : 0 : 0

#points=100000                ** Number of data point in the input file

!!for #point = 1 to #points step 1    ** Loop over data points

#line = #point + 2                ** Assuming there are 2 header lines to be ignored
in the input line.

#theta=FILEREAD("Unif_Random_FarField_100000_points", #line, 1) ** Read Theta
from input file, assuming the Theta value is in column 1

#phi=FILEREAD("Unif_Random_FarField_100000_points", #line, 2) ** Read Phi
from input file, assuming the Phi value is in column 2

FF 1 1 1 0    #theta #phi                ** Request far field at single point
(#theta,#phi)

DA 0 0 1 0 0 0    0 0 0 0 ** Export far field value to ASCII
*.ffe file

!!next                            ** End of loop

** FF: 1 : 181 : 1 : 0 : : 0 : 90 : 1 : 0 ** FarField1

** End of file

EN

** CADFEKO Checksum: adeaa93e8a1bcf91f533cd64f304e954

```

VITA

Endegenä Assefa

Candidate for the Degrees of

Master of Science

Thesis: VALIDATION AND IMPLEMENTATION OF EFFICIENT SIMULATION  
TECHNIQUES TO DETERMINE COUPLING TO A WIRE IN AN  
OVERMODED ENCLOSURE

Major Field: Electrical Engineering

Biographical:

Education:

Completed the requirements for the Master of Science in Electrical Engineering at Oklahoma State University, Stillwater, Oklahoma in May, 2012.

Completed the requirements for the Bachelor of Science in Electrical Engineering at Bahir Dar University, Bahir Dar, Ethiopia in 2005.

Experience:

Graduate Research Assistant, School of Electrical and Computer Engineering, Oklahoma State University, from 2010 to 2011.

Name: Endegen Assefa

Date of Degree: May, 2012

Institution: Oklahoma State University

Location: OKC or Stillwater, Oklahoma

Title of Study: VALIDATION AND IMPLEMENTATION OF EFFICIENT  
SIMULATION TECHNIQUES TO DETERMINE COUPLING TO A  
WIRE IN AN OVERMODED ENCLOSURE

Pages in Study: 111

Candidate for the Degree of Master of Science

Major Field: Electrical Engineering

Scope and Method of Study:

The efficiency of electromagnetic (EM) coupling computations depends on the methods employed. To solve coupling problems in a complex environment requires solving an EM problem for varying scenarios which is difficult to realize individually. In this work, the effect of change of certain parameters on the current coupling to a wire in a box is observed, which leads to the need to develop statistical methods. An effort is made to develop and verify efficient methods of representing a stochastic field environment using efficient sampling methods. FEKO, a commercial software package is used for simulating field radiations and the current coupled to a wire in a rectangular box with an aperture. MATLAB codes are used to post-process the FEKO output files. A method to implement reciprocity is verified and used in order to reduce the number of computations required to calculate the coupling to a wire in a box for random field encounters. The statistics for the current coupled to the wire is evaluated and compared with theories.

Findings and Conclusions:

A method to implement reciprocity is verified and used in order to reduce the number of computations required. Efficient methods of representing the stochastic field environment are verified and less computational times are achieved. Good agreement with theories is obtained for current statistics obtained by collecting current data using the efficient methods.

ADVISER'S APPROVAL: Dr. Charles F. Bunting

---